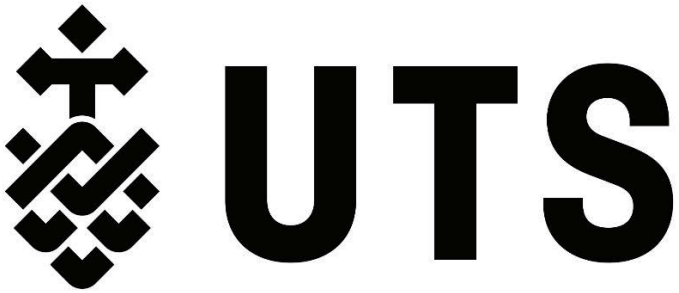

Investigating the Conditions that Trigger Filamentation in Uropathogenic *Escherichia coli*

Greg Iosifidis

Doctor of Philosophy

July 2018

CERTIFICATE OF ORIGINAL AUTHORSHIP

I certify that the work in this thesis has not previously been submitted for a degree nor has it been submitted as part of requirements for a degree except as part of the collaborative doctoral degree and/or fully acknowledged within the text.

I also certify that the thesis has been written by me. Any help that I have received in my research work and the preparation of the thesis itself has been acknowledged. In addition, I certify that all information sources and literature used are indicated in the thesis.

This research is supported by an Australian Government Research Training Program Scholarship.

Production Note:

Signature of Student: Signature removed prior to publication.

Date: 17.7.18

ACKNOWLEDGMENTS

Coming to the end of my PhD, there are so many people to whom I am forever grateful, without you I would never have made it to the end.

First, I would like to thank my primary supervisor Assoc. Prof. Iain Duggin for giving me the opportunity to undertake this very interesting project. I appreciate your guidance and support throughout these many years and for your help with my thesis. To Dr. Amy Bottomley, my co-supervisor, a massive thank you for all of your help and all that you have done for me. Thank you for proof reading my thesis many times over and collaborating with you has been so much fun.

To the members of the Duggin Lab, past and present: Emma, Daniel, Tamika, James, Shirin, Roshali, Solenne, Yan and Kirstine. Thank you for being such an amazing lab group. A special thanks to the UPEC team Daniel and Tamika who have been a great source of laughs, support and problem solving and as we navigated our way through all things UPEC. Thank you to Emma, who I have done my honours and PhD alongside. You are a great friend who has given me so much help and support.

I would also like to thank the Whitchurch Lab group who are a beacon of knowledge when it comes to flow cell models. Thank you for your help when I was setting up my flow cell model and lending me equipment when mine had broken or I had run out, my models will never look as neat as yours. Thank you to the Level 7 Technical Staff Mercedes, Sarah and Luke who have helped me out in the lab when I needed equipment training, disposing of something or had any tissue culture issues. Thank you to Dr. Michael Johnson for all his help with the microscopes, which have been extremely testing at times. In addition, I would like to thank Assoc. Prof. Mary Bebawy who allowed me to use her microscope and microfluidic equipment, it was nice having that all to myself for a while. Another thank you to Shirin, Amy and Iain who provided me with some of the bacterial strains I have used in this work.

To the ithree HDR students, too many to name, thank you for all of your support throughout these years and thanks for everything. Thank you to my best friend Oscar Almond, the very hard worker, who was always there to listen about my PhD escapades and always wanting to go out eating.

I would also like to give a big thank you to my parents and my brother who have always supported me and listened to my daily adventures and me talking about my work. Finally, I would like to thank everyone else in my life who have helped make this such an enjoyable and rewarding experience.

TABLE OF CONTENTS

LIST OF FIGURES AND TABLES

Figures

Tables

ABBREVIATIONS

°C	Degrees Celsius
µg	microgram
µl	microlitre
µm	micrometre
Amp	Ampicillin
AUM	Asymmetric Unit Membrane
cAMP	Cyclic Adenosine Monophosphate
CFU	Colony Forming Unit
CNF-1	Cytotoxic Necrotising Factor 1
CO_2	Carbon dioxide
Da	Daltons
ddH_2O	Double Deionised Water
DMEM	Dubecco's Modified Eagle Medium
DMSO	Dimethyl sulfoxide
DNA	Deoxyribonucleic Acid
DTI	Defined Trypsin Inhibitor
E.	*Escherichia*
EDTA	Ethylenediaminetetraacetic acid
EGFP	Enhanced Green Fluorescent Protein
et al.	and others
FITC	Fluorescein Isothiocyanate
g	gram
GFP	Green Fluorescent Protein
h	hours
H.	*Haemophilus*
HKGS	Human Keratinocyte Growth Supplement
IBC	Intracellular Bacterial Community
IL	Interleukin
IPTG	Isopropyl β-D-1-thiogalactopyranoside
kb	Kilo basepair
Km	Kanamycin
LPS	Lipopolysaccharide
M	Molarity
mg	milligram

min	minutes
ml	millilitre
mm	millimetre
mM	Millimolar
MOI	Multiplicity of Infection
ms	millisecond
NF	Nuclear Factor
nM	Nanomolar
PAMP	Pathogen-Associated Molecular Pattern
PBS	Phosphate Buffered Saline
PCR	Polymerase Chain Reaction
PFA	Paraformaldehyde
pH	Power of Hydrogen
PRR	Pattern Recognition Receptor
PS	Penicillin/Streptomycin
R	Resistance
rcf (xg)	Relative Centrifugal Force
rpm	Revolutions per Minute
SEM	Standard Error of the Mean
SHU	Synthetic Human Urine
TAE	Tris-acetate EDTA
TBE	Tris-borate EDTA
TLR-4	Toll Like Receptor 4
Tris	Tris(hydroxymethyl)methylamine
TRITC	Tetramethylrhodamine-isothiocyanate
UP	Uroplakin
UPEC	Uropathogenic *Escherichia coli*
UTI	Urinary Tract Infection
V	Voltage
v/v	Volume per Volume
w/v	Weight per Volume
WT	Wild Type
Δ	Deletion

ABSTRACT

Urinary tract infections (UTIs) are one of the most common and costly infections worldwide, primarily caused by Uropathogenic *Escherichia coli* (UPEC). Over recent years, there has been an increase in antibiotic resistant UTIs, which are diminishing the use of existing antibiotic therapies. This requires close surveillance as it has the possibility to greatly exacerbate the impact of UTIs. Therefore, there is a high need to develop new treatments that can replace current ineffective antibiotic therapies. In order to identify new treatment options, the different stages of UPEC infection need to be understood.

UPEC undergo a multi-stage infection cycle, which is initiated by UPEC binding to and being internalised into host bladder epithelial cells that line the bladder wall. The bacteria continue to grow inside the bladder cells where they develop into intracellular bacterial communities, which are internal biofilm-like colonies. Once the bacterial burden has overwhelmed the host, the bladder cell ruptures and releases the bacteria. A substantial proportion of the released bacteria consist of extensively elongated bacteria, many times longer than typical rod-shaped *E. coli*. This morphology change is known as filamentation, where the bacterial cell has continued to grow without dividing. This occurrence has been thought to offer survival advantages to the bacteria to allow it to cause such a successful and persistent infection.

Studies have demonstrated that one trigger that induces bacterial filamentation is concentrated urine, although the underlying mechanisms are unknown. This thesis aimed to further define and investigate the conditions and factors that trigger bacterial filamentation in a UTI. Initially, a method was required to accurately quantify the degree of filamentation by reproducing and improving on current *in vitro* bladder cell infection models. Through the development of an appropriate fluorescent UPEC strain to visualise the bacteria during infection of human bladder cells, a reproducible method, based on the combined use of microscopy and flow cytometry, was established to determine the degree of filamentation under different conditions.

By directly visualising the events before and during bacterial filamentation, it can develop an understanding of how and why filaments arise. Therefore, a novel microfluidic infection model was established to observe the infection of bladder cells by UPEC in real time. This model revealed the bacteria do not initially inactivate or kill their host cells,

but appear to use the bladder cells as protection to grow and develop. With this new model it was also demonstrated that cultured human bladder cells became immobilised, permeabilised and likely killed upon exposure to a flow of sterile human urine. This was unexpected but revealed a likely mechanism by which the bacteria could rapidly respond to form filaments, from inside the host bladder cells. Nevertheless, it was expected that the exposure to urine was a key factor that triggers the filamentation response of UPEC after bladder cell rupture both *in vitro* and *in vivo*. For the first time, UPEC filaments were directly observed to grow out from within permeabilised bladder cells after exposure to urine.

To begin to understand what initiates bacterial filamentation in UTI potential factors were investigated. The well-characterised SOS response was analysed for its importance to UPEC filamentation. This response is known to cause filamentation after bacterial DNA damage and there has been some conflicting reports over the role of SOS filamentation in a UTI. The work in this thesis indicated that it is unlikely that SOS induction is the primary cause of filamentation in a UTI.

Investigations were conducted into host factors, such as the composition of urine, as a condition that induces bacterial filamentation. The results showed that filamentation occurs in response to a certain urine constituent(s), that is pH dependent and of small molecular weight.

By developing and utilising *in vitro* infection models of UTIs, this thesis has initiated a new line of research into the effects of different factors, both bacterial (SOS) and host related (urine), on filamentation. Overall, this thesis provided evidence of the existence of other non-SOS pathways that are sensitive to urine composition that cause UPEC to filament during infection. This knowledge could be used in the future to help develop treatments that focus on preventing filamentation and the infection cycle, in the hope of attenuating this common infection.

CHAPTER 1

GENERAL INTRODUCTION

Urinary tract infections (UTIs) are one of the most common infections in the developed world. Every year these infections account for over 7 million clinical visits [1]. This in turn makes them extremely costly infections, with an annual cost estimated to be $3.5 billion [1]. Clearly, UTIs present a substantial burden on the health care industry.

The current treatment for this infection is a course of antibiotics. However, the emergence of antibiotic resistance is exacerbating this problem and has highlighted the need for new treatment options. In recent years, cases have been reported of patients presenting with UTIs resistant to last resort antibiotics. This is very problematic given how common UTIs are and could further push the limits of available care and treatments.

To begin to tackle this growing issue, a further understanding of UTIs and the bacteria that cause them is essential. This would provide a much-needed insight into the molecular pathways occurring during infection and could lead to the development of new treatments and prevention techniques for these infections. The work in this thesis aimed to improve upon current methods used to study the bacteria in a UTI and to understand the behaviour of the most common causative agent of UTIs, *Escherichia coli*. By further researching the underlying mechanisms in a UTI caused by *Escherichia coli*, it could help to understand the processes involved and to combat this infection and reduce its impact on society.

1.1 URINARY TRACT INFECTIONS (UTI)

Urinary tract infections (UTIs) can be separated into uncomplicated, affecting healthy individuals, and complicated, affecting those with abnormalities regarding the urinary tract such as catheters [2]. They are caused by both Gram negative and Gram positive bacteria with the most common organisms being *Escherichia coli*, *Klebisella pneumoniae*, *Proteus mirabilus*, *Enterococcus faecalis* and *Staphylococcus saprophyticus* [2]. Women are more susceptible to these infections than men, with 40-50 % of women compared to 5 % of men experiencing a UTI in their lifetime [3]. Antibiotics including co-trimoxazole, ampicillin and ciprofloxacin commonly treat these infections [2]. One reason for the high burden of UTIs is reoccurrence with around one in four women experiencing a second UTI within six months of an initial infection [4]. In addition to this, 3 % of these women will then experience a third UTI within the ensuing six month period, highlighting the ineffectiveness of current treatments [4]. It has also been shown that around one third of cases of reoccurrence are caused by the same bacterial strain that caused the initial infection [5]. This suggests that the initial infection had not been completely cleared, highlighting the existence of mechanisms implemented by the bacteria to evade current treatments and persist.

UTIs are classified depending on the position of the urinary tract in which they cause infection. An infection in the urine is referred to as bacteriuria, an infection of the bladder is called cystitis and once the infection has ascended into the kidneys it is termed pyelonephritis [6]. In some cases, the bacteria in the kidney can disseminate into the bloodstream causing sepsis, which can become life threatening rapidly [6]. Symptoms of a UTI can include pain and a burning sensation in urination, urgency in urination and a frequency of urination [6]. However, in some instances there are no associated symptoms such as in asymptomatic bacteriuria [6]. This can often prevent the urinary tract from becoming colonised by more pathogenic bacteria [7, 8]. Studies have demonstrated that the presence of non-pathogenic *E. coli* 83972 can inhibit infections by Gram positive, Gram negative and fungal uropathogens [7, 8]. This had the potential to be used as therapeutic agent to prevent symptomatic UTIs in people with spinal cord injury.

During a UTI, there is a lot of interplay between the host, particularly urinary tract epithelial cells, and the pathogen, most commonly *Escherichia coli*. As will be described later on in this chapter, the host cell plays an important role in the survival and

development of the bacteria to cause successful infection. The bacteria usually find their way into the bladder via the urethra where they invade and colonise the host bladder cells and then disseminate from there. To comprehend the infection process, an understanding of the host cell is required.

1.2 THE HOST CELL

The bladder collects urine before it is removed by the body through urination. The bladder wall is impermeable to passive diffusion of molecules, but allows active transport to occur between the blood and urine [9]. This ensures that the urine maintains essentially the same composition as when it leaves the kidneys [10]. The wall of the bladder is made up of several layers, including the lamina propria, muscularis mucosa, submucosa, muscularis and the serosa [10, 11]. The lumen of the bladder is lined by a layer of epithelial cells that sit on top of the lamina propria, termed the urothelium [10, 12].

The urothelium is a transitional epithelium consisting of three layers, a bottom layer of small germinating basal cells (5-10 μm), an intermediate layer of pyriform shaped cells (10-25 μm) and a top layer of large hexagonal multinucleate umbrella cells that range from 25-250 μm across, depending on how full or empty the bladder is (Figure 1.1) [13]. Each layer of the urothelium is generated continuously from the layer below; the umbrella cells are formed from the cell to cell fusion of intermediate cells and intermediate cells arise from the fusion of basal cells [10, 13].

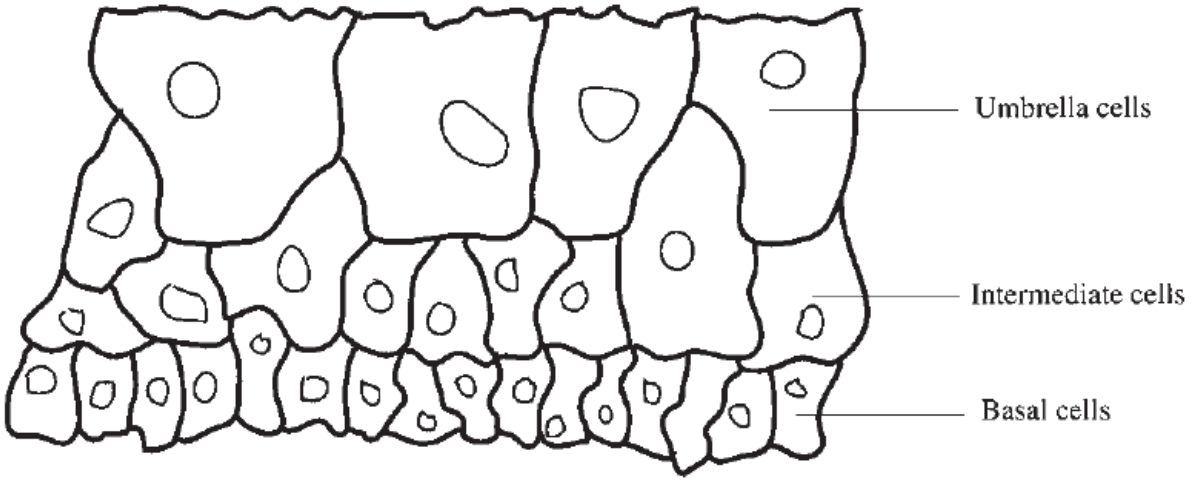

FIGURE 1.1: Diagram of the three cell layers that make up the urothelium of the urinary bladder: lower basal cells, intermediate cells, and upper umbrella cells [10].

The umbrella cells possess an asymmetric unit membrane (AUM). That is, the outer leaflet of the plasma membrane appears twice a thick as the inner leaflet (Figure 1.2) [10, 13, 14]. The surface of the umbrella cells consist of plaques that are separated by plasma membrane domains called hinges (Figure 1.2) [10, 13, 14]. The plaques are made up of proteins called uroplakins (UP), of which there are five types: UPIa, UPIb, UPII, UPIIIa and UPIIIb [13]. UPIa and UPIb cross the plasma membrane four times and are known as the tetra-span family members, while UPII, UPIIIa and UPIIIb are type I single-span proteins [13]. The role of the plaques has not yet been fully elucidated; however, it is thought that they have a role in the permeability of the bladder wall [13]. When bacteria invade the urinary tract, they may bind to the uroplakins UPIa and UPIb on the surface of the umbrella cells [13, 15].

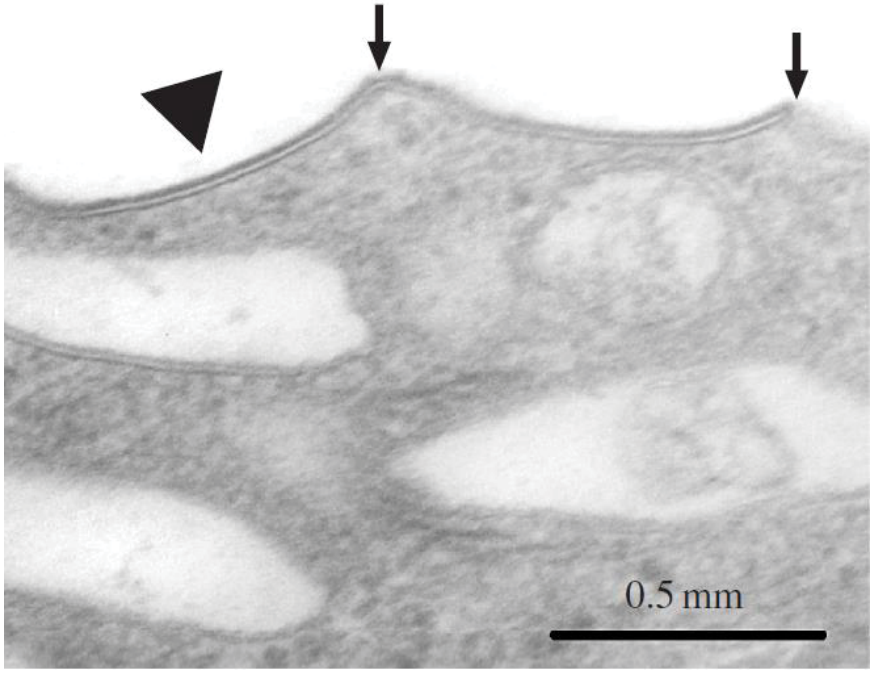

FIGURE 1.2: Transmission electron micrograph showing the umbrella cells of a rat urinary bladder, the hinge regions are indicated by the arrows, whereas the arrowhead indicates a plaque with an asymmetric unit membrane [13].

1.3 UROPATHOGENIC *ESCHERICHIA COLI* (UPEC)

There are many strains of *E. coli* that range from harmless intestinal commensal strains to severely pathogenic strains that can cause very serious disease in animals and humans. UPEC is one such pathogenic strain that causes a high health burden and yet there remains a lack of detailed knowledge about some of the underlying mechanisms involved in this infection process.

UPEC is the predominant cause of UTIs, responsible for more than 85 % of cases [16]. It is classified as a type of extraintestinal pathogenic *E. coli* (ExPEC), which include all strains that can cause infection outside the gut [17]. UPEC has evolved to colonise the urinary tract, invade host cells, suppress and evade the immune system whilst obtaining much-needed nutrients, such as iron [17]. These adaptations include so-called virulence factors, components of pathogens that contribute to damaging the host during infection, such as flagella, adhesins, toxins and iron acquisition systems [18], or physical adaptations such as morphological changes. Virulence factors are typically encoded in the genome on what is known as a pathogenicity island, which is a block of adjoining virulence genes, inserted into the core genome, that are not present in commensal strains of *E. coli* [17, 18].

1.3.1 Adaptations of UPEC

UPEC has many associated virulence factors that allow it to survive and cause infection outside the intestine. One such virulence factor is the flagellum, involved in bacterial motility. The flagella assists in the spread of a UTI by allowing the bacteria to ascend the urinary tract into the bladder and kidneys [19].

Another group of virulence factors, mainly associated with the adherence of the bacteria to host bladder cells, are the adhesins. UPEC possess adhesins on the surface of the cell in the form of fibres called pili and fimbriae. These include S pili, Dr family adhesins, P pili and Type 1 pili [20]. Of these, Type 1 pili are the most common amongst UPEC as they specifically bind to bladder epithelial cells [20, 21]. These Type 1 pili are comprised of protein subunits encoded by the *fim* genes, *fimA – H* [22]. These pili appear 1-2 μm long and contain two combined fibres with a helical rod 7 nm in thickness made up of more than 1000 repeating FimA subunits (Figure 1.3) [23-26]. This is connected to a 3

nm wide distal tip structure which contains two adaptor proteins FimF and FimG and then the tip adhesin FimH (Figure 1.3) [23-26].

The pili form through a chaperone-usher pathway, where the usher anchors the pili to the outer membrane and the chaperone FimC recruits the subunits to the growing pili [23]. The usher comprises the transmembrane pore domain FimD, two C-terminal domains, plug domain and an N-terminal domain, all of which work together to form the pilus structure [23]. FimB and FimE are regulatory genes, which are responsible for the phase variable expression of the Type 1 pili [22, 27, 28].

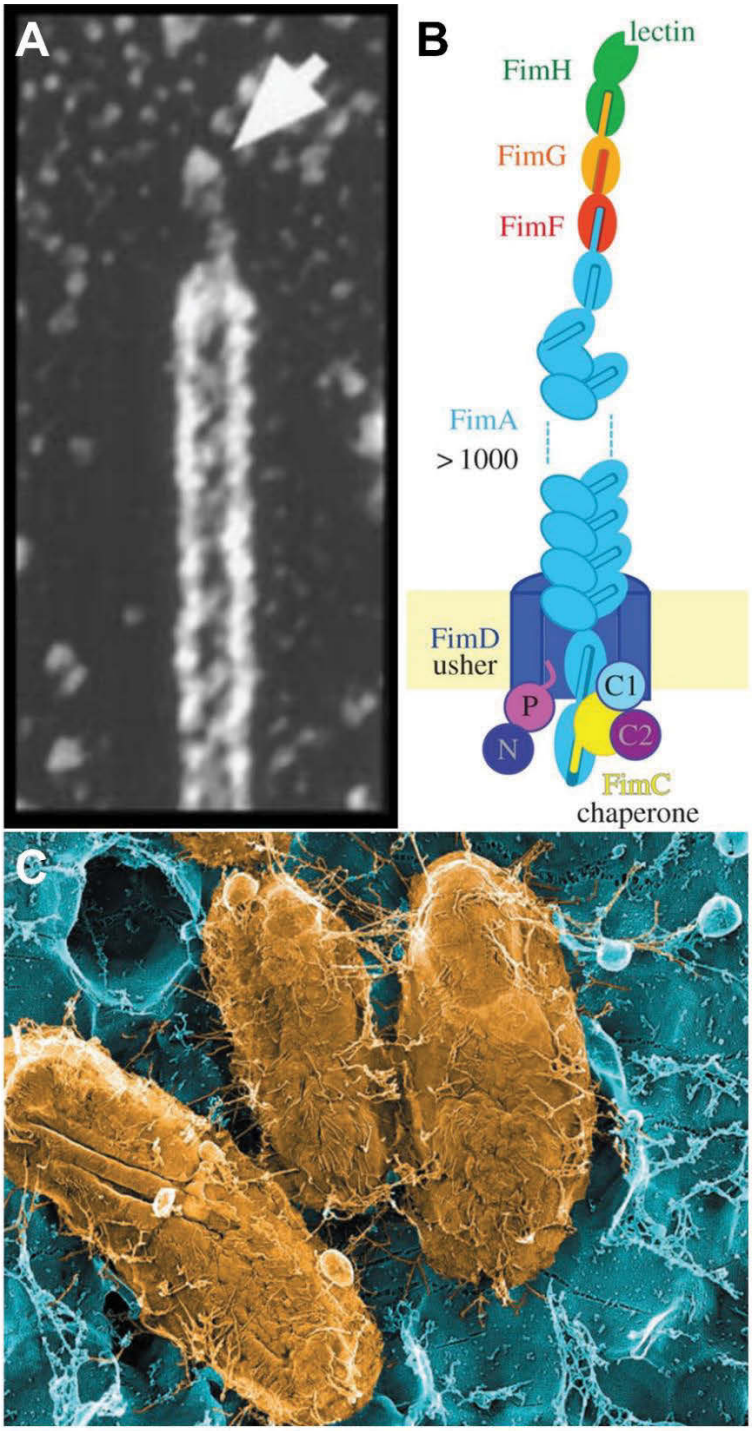

FIGURE 1.3: *E. coli* and the type 1 pili. (A) Electron micrograph of the structure of the type 1 pili, FimH adhesin is indicated by the arrow [20]. (B) Schematic diagram showing the assembly of type 1 pili [23]. (C) Electron micrograph showing *E. coli* (yellow) attaching to the bladder epithelial cells (blue) and the fibrous projections that are the pili [20].

Another feature of UPEC that contributes to virulence relates to the ability for UPEC to form biofilms, which is thought to be one essential component of persistent infection by this organism. A biofilm is an organised bacterial community encased within a self-made matrix, adherent to a natural or artificial surface [29]. Biofilms have been associated with many chronic bacterial infections and have been observed in a wide range of bacteria including *Pseudomonas aeruginosa* and *Staphylococcus aureus* [29]. Biofilms offer several advantages including increased resistance to antibiotics and the defence mechanisms of the host due to their very low penetrability [29]. Biofilms have also been associated with increased expression of other virulence factors [30]. In the pyelonephritis-causing UPEC strain CFT073, an autotransporter protein called UpaH was found to be involved in biofilm formation, as its deletion from CFT073 was associated with a decreased ability to form biofilms [31]. In addition, it was suggested to provide a survival advantage in colonisation of bladder epithelial cells as the UpaH CFT073 deletion showed a decreased ability to colonise the urinary tract when co-infected with wild type CFT073 [31]. In addition, a cystitis UPEC strain, UTI89, was found to have upregulated genes involved in a range of processes such as iron acquisition, toxin release and motility in an intracellular biofilm [1].

Iron is an essential nutrient for bacterial growth; however is in low abundance in many settings such as the urinary tract. UPEC possess iron acquisition systems that allow them to obtain this essential growth nutrient from the iron limited urinary tract of the host [32]. For example, UPEC implements siderophores, which are small iron-chelating molecules, which carry iron into the bacterial cell through cell surface receptors [33]. Enterobactin is one such siderophore that is expressed by UPEC and has a very high affinity for iron [34]. This outcompetes transferrin, a host iron-binding protein, and sequesters the iron to be used by the bacteria [34].

Bacterial toxins are secreted molecules that improve bacterial growth and survival during infection and cause specific damage to the host. UPEC strains are known to secrete toxins that can cause tissue damage or disrupt the function of the host immune system [21]. UPEC produced toxins can cause the removal of the upper layers of bladder epithelial cells to give UPEC access to underlying cell layers and tissues [35, 36]. One such toxin is α-hemolysin, which is mainly associated with pyelonephritis, and to a lesser extent cystitis [6]. This toxin is able to lyse both blood and host cells, giving the bacteria access to iron stores [36], which can then be sequestered by the siderophores. Toxins can also

allow UPEC to cross mucosal barriers by destroying bladder cells and also impair immune cells [6]. Another toxin that is secreted is cytotoxic necrotising factor 1 (CNF-1), but the actions of this toxin still remain unclear. It has been reported that CNF-1 can induce apoptosis of host cells and promote exfoliation of bladder epithelial cells, as well as suppress phagocytosis [35, 37]. However, a study by Miraglia *et al.* (2007) has shown that this toxin can prevent apoptosis of mammalian cells [38]. Apoptosis involves a complex process with many components, and so it is possible that different cell lines have unique variations of the apoptosis pathway. Therefore, CNF-1 may act differently in these pathways and thus account for different views on the actions of CNF-1. Further research is required to form a clear idea of the actions of CNF-1 on the apoptosis pathway of mammalian cells.

A type of physical adaptation thought to provide a survival advantage, which has been adopted by UPEC and other bacteria, is the ability to change morphology in response to certain factors. It has been observed that UPEC and other bacteria can elongate to many times their typical length, an occurrence known as filamentation. Filamentation has been shown to be a survival mechanism implemented by bacteria in response to various harsh conditions and stresses.

One such example is *Flectobacillus* filamenting in the presence of protists, which prevents the protest from engulfing the bacteria (Figure 1.4) [39]. *Flectobacillus* are susceptible to predation by the protist *Ochromonas*, however become resistant to predation when filamentous [40]. This morphology change was thought to arise from products excreted from *Ochromonas* and not from direct contact [40]. This demonstrated that filamentation could prevent bacteria being phagocytosed by larger cells.

Another example is filamentation occurring in the presence of antibiotics (Figure 1.4) [39]. *Burkholderia pseudomallei* were shown to filament when exposed to the antibiotics ceftazidime, ofloxacin and trimethoprim [41]. Their virulence attenuated in their filamentous form but once the antibiotic was removed, the virulence returned [41]. When *B. pseudomallei* was again exposed to these antibiotics, it was noted that in some cases, the MIC had increased for ofloxacin and some resistance began to emerge against ceftazidime [41]. This demonstrated that adopting a filamentous morphology can assist in survival against current and future antibiotic exposure.

In both examples of filamentation, the bacteria appear to be sensing external molecules, which most likely trigger an internal bacterial pathway that causes them to change morphology and become filamentous.

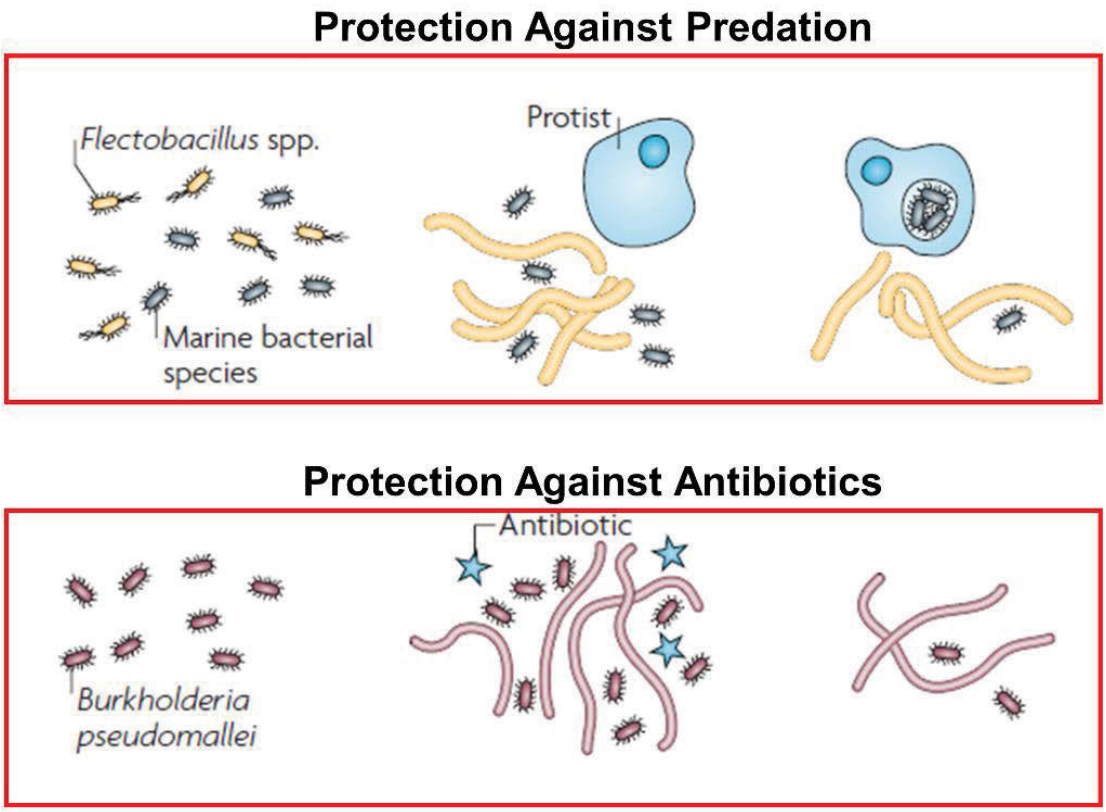

FIGURE 1.4: Examples of different types of bacteria changing their morphology to survive. *Flectobacillus* has elongated in the company of protists to prevent their engulfment, while the rod-shaped bacteria have been consumed. *Burkholderia* has elongated when exposed to an antibiotic, which has successfully killed most of the rod-shaped bacteria. Adapted from [39].

There are also some reasons why it may be advantageous for UPEC to filament in the bladder. One such example is to evade the host immune response. It has been observed that in mice with defective signalling of Toll like Receptor-4 (TLR-4), a host immune sensor of bacterial pathogens, filamentous bacteria were not produced (Figure 1.5) [39, 42]. This proposes that filamentation is a bacterial response to host immunity [39, 42]. Filamentation can also prevent phagocytosis by neutrophils in the same way that *Flectobacillus* survive protist engulfment (Figure 1.5) [42].

Another advantage is the enhanced binding ability of the filaments. As the filaments are longer, they contain more pili, which allows them to bind to the bladder cells on the bladder surface [43]. This prevents the bacteria being removed from the bladder by the flow of the urine and allows them to remain where they can revert to rod-shaped bacteria and continue with the infection [43].

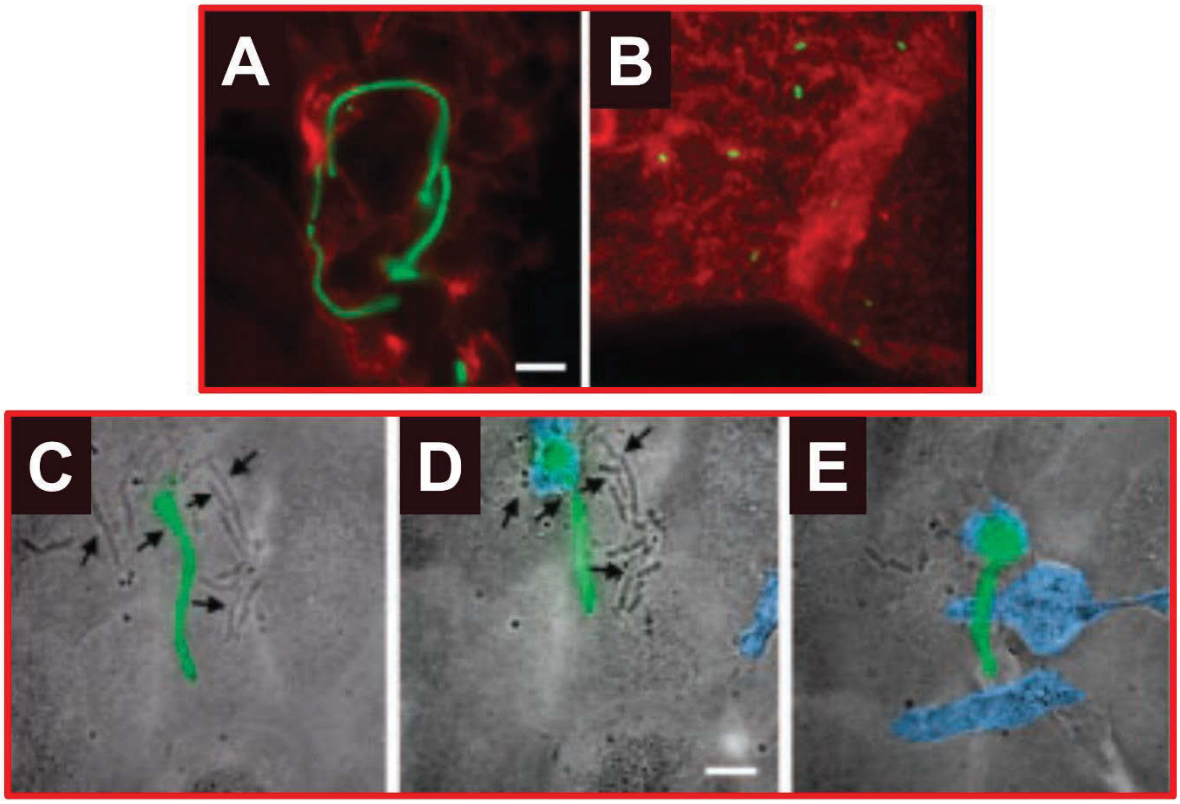

FIGURE 1.5: Filamentation is advantageous for UPEC to survive the urinary tract. Filamentous bacteria (green) were present in wild type mice (A) but were absent in TLR-4 deficient mice (B); (C – E) Neutrophils (blue) were unable to consume the filamentous bacteria (green) but could easily engulf the shorter bacteria (arrows); scale bars = 10 μm; adapted from [42].

1.4 THE INFECTION CYCLE OF UPEC

UPEC infect the urinary tract in a process that has been extensively studied and modelled in mice [1, 42, 44, 45]. A similar occurrence is seen in a human infection [16]. The infection is a multi-stage process that results in colonisation and infection of the urinary tract (Figure 1.6). UPEC bind to the uroplakins on the surface of umbrella cells via their type 1 pili, or through other fimbria-host cell interactions. They are internalised by the umbrella cells where they undergo intracellular replication to form intracellular bacterial communities (Figure 1.6). Infected umbrella cells can also be exfoliated in a host attempt to rid the body of bacteria. In umbrella cells that have not shed, they burst open due to a high bacterial burden and release rod-shaped and filamentous bacteria, capable of reinfecting other urothelial cells (Figure 1.6). Each stage of the infection cycle is described in the following sections.

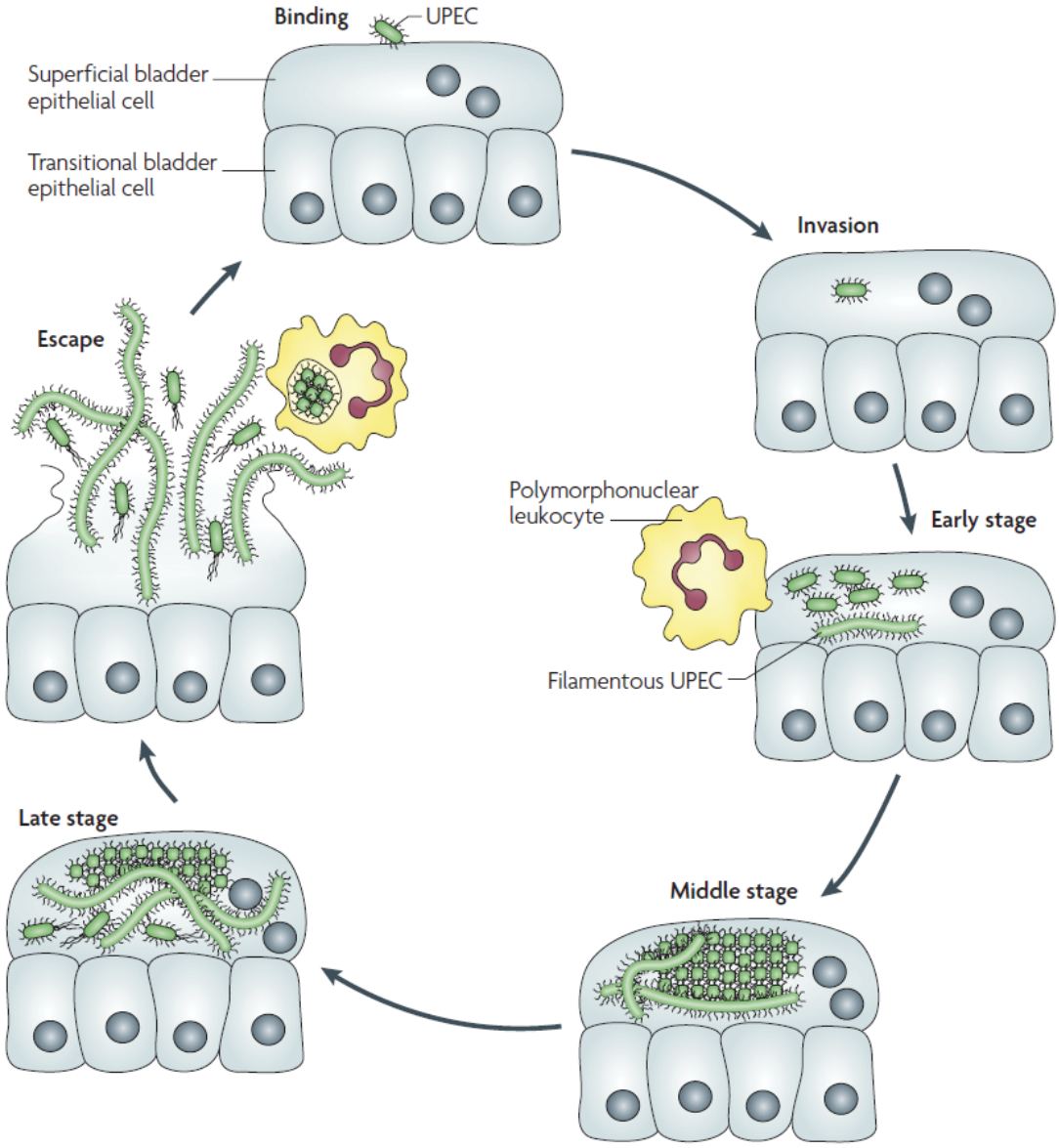

FIGURE 1.6: The infection cycle of UPEC infecting bladder epithelial cells. UPEC bind to the superficial bladder cell and subsequently invade, offering protection against immune cells such as polymorphonuclear leukocytes. The bacteria begin to grow inside the bladder cell to form an intracellular bacterial community (IBC), which undergoes multiple developmental stages beginning with a loosely packed early IBC, followed by an organised middle stage IBC, where some of the bacteria have become coccoid, and ending in a late stage IBC, where a subpopulation of bacteria have become filamentous. The bladder cell ruptures due to a high bacterial burden and the UPEC escape into the bladder lumen, where the infection cycle is reinitiated [39].

1.4.1 Adhesion and Invasion

Adhesion of the UPEC cells to the bladder epithelial cells is the first – and thought to be one of the most important – steps in the infection cycle. It is guided by the virulence factors adhesins and pili, described earlier in Section 1.3.1, located on the bacterial cell surface. Type 1 pili attach to the epithelium via the FimH adhesin (Figure 1.7 A and B), which binds to the uroplakins (UPIa and UPIb) on the surface of the bladder epithelial cells [15, 46]. This initial adhesion stage is one of the most important as it initiates the infection cycle and prevents the removal of the UPEC by the flow of the urine in the bladder [46].

Invasion of the bacteria into the bladder epithelial cells is the next step of the infection and is thought to aid in bacterial survival and development. The AUM of the bladder epithelial cells, described in Section 1.2, has been shown to envelope and internalise the bacteria, described as 'zippering' around the bacterial cell (Figure 1.7 C – E) [20, 47]. The adhesin FimH has also been shown to assist in the invasion of UPEC by stimulating host signals and effector molecules that result in modifications to the cytoskeleton via interactions between FimH and the uroplakins, leading to internalisation of the bacteria [20, 24]. However, an exact mechanism of UPEC invasion has not yet been proven. In this field, this process is widely referred to as invasion, which is an active process driven by the bacteria. However, due to the absence of supporting evidence, this process will be referred to as bacterial internalisation for the remainder of this thesis.

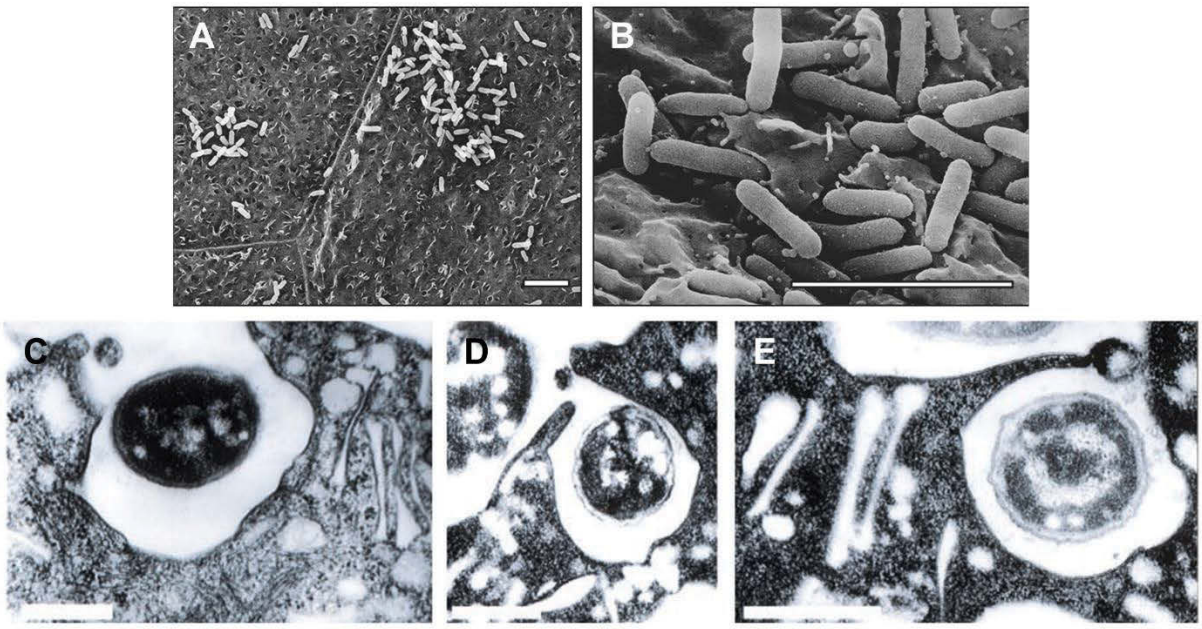

FIGURE 1.7: (A and B) Scanning electron micrographs showing UPEC attaching to umbrella cells; scale bar = 5 μm [47]. (C – E) Transmission electron micrographs showing UPEC at various stages of envelopment by the umbrella cells; scale bar = 0.5 μm [20].

1.4.2 Intracellular Bacterial Communities (IBCs)

Once the UPEC have been internalised by the cells, they begin to proliferate and form what are known as intracellular bacterial communities (IBCs). These appear as organised colonies within the bladder epithelial cells that possess biofilm-like properties [42, 44, 45]. This ability to form biofilms is another virulence factor, as described in Section 1.3.1, which aids the bacteria in surviving the bladder environment. These biofilms eventually occupy the majority of the host cell cytoplasm, leading to a distortion of the host cell morphology. IBCs appear as a globular shape containing tightly packed coccoid bacteria (Figure 1.8 g and h) [1, 42].

IBCs occur between 6 to 24 hours after initial UPEC infection [1]. They express type 1 pili, antigen 43, and secrete a polysaccharide matrix [1]. Antigen 43 is a surface protein responsible for bacterial aggregation by forming a complex with itself on adjacent bacterial cells [48], and is thought to be involved in maintaining an IBC. Type 1 pili have been shown to eliminate the effect of antigen 43 and disperse aggregated cells [48], which could be involved in breaking up an IBC. Several genes have been found to be essential for the formation of IBCs, including *leuX*, *fimH* and *surA*, as well as the up regulation of several iron acquisition systems [1, 49, 50]. Justice *et al.* have observed that UPEC mutants lacking in *surA* are less likely to attach to and be internalised by bladder epithelial cells due to improperly formed type 1 pili, and also have a greatly reduced ability to form IBCs [51], suggesting that pili formation is involved in IBC development.

Bacterial morphology changes have been observed during the different developmental stages of an IBC. In the early stage of an IBC, the UPEC cells appear loosely packed and the bacteria have a typical rod-shaped appearance (Figure 1.8, a – e) [51]. During the middle stage, the bacterial cells have become more organised and tightly packed together, appearing smaller, rounder (coccoid) in shape (Figure 1.8, f – h) [51]. In the late stage, the bacterial cells on the edges of the IBC elongate back to rod shaped cells or progress to form filamentous cells [51].

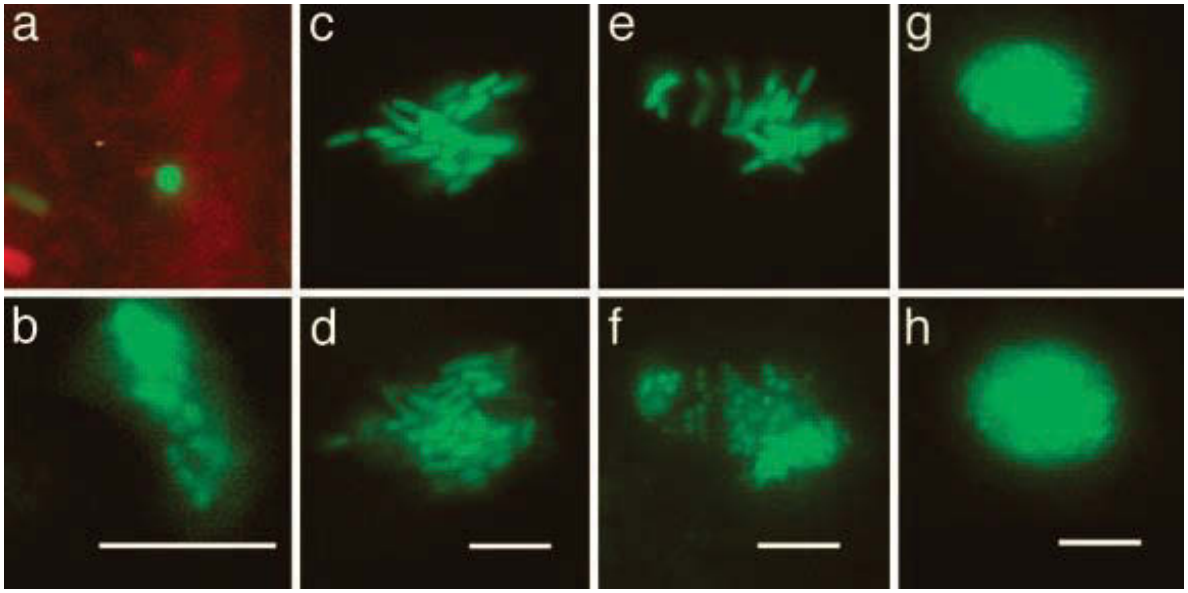

FIGURE 1.8: The development of an IBC using videomicroscopy and fluoresent bacteria; (a) A bacterium (green) is internalised by a bladder epithelial cell (red); (b – d) An early IBC develops within the bladder cell; (e and f) The early IBC progresses to a middle stage IBC with coccoid bacteria; (g and h) The growth of a middle stage IBC; Scale bars = 10 μm; [42].

1.4.3 Escape of UPEC from the Bladder Epithelial Cells

Upon reaching the end of the infection cycle, the bacterial burden overwhelms the bladder epithelial cell and forms protruding pod-like structures. This causes the bladder cell to rupture and release the UPEC into the lumen of the bladder (Figure 1.9) [16]. However, the exact signals that trigger the bladder cell rupture are unknown [42]. During this phase, the rod-shaped bacterial cells are released as well as long filamentous cells (Figure 1.9). The rupturing of bladder cells and release of UPEC was observed to occur asynchronously [42]. This release of a high number of cells allows the UPEC to infect other nearby bladder epithelial cells and re-initiate another infection cycle. This reinitiation of the infection was demonstrated by the presence of small groups of UPEC within other bladder cells that coincided with the rupture of other nearby infected bladder cells [42].

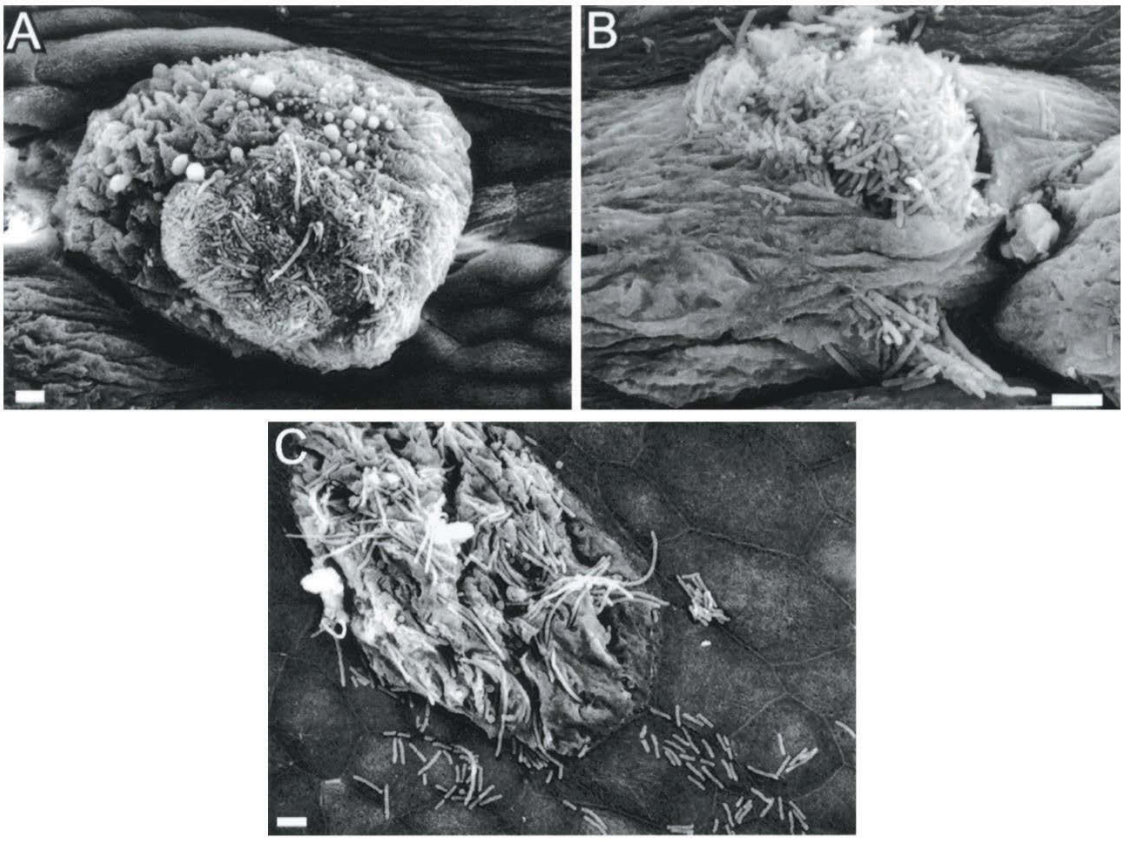

FIGURE 1.9: Scanning electron micrographs showing UPEC rupturing from infected bladder epithelial cells; (A) shows the bladder cell bulging under the incredible burden of a late stage IBC or 'pod', (B) and (C) depict the bladder cell rupturing and releasing the UPEC into the lumen; Scale bars = 5 μm; [44].

1.5 HOW HAVE UTIs BEEN MODELLED?

The infection cycle of UPEC has long been modelled *in vivo* using mice and more recently using *in vitro* cell culture based models. The mouse model involves transurethral injection of bacteria, and then collection of urine or sacrifice of the animal and analysis of the bladder or other organs for evidence of infection. A variation of this model involves taking bladder explants after infection and continuing to monitor the progress of infection on the splayed bladder surface [44]. One main advantage of the mouse model is that the impact of the majority of clinically relevant host environmental factors, such as the various facets of the immune system, can be observed. The main disadvantage of this model is that the mouse infection might not always accurately reflect a human infection. Nevertheless, the mouse model has allowed the reproduction of the main features of infection in humans [16].

Within the last 10 years, *in vitro* infection models have been developed to model the infection cycle of UPEC. These models used immortalised human epithelial cell lines, and while they carry the advantage of a human-derived cell line host, *in vitro* models currently cannot precisely mimic what happens *in vivo*. There are many factors that could play a role in altering the infection *in vivo* that an *in vitro* model would need to try to address. Various improvements to the basic infection *in vitro* have been proposed and developed, including reproduction of the full overall bladder cell infection cycle, which includes IBC dispersal and filamentation, and incorporation of multiple different host and bacterial cells into the same culture system to study the interactions and roles of these differing cell types.

1.6 HOST DEFENCES AND HOW UPEC EVADE THEM

There is a significant arms race between host and pathogen taking place in the bladder. While UPEC possess multiple virulence factors to assist in colonising the urinary tract, multiple defence mechanisms are implemented by the host to combat the infection of UPEC. It appears that for most virulence factors of the bacteria, there is a host defence against it.

1.6.1 UPEC Recognition

The innate immune system uses so-called 'pattern recognition receptors' (PRR) to recognise 'pathogen-associated molecular patterns' (PAMPs) that are unique to invading bacteria [52]. In UPEC, these include the abundant surface features of bacteria: lipopolysaccharide, flagella and type 1 pili [52]. The activation of the immune system by UPEC is thought to commonly involve a type of PRR known as Toll-like receptors (TLR), which recognise structurally conserved components of microorganisms [6]. This recognition leads to the activation of NF-κB signalling, which activates pro-inflammatory mediators like cytokines and chemokines [6], in order to stimulate bacterial clearance by the innate immune system.

There are multiple pathways present that can activate the immune system during a UTI. One of the most studied pathways is the TLR-4 pathway. TLR-4 responds to the lipopolysaccharides on Gram-negative bacteria, activating NF-κB [53]. NF-κB then proceeds to induce the expression of pro-inflammatory molecules, including interleukin-6 (IL-6) , which activate neutrophil signaling and acute phase proteins, and interleukin-8 (IL-8), which recruits neutrophils to the bladder [6, 53]. Alternatively, TLR-4 may induce expression of pro-inflammatory molecules in a pathway independent of NF-κB, by implementing secondary messengers such as calcium and cAMP response element binding (CREB) protein [53]. The presence of these two pathways is thought to be an adaptation by the immune system to prevent UPEC completely dampening the host immune response [53]. TLR-4 is thought to play a role in bacterial filamentation [42, 54]. It was suggested that the filamentation of UPEC is induced as a response to stress by immune components released by the TLR-4 pathway [42]. However, there are other possible interpretations and a full understanding of the role of innate immunity during

UTI awaits a more comprehensive analysis of the role of TLR-4 and other receptor-mediated signaling during the UTI infection cycle in mice and a deeper analysis of the bacterial responses that take place during these infections.

1.6.2 UPEC Evasion of Host Defences

The host benefits from preventing pathogenic bacterial attachment to host surfaces through, for example, pili and adhesins. The flow of urine works as a preventative measure by washing away any unbound or weakly bound bacteria before they have a chance to adhere to and be internalised by any bladder epithelial cells [6]. The urine also has certain properties that can decrease the survival of bacteria including the presence of urea, salts and organic acids as well as having a low pH [6]. The urine also contains various antimicrobial peptides or macromolecules that can prevent bacterial attachment to host cells. One such molecule is the Tamm-Horsfall glycoprotein, which binds to type 1 pili on the surface of UPEC and thus renders the UPEC unable to bind to the host cells [15, 55]. Antimicrobial peptides called defensins also exist in the urine, which bind to the bacterial cell surface and kill bacteria by disrupting their membrane structure [6]. In addition, the urothelium secretes glucosamines, which coat the surface in a mucin layer and help prevent bacterial attachment [6]. Another physical defence mechanism involves the exfoliation and subsequent removal of infected bladder epithelial cells by an apoptosis-like pathway [6].

Internalisation of UPEC into bladder epithelial cells is thought to be a protective mechanism for the bacteria as it helps to shield the bacteria from the phagocytic immune system, and the relative harshness of pure urine, and possibly grants them access to more nutrients need for growth and development. For example, once UPEC attach to the bladder cells, they can overcome the effects of the urine on their Type 1 pili [55]. Type 1 pili remain on the bacterial surface and the UPEC are even able to form more pili as needed [55].

Lactoferrin and lipocalin are other host defences that hinder the UPEC from taking iron from the host. Lactoferrin affects the membrane integrity of bacterial cells and lipocalin 2 binds to the siderophores released by UPEC and prevents them returning iron to the bacterial cells [56]. Lipocalin 2 mainly interacts with the siderophore enterobactin and renders it unable to bind to iron [34]. UPEC can express multiple siderophores aside from enterobactin, such as salmochelin, yersiniabactin and aerobactin, none of which are

recognised by lipocalin [34]. For instance, the *iroA* gene cluster, present within some bacteria, modifies enterobactin by glucosylation to form salmochelin [34, 57, 58].

UPEC strains have also been shown to suppress the capacity of the bladder epithelial cells to produce pro-inflammatory cytokines such as IL-6 and IL-8 [59]. It was hypothesised that UPEC possess surface features that inhibit the TLR-4 pathway including by altering the way LPS or other surface molecules are presented. Although these features are currently unknown, Hunstad *et al.* (2005) have found that when certain genes involved in bacterial surface assembly were mutated, including the *rfa* and *rfb* operons responsible for lipopolysaccharide synthesis and the *surA* gene responsible for outer membrane protein synthesis, the cytokine inhibitory effect was attenuated[59]. This suggested that UPEC have adapted their structure to dampen the host immune response.

It has also been shown that UPEC avoid recognition by PRR early on in an infection by reducing the production of PAMPs on the bacterial cell surface and hence preventing the production of pro-inflammatory molecules [52]. Genes involved in cell surface assembly, including *ampG* and *alr* for peptidoglycan synthesis and *waaL* for LPS synthesis, were shown to aid in the virulence of UPEC [52]. This may grant UPEC sufficient time to be internalised by bladder epithelial cells before the neutrophils have been recruited to the area [52]. This is a clear demonstration that UPEC are capable of slowing down the immune response.

Although alteration of surface structures has been used by UPEC to evade the host defences, there is another less characterised tactic that UPEC appears to use to help in its survival in the bladder and urinary tract environments. This approach involves bacterial filamentation, and relies on modifications in bacterial cell division.

1.7 CELL DIVISION OF BACTERIA

Morphological changes of bacteria have been thought to be advantageous in survival and have been observed in several different types of bacteria [39]. As discussed previously, bacteria have been observed to elongate and become filamentous in multiple examples including UPEC in UTIs; the focus of this thesis was to identify conditions that trigger UPEC filamentation. Filamentation is known to be caused by a block to bacterial cell division, involving constriction and separation, whilst maintaining apparently all other aspects of bacterial growth and elongation. The process of filamentation therefore requires bacteria to sense environmental conditions where a filamentation response is warranted (Section 1.3.1), transducing the signal(s) into the bacterium and bring about the appropriate arrest of cell division.

Rod shaped bacteria divide by the process of binary fission, which involves a constriction in the middle of the cell, known as the division septum, that eventually splits down the middle to form two identical daughter cells [60, 61]. Precise positioning of the division septum ensures that each daughter cell is fully functional [60]. FtsZ is a highly conserved and key bacterial cell division protein that forms a ring structure at mid-cell, which can then contract to separate the cell by cytokinesis [61, 62]. The positioning of the division site in the middle of the bacterium is aided by at least two known systems in *E. coli*: nucleoid occlusion and the Min system [61] (Figure 1.10).

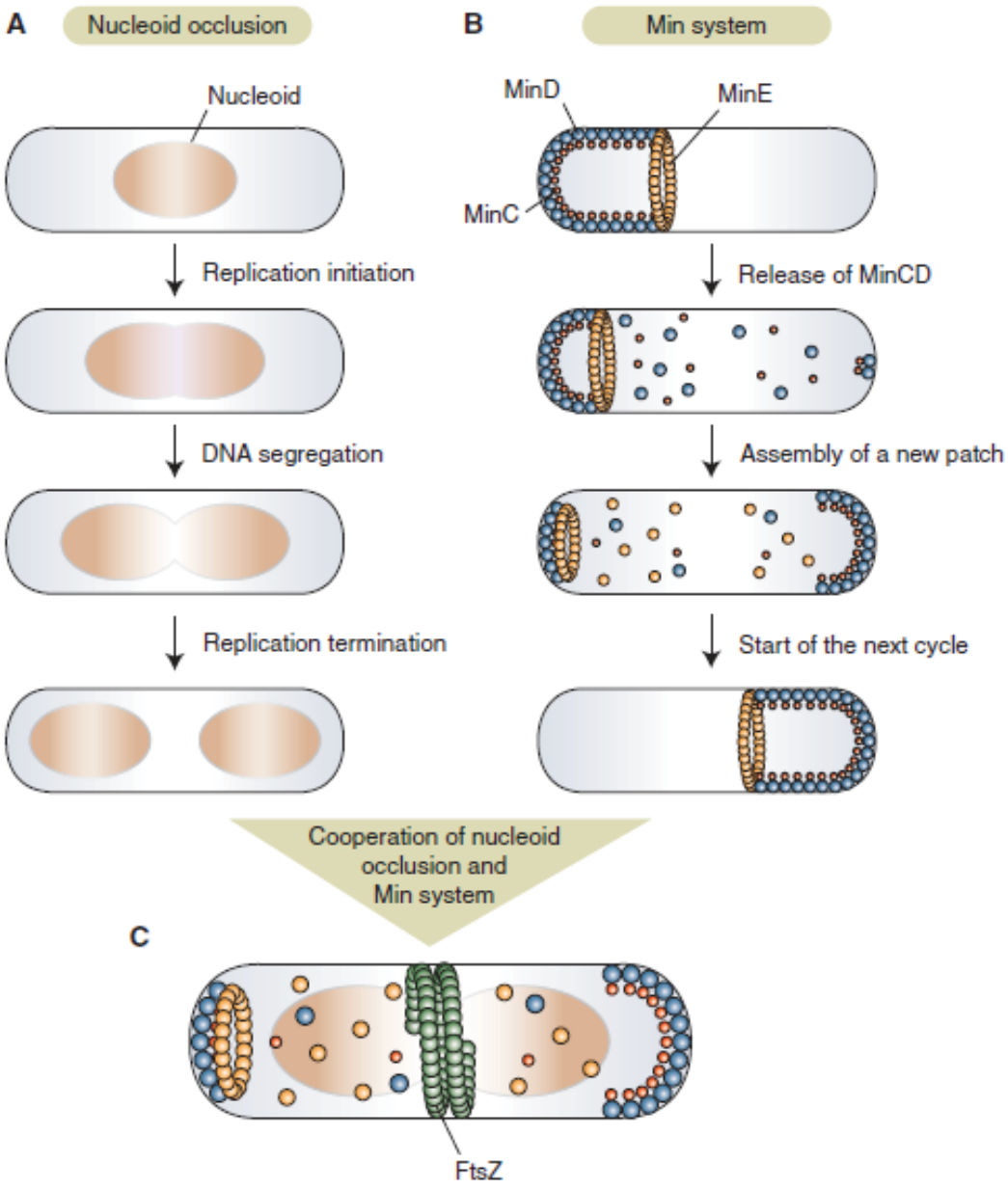

FIGURE 1.10: The two known negative-regulators of cell division: nucleoid occlusion and the Min system, with nucleoid occlusion preventing cell division over the nucleoid, implementing SlmA, and the Min system acting to prevent division near the cell poles through an oscillatory wave; [63].

Nucleoid occlusion ensures that the division septum does not form over any chromosomal content in the bacterial cell (Figure 1.10), helping ensure that the chromosome is not damaged by cytokinesis [64, 65]. Chromosome replication occurs simultaneously with chromosome segregation and many bacteria, such as *E. coli*, have been found to possess their replication mechanism towards the centre of the cell [66]. The origin of replication is replicated first and then both copies of the chromosome move to either pole of the cell, while the terminus remains in the centre before chromosome replication is complete [67]. Once the chromosome is fully replicated and segregated, an area of reduced chromosome content is created in the centre of the cell (Figure 1.10), which allows cell division to occur [62, 65]. Little is known about how cell division is blocked by nucleoid occlusion, however in recent years a DNA binding protein required for nucleoid occlusion called SlmA has been identified in *E. coli* as having a major role [68, 69]. SlmA inhibits cell division over the bacterial chromosome by interacting with both the chromosome and FtsZ directly [68]. Being bound to the chromosome means SlmA is positioned at mid-cell while the chromosome is still replicating. It has been observed that SlmA prevents FtsZ from forming a proper Z-ring [69].

The Min system prevents the Z-ring from forming at the cell poles and thus promotes its formation in the centre of the bacterial cell (Figure 1.10) [70]. In *E. coli*, this involves the interactions between the proteins MinC, MinD and MinE [71, 72]. MinD binds to the inner surface of the cell membrane, dependent on ATP binding, and self-associates there, forming a polymeric sheet that extends towards the cell pole [72, 73]. MinC is recruited by MinD to the membrane, and is the effector protein in this system as it prevents the polymerisation of FtsZ and consequently inhibits Z-ring formation [72]. MinE displaces MinC and causes the hydrolysis of MinD-bound ATP to ADP, which releases MinD from the membrane [73]. The released MinD then binds to the cell membrane on the other cell pole and begins the cycle again, which gives rise to an oscillatory motion between cell poles. The effect of this pattern-forming system is to maintain a higher concentration of MinC at the poles and a lower concentration at the cell centre [73]. This effectively prevents division at the poles.

1.7.1 Filamentation

Bacterial filamentation involves a process where the bacteria cease to divide but continue to grow and elongate becoming many times longer than rod-shaped bacteria [39] (Figure 1.11). In a UTI, these filaments are able to revert into rod-shaped bacteria, capable of re-infecting other bladder epithelial cells [43].

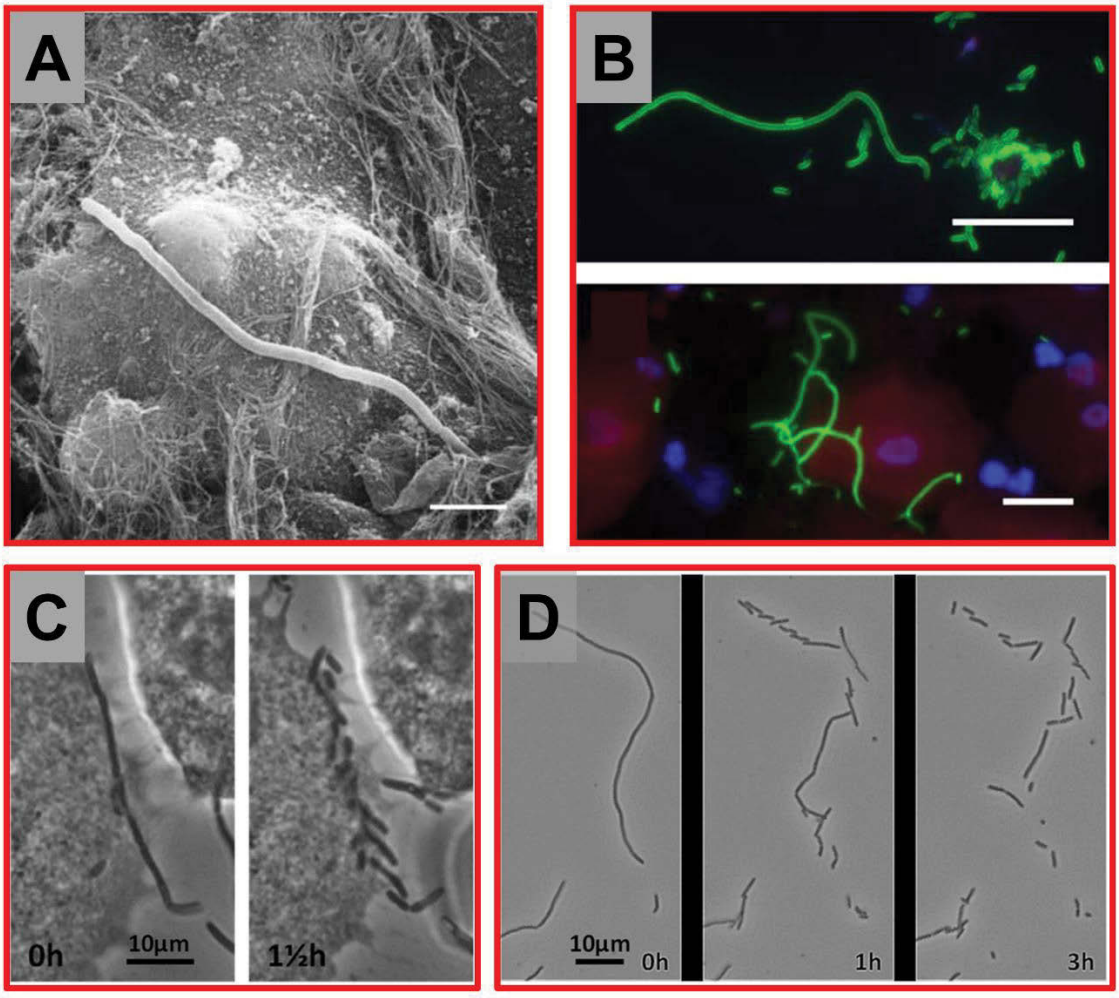

FIGURE 1.11: Microscopy images of bacterial filaments. (A) Scanning electron micrograph of a filament associated with a bladder cell, scale bar = 5 µm [16]; (B) Immunofluorescence microscopy of filaments found in urine samples, scale bars = 20 µm [16]; (C) Filament associated with a bladder cell undergoes reversal [43]; (D) Filament collected from an infection model undergoes reversal [43].

The best characterised pathway of filamentation is due to damage to the DNA, typically caused by UV exposure or oxidative stress, which initiates the so-called SOS response (Figure 1.12). Justice *et al.* (2006) has reported that filamentation occurs due to the SOS response, which normally stops cell division temporarily to allow time for DNA repair and completion of chromosome replication, to prevent any defective DNA being passed onto daughter cells [54]. To initiate the SOS response, the protein RecA, which is activated by the sensing of damaged DNA, induces degradation of the LexA protein [54]. LexA is the repressor of many DNA repair genes and the cell division inhibitor SulA, so without LexA these genes and proteins can go about and fix the DNA while SulA prevents the cell from dividing [54]. The expressed SulA inhibits cell division by binding to FtsZ and inhibiting its polymerisation to form the Z-ring [74, 75]. Therefore, SulA plays a role in filamentation and was therefore hypothesised to play a role in filamentation of UPEC in bladder epithelial cells [54].

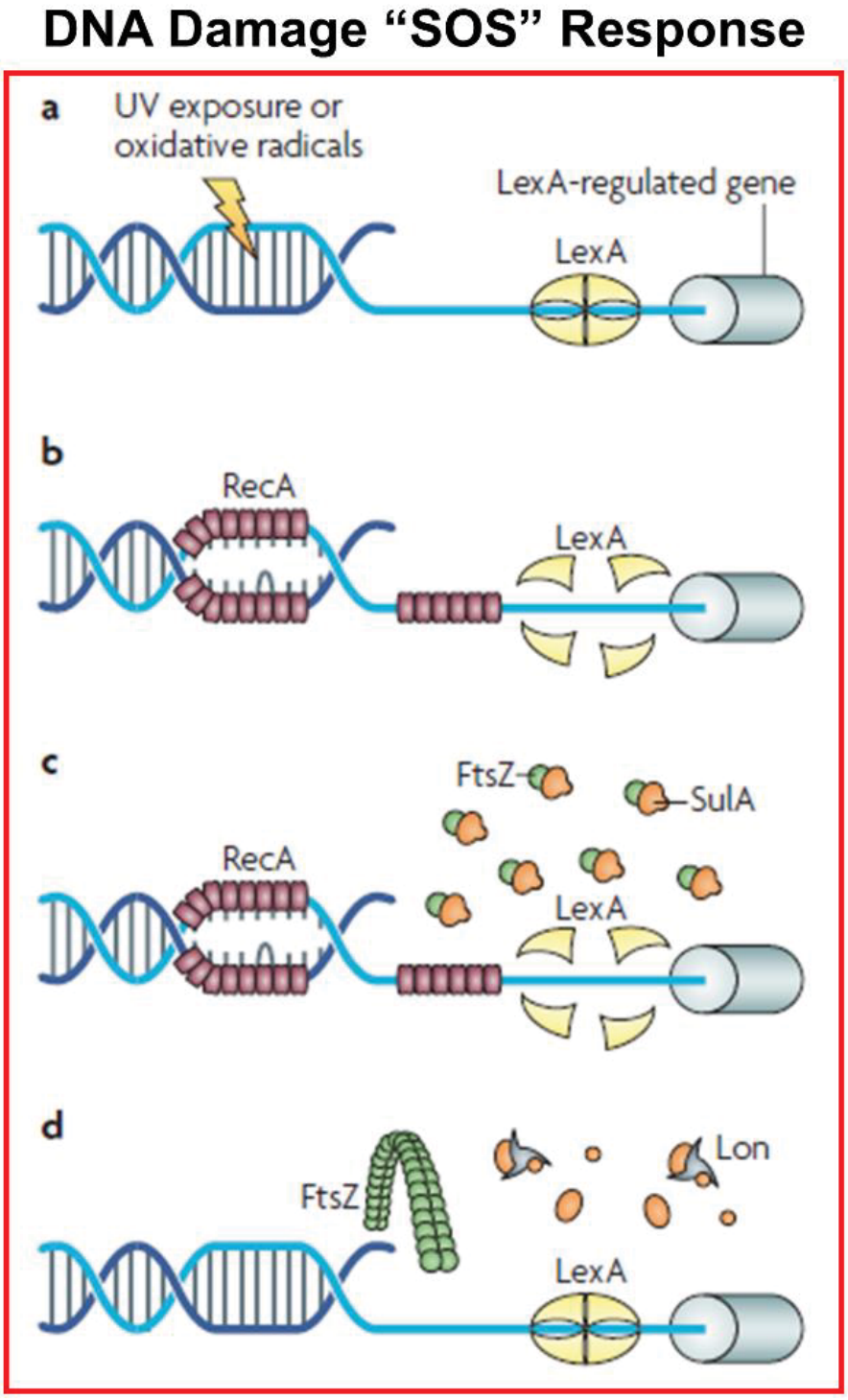

FIGURE 1.12: A diagrammatic representation of the SOS response, which is initiated by RecA binding to damaged DNA and causing the breakdown of the SOS repressor LexA. This allows the downstream proteins, including the cell division inhibitor SulA, to activate and repair the damage. Adapted from [39].

An alternative proposal for the mechanism of filamentation in UTIs involves the *E. coli* gene *damX*. *damX* is a cell division gene that has been shown to localise at the division site and contributes to the cell division process, where it is thought to play a redundant role with *ftsN* [76, 77]. Overexpression of this gene is known to inhibit cell division [76, 77]. Khandige et al. observed that *damX* was overexpressed during the late infection stage where the bacteria adopted the filamentous morphology. They demonstrated that when *damX* was deleted from UTI89, the bacteria were unable to form filaments. Further research showed that an overexpression of *damX* by arabinose induction could induce filamentation and when the overexpression was stopped by glucose suppression, the bacteria began to revert to rods. This demonstrated another pathway by which the filamentous response in bacteria is regulated; however, the underlying conditional triggers and signalling mechanisms remain unknown.

Bacterial filamentation is still a poorly characterised occurrence and there is the need to resolve the apparently conflicting observations of the role of known genes that can cause filamentation, *damX* and *sulA* (SOS). The reasons for filamentation have been suggested and observed [39, 43, 54], however it appears that bacteria only become filamentous under certain conditions. Whether bacterial filamentation in UTIs is a general stress response of many bacteria to conditions experienced in the bladder, or a specific adaptation of certain UPEC strains is still unknown because the mechanism inducing and regulating filamentation is unknown. In a urinary tract infection, the formation of filaments appears to be a crucial part of secondary infection. However, it is not known what triggers these filaments to form towards the end of an infection cycle.

1.8 AIM AND OBJECTIVES

UPEC undergo a multi-stage infection cycle involving many acquired adaptations that have allowed them to be able to cause one of the most successful and persistent infections worldwide. One such adaptation is the ability to change morphology at different stages of their infection cycle. Towards the end of their infection cycle, a subpopulation of bacteria cease cell division and adopt a filamentous morphology. Filamentation appears to be largely advantageous to UPEC and allows this organism to survive and thrive in the bladder. The conditions and mechanisms that trigger and then carry out this response remain unknown.

The overall aim of this thesis was to determine the conditions that trigger bacterial filamentation in UTIs caused by uropathogenic *E. coli*. This aim was broken down into three main objectives. The first two objectives were intended to develop appropriate new tools to help achieve the third objective, which reflected the overall aim.

The first objective intended to determine whether an appropriate method could be established to measure the filamentous response in UPEC. Filamentous bacteria had been previously observed in the infection cycle using both *in vivo* and *in vitro* models, however their formation had not been substantively researched. In this first objective, current *in vitro* bladder infection models were expanded upon and improved in our laboratory to reproduce and quantify bacterial filamentation. In order to investigate filamentation, an appropriate model was required to measure the extent to which the bacteria filamented. Different infection models have been previously established to look at different aspects of the infection cycle. One such model primarily looks at the growth of bacteria within bladder cells and uses bacterial counts to model the first stages of the infection cycle being attachment, internalisation and intracellular growth. Another model uses a flow cell to replicate the later stages of infection and achieve filamentation. These current infection models primarily achieve qualitative data and the expectation was to expand these to also obtain quantitative data.

For the second objective, the goal was to develop a novel method to observe and explore the live progression of the infection cycle and the development of filamentous bacteria. This has not been done before and would provide further insight into when the bacterial filaments are formed and how they emerge from the bladder epithelial cells. It would also

allow real time observations of the entire *in vitro* infection to examine the behaviour of the bladder host cells. This could potentially highlight differences between the *in vitro* and *in vivo* infections and show how well *in vitro* infection models reflect an actual infection in the human body. This model would be optimised for microscopy and could further expand the understanding of the underlying mechanisms involved in infection and filamentation.

The third objective, made possible by achieving the first two objectives, was to investigate the conditions involved in triggering bacterial filamentation. Initially, the involvement of the SOS response was addressed as this had been implicated in many cases of filamentation, as described in Section 1.7.1. Previous studies have suggested that a likely trigger is present in urine itself. Chapter 5 reported the results of investigating the role of different properties of urine to determine the role of urine in inducing filamentation in UPEC.

By achieving these objectives, the conditions that trigger the filamentous response in uropathogenic *E. coli* may be further understood. This could lead to the development of alternative treatments that move away from antibiotics, which suffer from the development of resistance.

CHAPTER 2

GENERAL MATERIALS AND METHODS

2.1 MATERIALS

TABLE 2.1: The list of chemicals, media and antibiotics used and their supplier.

NAME	SUPPLIER
Agarose	Bioline, Australia
Ampicillin	Genlantis, USA
Bacteriological Agar	Oxoid, USA
Calcium chloride	Sigma-Aldrich, USA
Casein hydrolysate	Oxoid, USA
Defined Trypsin Inhibitor	Gibco by Life Technologies, USA
DMEM	Gibco by Life Technologies, USA
DMEM + GlutaMAX	Gibco by Life Technologies, USA
DMEM/F12	Gibco by Life Technologies, USA
EpiLife	Gibco by Life Technologies, USA
FBS	Gibco, USA
Gel Red	Biotium, USA
Gentamicin sulfate	Sigma-Aldrich, USA
Glycerol	Sigma-Aldrich, USA
Human Keratinocyte Growth Supplement (HKGS)	Gibco by Life Technologies, USA
Kanamycin	Sigma-Aldrich, USA
LB	Becton Dickinson, USA
Paraformaldehyde (PFA)	ProSciTech, Australia
PBS Tablets	Astral Scientific, Australia
Penicillin/Streptomycin	Life Technologies, USA
Spectinomycin	Sigma-Aldrich, USA
SYTOX Orange	Thermo Fisher Scientific, USA
Triton X-100	Sigma-Aldrich, USA
Trypsin-EDTA	Gibco by Life Technologies, USA

TABLE 2.2: The list of solutions used and the composition of each.

SOLUTION	COMPOSITION
TAE	40 mM Tris, 20 mM Acetate, 1 mM EDTA, pH 8.6
TBE Buffer	89 mM Tris, 89 mM Boric Acid, 2.5 mM EDTA, pH 8.3
Lysis solution	0.5% (v/v) Typsin-EDTA, 0.1% (v/v) Triton X-100
PBS	1X PBS tablet (137 mM NaCl, 2 mM KCl, 10 mM Phosphate Buffer) in 100 ml ddH_2O
10% Paraformaldehyde	10% (w/v) PFA, 0.01% (v/v) 1M NaOH, ddH_2O

TABLE 2.3: The mammalian cell lines and the *E. coli* strains used throughout this work.

	STRAIN	PHENOTYPE	SOURCE
Mammalian Cell Lines	PD07i	Bladder epithelial cell line	Jakob Moller-Jensen, Denmark; Halbert *et al.* 1991 [78]
	HEK293	Kidney epithelial cell line	Sarah Bajan, UTS; Graham *et al.* 1977 [79]
Bacterial Strains	UTI89	Uropathogenic strain	Jakob Moller-Jensen, Denmark; Mulvey *et al.* 2001 [44]
	MG1655	Non-pathogenic K12	Maurizio Labbate, UTS
	DH5α	Non-pathogenic K12 for cloning	Invitrogen, USA

TABLE 2.4: The media used to grow the mammalian and bacterial cells and their composition.

	MEDIA	PURPOSE	COMPOSITION
Mammalian Growth Media	EpiLife	Grow PD07i cells	EpiLife, 10% (v/v) HKGS, 1% (v/v) PS (Base medium composition as stated in EpiLife Medium Specifications sheet)
	DMEM	Grow HEK293 cells	DMEM, 10% (v/v) FBS, 1% (v/v) PS
	E Medium	Differentiate PD07i cells	DMEM, DMEM/F12, FBS, 0.1 M calcium chloride
Bacterial Growth Media	LB	To grow bacterial cells	1% (w/v) tryptone, 0.5% (w/v) yeast extract, 1% (w/v) NaCl
	SOC	For transforming electro-competent bacteria.	2% (w/v) tryptone, 0.5% (w/v) yeast extract, 10 mM NaCl, 2.5 mM KCl, 10 mM MgCl2, 10mM MgSO4, 20 mM glucose

2.2 METHODS

2.1 Culturing Mammalian Cells

The bladder cell line used in this project was PD07i, which was obtained from a human bladder and immortalised with human papillomavirus type 16 E6E7 [1]. The bladder cells were cultured in EpiLife medium with 60 mM calcium, supplemented with 1% Human Keratinocyte Growth Supplement (HKGS) and 1% Penicillin/Streptomicin (PS).

The kidney cell line used in this project was the human embryonic kidney cells HEK293, which was transformed with Adenovirus type 5 [79]. The kidney cells were cultured in DMEM medium supplemented with 10% fetal bovine serum (FBS) and 1% Penicillin/Streptomicin (PS).

Both cell lines were seeded into a T75 culture flask and left to incubate at 37 ºC with 5 % CO_2 until approximately 80 % confluent (coverage of the base of the culture flask). The media was changed every two days.

2.2 Splitting Mammalian Cells for Continuous Growth in Culture

The media was removed from the flask and the cells were washed once with PBS. Enough 0.5 % Trypsin-EDTA was then added to cover the base of the flask and it was incubated at 37 ºC with 5 % CO_2 for 10 minutes. The plate was tapped gently to release the cells from the surface and then tapped vigourously to remove all remaining cells. A 1x volume of Defined Trypsin Inhibitor was added and the cell suspension was transferred to a centrifuge tube. The tube was centrifuged for 4 minutes at 1000 xg, the supernatant removed and the cell pellet resuspended in PBS.

A small volume (approximately 100 µl) was taken to obtain a cell count per millilitre using a coulter counter. The cells were then centrifuged again as before, the supernatant removed and the pellet then resuspended in EpiLife media to a concentration of 3×10^6 cells/ml.

The cells were dispensed into new T75 culture flasks to continue the culture, or into the appropriate apparatus to undergo an infection with bacteria.

2.3 Preparation of Urine Samples

The work in this thesis relied on concentrated urine, which was achieved by the donor collecting the urine while being in a dehydrated state, having not consumed water for some time, such as first thing in the morning. The urine samples were collected and stored at – 4°C for 2 – 3 days. The samples were centrifuged at 4000 x g for 10 mins to remove any precipitate and debris and passed through a 0.2 μm filter. To measure the concentration of urine, creatinine concentration, osmolality and specific gravity can be used. For the experiments in this thesis, specific gravity was used to determine the concentration of the urine by comparing it to the density of pure water. To ensure that filamentation was successfully induced, the specific gravity of each batch was measured. Only urine with a specific gravity of 1.020 g/ml and higher was used, which also helped to reduce the variability of the urine batches. Although the specific gravity was a simple method to measure concentration, there was a high degree of variability in measurements. Consequently, the determined urine concentrations were not completely accurate but only a close estimation. In some instances, the concentration of the urine was determined to be just below 1.020 g/ml but still managed to induce filamentation. Upon measuring the specific gravity a second time, it was just above 1.020 g/ml. The filter sterilised samples were stored at – 4°C until used.

The complex nature of urine introduced variability into the experiments conducted in this thesis. For an accurate study into the effect of urine on bacterial filamentation, the urine needed to be relatively consistent. By using only a single donor for the majority of this work, this helped to reduce the variability.

2.4 *In Vitro* Flow Cell Infection Model

A volume of 100 µl of PD07i cells at a concentration of 3×10^6 cells/ml was added to an IBIDI flow chamber and incubated overnight at 37 ºC with 5 % CO_2. The flow cell system was set up as shown in Figure 2.1; a media bottle passing through to the bubble trap, which flows on to the flow chamber, peristaltic pump and then into the waste container. The entire setup was placed into an incubator, at 37 ºC with 5 % CO_2, the flow rate was set to 50 µl/min and EpiLife media without antibiotics was pumped through the system overnight. Alongside the flow cell set up, static bacterial cultures of the required strains were set up and incubated at 37 °C overnight.

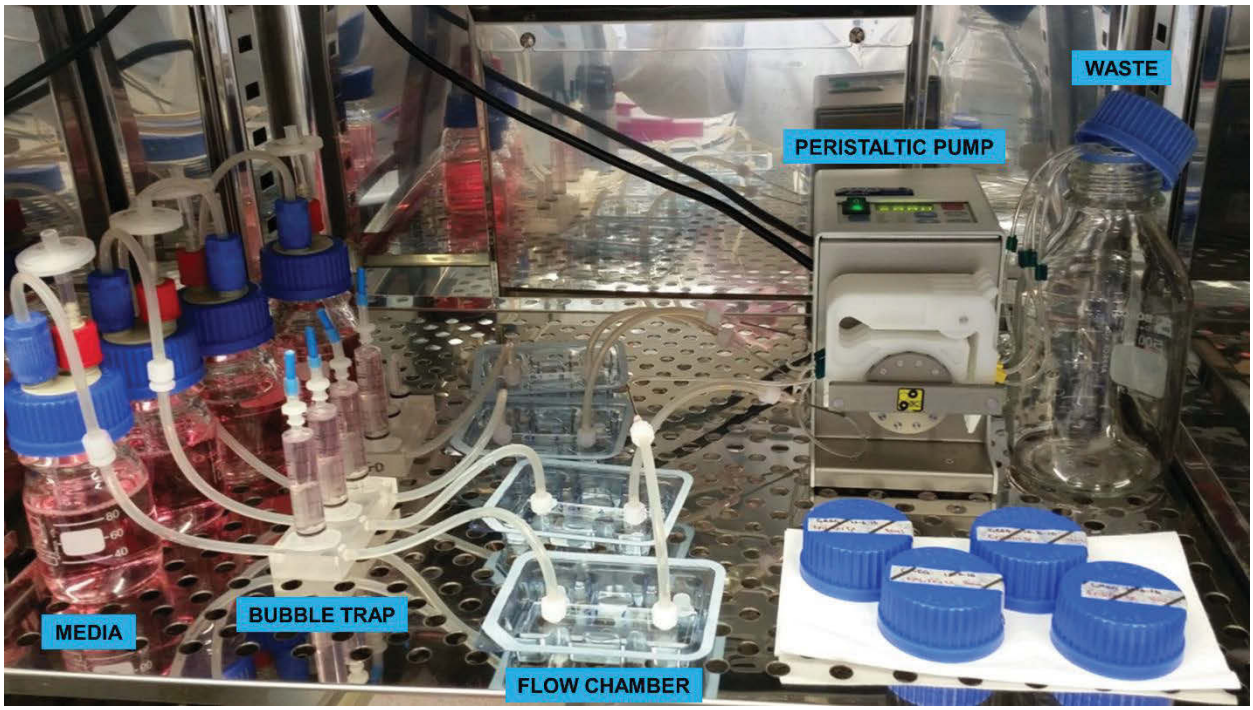

FIGURE 2.1: The setup of the flow cell infection model. The media bottle is connected to a bubble trap, which continues on to the flow chamber. The flow chamber is connected to the peristaltic pump, which pulls the media through and into the waste bottle.

2.4.1 Infection

The bacterial culture was centrifuged and resuspended in PBS to an absorbance (600nm) of 0.2. The flow cell system was stopped and the tubing before the flow chamber was disconnected. Using a pipette, a small piece of tubing was filled with the bacterial suspension and connected to the flow chamber, ensuring no bubbles enter the system. The other end of the tubing was placed in the bacterial suspension and the flow was resumed for 20 mins. The pump was stopped, the small piece of tubing was disconnected, the initial tubing was reconnected and the flow was resumed for 9 hours.

2.4.2 Intracellular Growth

The pump was stopped and all the tubing before the flow chamber was drained and filled with EpiLife media containing 100 µg/ml gentamicin. This new media was flowed through the flow chamber for 20 hours. To harvest the bacteria at this stage, the flow chamber was disconnected and washed three times with PBS. Lysis buffer (200 µl) was then added to the chamber and incubated for 15 mins at 37 °C. The buffer was then removed with a pipette and repeated with another 200 µl of lysis buffer. The lysis buffer was pooled together, centrifuged at 5000 xg for 5 mins and the pellet was resuspended in 2% paraformaldehyde and stored at 4 °C.

2.4.3 Egress and Filamentation

The pump was stopped and the tubing before the flow chamber was drained, washed out with sterile water to remove the gentamicin and then filled with concentrated urine (Section 2.3). The urine was allowed to flow through the chamber for another 20 hours. To harvest the bacteria, the flow chamber was disconnected and the supernatant removed using a pipette into a 1.5 ml centrifuge tube. PBS (200 µl) was then added to the chamber, pipetted back and forth and then removed and pooled with the supernatant. The bacteria were centrifuged at 5000 xg for 5 mins and the pellet was resuspended in 2% paraformaldehyde and stored at 4 °C.

2.5 Analysis of Bacterial Cell Length

2.5.1 Microscopy

2.5.1.1 Zeiss Microscopy

A 1 % agarose pad was made using PBS and 2 µl of the culture was placed onto the slide. The cells were viewed using a Zeiss Axioplan 2 fluorescence microscope at 100x magnification using a phase contrast PH3 Plan-APOCHROMAT 100x/1.4 Oil objective. For fluorescence microscopy, the FITC or Rhodamine filter blocks were used. Images were taken using a Zeiss AxioCam MRm camera and analysed using the software AxioVision Rel (version 4.8) and FIJI.

2.5.1.2 Nikon Ti Microscopy

A 1% agarose pad was made using PBS and 2 µl of the fixed bacterial suspension was placed onto the slide. The bacteria were viewed using a Nikon Ti Epifluorescence microscope at 100x magnification using a Plan Apo λ 100x Oil Ph3 DM objective. For fluorescence microscopy, the GFP, TRITC or TEXAS RED filter sets were used. Images were taken using a Nikon DS-Qi2 camera and analysed using the software FIJI.

2.5.2 Flow Cytometry

In a FACS tube, 200 µl of the fixed bacterial suspension was added along with 300 µl of PBS to dilute the sample. Where a sample was already dilute, only 200 µl of the sample was added to a tube. The samples were run on a BD LSRII flow cytometer and 100000 events were recorded and visualised in real time using the BD FACS software. The parameters that were selected were forward scatter (FSC), side scatter (SSC) and fluorescence (GFP), with the side scatter also set as the threshold. Before the samples were run, a tube containing sterile water was run for 5 mins. After the samples had been run, a tube of 1% bleach was run for 5 mins followed by a tube of FACS rinse and sterile water, each for 5 mins. To further analyse and present the flow cytometry data, FlowJo V.10.1 was used.

2.5.2.1 Quantification of Filamentous Bacteria

This analysis was performed using FlowJo. The histogram of the bacterial population was generated and then gated to distinguish between the short and filamentous bacteria. The "short population" control was the sample known to contain the short bacteria in each experiment, which was gated to contain approximately 99% [80]. To determine the proportion of filamentous bacteria, the histogram was gated from the end of the assumed short population, determined from the control, to estimate the proportion of filamentous bacteria.

CHAPTER 3

ESTABLISHING AN *IN VITRO* CELL CULTURE INFECTION MODEL TO MEASURE BACTERIAL FILAMENTATION

3.1 INTRODUCTION

Mouse models have been used extensively to model UPEC infection of the urinary tract, as thoroughly described in the review by Carey *et al.* 2016 [81], and have successfully characterised the multi-stage infection cycle [42, 45, 82]. These models have shown that UPEC undergo an intracellular lifecycle, as described in Section 1.4, and efflux from the bladder cells, some with a filamentous morphology [44]. Although there was an abundant use of mouse models, the infection cycle had not yet been studied in humans. In 2007, Rosen *et al.* demonstrated the existence of IBCs and filamentous bacteria, exfoliated from the bladder, in the urine collected from women with cystitis [16]. This was the first example in humans and further strengthened the notion that the mouse models were a reasonably accurate reflection of bladder infection in humans.

Although mouse models are effective at observing *in vivo* infection i.e. within the host environment, they do present with some challenges such as being difficult to undertake and time consuming. Modelling UPEC infection *in vitro*, by using immortalised human bladder cell lines, had been very limited due to the difficulty in reproducing clinically relevant infections. However, a model was developed that looked at the penetration of bacteria into cultured epithelial cells [83]. This model used a gentamicin protection assay, which determined the number of bacteria infecting a population of host (epithelial) cells. Gentamicin is unable to penetrate the epithelial cells, so only the internalised bacteria can survive. This model was used to study many different enteric bacteria using different cell lines, such as *Salmonella* and many types of *E. coli* [83]. Later on, it was used to study the internalisation of the UPEC strain NU14 into the 5637 human bladder epithelial cell line [24, 44]. This progress paved the way for the development of *in vitro* infections that modelled many types of infections, including UTIs and that produced results similar to mouse infection models.

Using this gentamicin protection assay, Berry *et al.* (2009) developed an *in vitro* static bladder cell infection model that proceeded through to the IBC development stage [1]. The IBCs that arose from this model appeared similar in morphology to those reported in the mouse models. This static infection model is performed in multi-well plates and typically uses bacterial colony counting on agar plates to determine the number of bacteria at defined infection stages of bacterial adhesion, internalisation and intracellular growth (IBC stage), representative of what has previously been observed in mouse models.

The initial infection stages (Figure 1.6) have been widely studied using mouse models and the above mentioned static *in vitro* model. However, the later infection stages (Figure 1.6), being bacterial filamentation and release, as well as secondary host cell infection, have not been as well studied. An *in vitro* flow cell model was then established a few years later, by Andersen *et al.* (2012), to model and study these later infection stages [43]. This model is undertaken in a flow chamber that is subjected to a constant flow of media and urine and utilises the gentamicin protection assay, mentioned above. This model was the first to replicate filamentous bacteria *in vitro* allowing further research into this bacterial morphology change, which had not been possible with previous models. This model, like the static model, gave rise to IBCs as shown in the well-established mouse models as well as filamentous bacteria, which were also observed using previous mouse models. Additionally, it was observed that the filamentous bacteria reverted into rods capable of reinitiating the infection cycle [43]. By replicating bacterial filaments, further research can now be conducted into the mechanisms associated with this occurrence.

Both of these static and flow cell *in vitro* models have used the immortalised bladder epithelial cell line PD07i [1, 43], and this cell line was used for all the work conducted in this thesis. This epithelial cell line has been widely used and closely resembles the intermediate bladder cells found in the wall of the bladder (Figure 1.1). PD07i epithelial cells were derived from paediatric human bladder cells and were transfected with the human papillomavirus type 16 E6E7 [78]. The human origin of this cell line provides an advantage over using mouse models as they are relevant for human infections and eliminate the need to use lab animals for experimentation.

To begin to investigate the triggers of bacterial filamentation in a UTI, an appropriate model was required to quantify this filamentation. Although previously established models existed, they were either not designed for filamentation, such as the static model, or not optimised to obtain quantitative data, such as the flow cell model. Therefore, the aim of this chapter was to expand and improve upon the current models to effectively measure bacterial filamentation. By achieving this aim, it would allow further research into the triggers of this morphology change as the degree of filamentation would be clearly observed in response to different factors.

In addition, reproducing the static infection model would allow research to further understand the mechanisms behind the infection cycle. This model has been successfully used to study the role different genes required for IBC development, and can be used to

look at many other potential genes involved in different stages of infection. One such gene is the uncharacterised *ytfB* which was identified in a genetic screening of filamentous *E. coli* [80]. It was shown to have homology to *oapA* in *Haemophilus influenzae*, which is involved in bacterial adherence during infection [84]. Preliminary work had suggested that this gene has the potential to play a role in some part of the infection cycle of UPEC and was performed in collaboration with Dr. Amy Bottomley.

Fluorescent bacterial strains have been used in many other studies to visualise the bacteria in an infection setting. Bladder epithelial cells are very complex and contain many organelles, therefore making it difficult to distinguish the infecting bacteria. By adding a GFP-expression plasmid to the bacteria, they can be easily differentiated from the internal structures of the host cell, allowing their morphology and behaviour to be observed. This chapter also described the development of fluorescent *E. coli* strains of UTI89 (UPEC) and MG1655 (non-pathogenic) that were optimised for inclusion in the infection models. The use of well-known fluorescent plasmids and the development of a new fluorescent plasmid were addressed that lead to the development of fluorescent *E. coli* ideal to discern the bacteria during the infection cycle.

3.2 MATERIALS AND METHODS

3.2.1 Static Infection of PD07i Bladder Cells with UTI89

A volume of 1 ml of PD07i bladder epithelial cells at a concentration of 1×10^5 cells/ml was seeded into 24-well plates (Section 2.2) and incubated for 2 days at 37 ºC with 5 % CO_2. 5 ml of LB broth was inoculated with UTI89 or MG1655 and grown statically overnight at 37 ºC.

On the day of the infection, the PD07i cells were washed with PBS three times to remove all traces of the Penicillin/Streptomycin antibiotic. EpiLife + HKGS was then added at a volume of 4 µl/mm^2. The static *E. coli* cultures (UTI89 and MG1655) were gently resuspended. The *E. coli* culture was diluted to 10^9 cells/ml ($A_{600} = 1$). To infect the PD07i cells, 0.1 µl/mm^2 of bacterial culture was added to each well, to give a multiplicity of infection (MOI) of 100. The wells were centrifuged at 600 xg for 5 minutes and incubated statically for 2 hours at 37 ºC with 5 % CO_2.

For an adhesion assay, the media was removed and the wells washed six times with PBS. To lyse the bladder cells, 4 µl/mm^2 lysis solution (Table 2.2) was added to the wells, incubated for 15 mins at 37 ºC with 5 % CO_2 and resuspended by pipetting. The bacteria were plated out onto LB agar and incubated overnight at 37 ºC to determine CFU counts.

For the bacterial internalisation and intracellular growth assays, the EpiLife media was removed and replaced with 4 µl/mm^2 of EpiLife + HKGS + 100 µg/ml Gentamicin. This was incubated statically for 1 hour (internalisation assay) or 24 hours (intracellular growth assay). The media was then removed and the wells washed with PBS four times. The bladder cells were lysed as described previously and the bacteria were plated out onto LB agar and incubated overnight at 37 ºC to count the colonies.

3.2.1.2 Differentiating PD07i Bladder Epithelial Cells

A culture of PD07i bladder epithelial cells were split and seeded into 24-well plates (Section 2.2), and grown to the point of confluence. The EpiLife media was then removed and replaced with E Medium (Table 2.4). The bladder cells were grown for 10 days in E Medium, where the media was replaced every 3 days.

3.2.2 Transformation of Fluorescent Plasmids into *E. coli*

3.2.2.1 Making Electro Competent UTI89 *E. coli* Cells

A 5 ml culture of LB broth (no NaCl) and any relevant antibiotics was inoculated with the bacteria and incubated overnight at 37 ºC at 250 rpm. A 1:50 dilution was then made and the new culture was grown, at 37 ºC at 250 rpm, to an absorbance at 600 nm (A_{600}) between 0.6 – 0.8. The culture was then left on ice for 30 mins before being centrifuged at 4000 xg for 15 mins. The pellet was resuspended in 50 ml of ice cold water and centrifuged as before. This was repeated another two times with decreasing volumes of ice cold water. After the final centrifugation, the pellet was resuspended in ice cold 10% glycerol, aliquoted and snap frozen with liquid nitrogen.

3.2.2.2 Transformation by Electroporation

Electro-competent *E. coli* cells were transformed with the plasmids using the electroporation method based on [85]. In an electroporation cuvette, 40 µl of competent cells (made in section 3.2.2.1) and 1 µl of DNA were mixed and incubated in ice for 1 min. The pulse generator was set to 2.5 µF, 2.5 kV and 200 Ω. The cuvette was placed in the pulse generator and the pulse was applied for a few seconds. Immediately after, 1 ml of SOC media was added to the cuvette and the contents then transferred to a 1 ml centrifuge tube and incubated for 1 hour at 37 ºC at 700 rpm. After the incubation, 100 µl was spread onto an LB agar plate with the appropriate antibiotics and incubate overnight at 37 ºC.

3.2.2.3 Growth of UTI89 *E. coli* Cultures

A 5 ml culture of LB broth was inoculated with a colony and incubated at 37 ºC at 250 rpm for 2 hours. The culture was diluted to an A_{600} of 0.04. The culture with UTI89/pEGFP-AmpR contained 0.5 mM IPTG. The culture was then grown to an A_{600} of 0.4 and a sample taken to observe the bacteria at log phase. To observe the bacteria at stationary phase the culture was allowed to grow overnight where a sample was then taken. Microscopy was then performed to visualise the bacteria (Section 2.5.1.1).

3.2.3 Lambda Red Recombination

3.2.3.1 Constructing the Fluorescence/Kanamycin Cassette

TABLE 3.1: Oligonucleotides used for PCR and sequencing of the Florescence/Kanamycin Resistance cassette. The bold denotes the regions of homology for the primers used to construct the cassettes.

Oligonucleotide	Sequence	Description
GFP_F_lacFtail	TATGTTGTGTGAAATTGTGAGC GAATAACAATTTCACACAGGAT ACAGCT**ATGGTGAGCAAGGGCG AGGAGC**	Amplify the GFP region from the plasmid pEGFP-Amp^R
GFP_R_P1tail	CTTCGAAGCAGCTCCAGCCTAC AC**TTACTTGTACAGCTCGTCCA TGCCG**	
mCh_F_lacFtail	TATGTTGTGTGAAATTGTGAGC GAATAACAATTTCACACAGGAT ACAGCT**ATGGTGAGCAAGGGCG AGGAGGATAAC**	Amplify the mCherry region from the plasmid pRod17
mCh_R_P1tail	CTTCGAAGCAGCTCCAGCCTAC AC**TTACTTGTACAGCTCGTCCA TGCCAC**	
P1	**GTGTAGGCTGGAGCTGCTTCGA AG**	Amplify the kanamycin resistance gene from the plasmid pKD4
P2_lacRtail	AATGGATTTCCTTACGCGAAAT ACGGGCAGACATGGCCTGCCCG GTTATTA**GAATTAGCCATGGTC CATATGAATATCCTCC**	
LacZ_US	GAGTCAGCTCACTCATTAGGCA CC	To check the cassette had inserted itself in the correct location on the chromosome
K1	CAGTCATAGCCGAATAGCCT	Used with LacZ_US to check that the fluorescence and kanamycin resistance products had combined correctly
mCh_5prime_R_seq	TTAACAGAACCCTCCATGTGAA CTT	Used with LacZ_US to check insertion of cassette for mCherry fluorescence
EGFP-N	CGTCGCCGTCCAGCTCGACCAG	Used with LacZ_US to check insertion of cassette for GFP fluorescence

The primers GFP_F_lacFtail and mCh_F_lacFtail contained a complementary region just upstream of the LacZ gene in UTI89 and the primer P2_lacRtail contained a complementary region downstream of the LacZ gene. The primers GFP_R_P1tail and mCh_R_P1tail had a complementary region to the primer P1 to allow the fluorescence products to be joined to the kanamycin resistance gene.

The PCR reactions were set up based on the NEB Phusion High-Fidelity DNA Polymerase protocol. A reaction mixture of 50 µl was made in sterile water containing 10 ng template DNA, 0.5 µM forward and reverse primers, 1× GC Buffer, 200 µM dNTPs, 3% DMSO and 1 unit/50 µl Phusion DNA Polymerase. The thermocycling conditions for the PCR reactions used the NEB Phusion High-Fidelity DNA Polymerase protocol. The products were analysed on a 1 % agarose TBE gel at 150 V for 30 mins.

Overlap extension PCR was used to combine the fluorescence and kanamycin resistance DNA products into one cassette. Both an amplification and non-amplification PCR were run alongside each other. The products were mixed equimolar and added to the reaction mixtures as the template. A 50 µl reaction mixture for both overlap extension PCRs was set up as described above. However, the non-amplification overlap extension PCR did not include any primers and was made up in a solution of the template DNA instead of water. The thermocycling conditions for the PCR reactions used the NEB Phusion High-Fidelity DNA Polymerase protocol. The products were run on a 1% agarose TAE gel at 65 V for 90 mins.

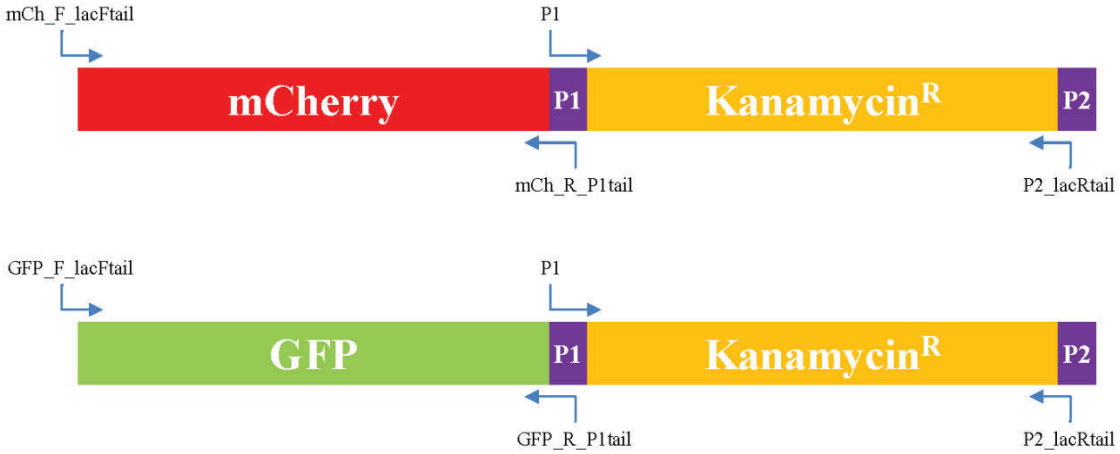

FIGURE 3.1: The structure and primer positions of the fluorescence and Kanamycin^R cassettes.

3.2.3.2 Transforming the Cassette into *E. coli*

Electro-competent UTI89 and MG1655 cells (Section 3.2.2.1) were transformed with the red recombinase expression plasmid pKD46 at 30 °C (Section 3.2.2.2). The newly made UTI89/pKD46 and MG1655/pKD46 were again made electro-competent and transformed with the DNA products from the overlap extension PCR described above, GFP/Km^R and mCh/Km^R.

3.2.3.3 Confirmation of the Cassette Insertion into the *E. coli* Chromosome

Colony PCRs were performed on the new strains to check for the inserted cassette. A colony suspension was made in 50 µl of sterile water and 1 µl of this suspension was used for the 50 µl PCR reaction mixture. The PCR reactions were set up based on the NEB Phusion High-Fidelity DNA Polymerase protocol. A reaction mixture of 50 µl was made in sterile water containing 1 µl of the colony suspension, 0.5 µM forward and reverse primers, 1× GC Buffer, 200 µM dNTPs, 3% DMSO and 1 unit/50 µl Phusion DNA Polymerase. The thermocycling conditions for the PCR reactions used the NEB Phusion High-Fidelity DNA Polymerase protocol. The products were analysed on a 1 % agarose TBE gel at 150 V for 30 mins.

3.2.3.4 Growth of UTI89 *E. coli* Cultures

The bacteria were grown up in cultures as described in Section 3.2.2.3.

3.2.4 Plasmid Construction for Constitutive Fluorescent Expression

3.2.4.1 Constructing the Components of the Plasmids

TABLE 3.2: Oligonucleotides used for PCR and sequencing of the fluorescent plasmids. The bold denotes the regions of homology and the underline denotes the restriction sites.

Oligonucleotide	Sequence	Description
PlacIq_F	GGGCCCGAATTC**GCGGATTTGAACGTTGCG**	Amplify the PlacIq promoter from the plasmid pNDM220
PlacIq_R	GGGCCCGGATCCATTAATTCCCATGG**TCACCACCCTGAATTGACTC**	
msfGFP_F	GGGCCCCCATGG**GTAAAGGTGAAGAACTGTTCACC**	Amplify first half of msfGFP from pDG57
msfGFP_noNco_R	**CCAGAGTCGGCCACGGAACCGGCAGTTTAC**	
msfGFP_R	GGGCCCAGATCTTTAGGATCC**TTTGTAGAGTTCATCCATGCC**	Amplify second half of msfGFP from pDG57
msfGFP_noNco_F	**GTAAACTGCCGGTTCCGTGGCCGACTCTGG**	
PlacI_F	AATTC**GCGCAAAACCTTTCGCGGTATGGCATGATAGCGCCCGGTCTAGAGGAGGTACTA**C	Annealed to create the promoter placI
PlacI_R	CATGG**TAGTACCTCCTCTAGACCGGGCGCTATCATGCCATACCGCGAAAGGTTTTGCGC**G	
PlacIQ_F	AATTC**GTGCAAAACCTTTCGCGGTATGGCATGATAGCGCCCGGTCTAGAGGAGGTACTA**C	Annealed to create the promoter placIQ
PlacIQ_R	CATGG**TAGTACCTCCTCTAGACCGGGCGCTATCATGCCATACCGCGAAAGGTTTTGCAC**G	
PlacIQ1_F	AATTC**TTGACACCACCTTTCGCGGTATGGCATGATAGCGCCCGGTCTAGAGGAGGTACTA**C	Annealed to create the promoter placIQ1
PlacIQ1_R	CATGG**TAGTACCTCCTCTAGACCGGGCGCTATCATGCCATACCGCGAAAGGTGGTGTCAA**G	

The plasmid pDG57 [86] was used to obtain the msfGFP region. This region was PCR amplified (Section 3.2.3.1) in two parts to remove an internal NcoI site using the primers indicated in Table 3.2. The two products were joined using an overlap extension PCR as described in Section 3.2.3.1. The final product was digested with the enzymes BglII and NcoI.

The backbone, consisting of pSC101 and the spectinomycin resistance gene *aadA*, was also taken from pDG57. The plasmid underwent a double digestion in CutSmart buffer with the enzymes BamHI and EcoRI. The plasmid was then subjected to a further digestion with ZraI and the DNA was run on a 1% agarose TBE gel at 100 V for 70 mins to gel purify using the Bioline Isolate II PCR and Gel Kit.

The PlacIq promoter, from the plasmid pNDM220, was PCR amplified (Section 3.2.3.1) using the primers indicated in Table 3.2. The product was then double digested with EcoRI and BamHI and cleaned up using the Bioline Isolate II PCR and Gel Kit.

The other promoters to be tested, placI, placIQ and placIQ1, were made by annealing the primers together, indicated in Table 3.2, to create the sequence flanked by NcoI and EcoRI restriction site overhangs.

3.2.4.2 Assembling the Components of the Plasmids

The backbone and the PlacIq promoter were ligated together using the NEB Ligation Protocol with T4 DNA Ligase. The product was transformed into DH5α *E. coli* cells using heat shock by mixing 1 µl DNA with 100 µl of competent DH5α. The mixture was incubated on ice for 30 mins, placed at 42 °C for 1 min and then back on ice for 2 mins, where 900 µl of LB broth was added. The bacteria were incubated at 37 °C at 250 rpm for 1 hour before being spread onto an LB agar plate with Spectinomycin antibiotic for overnight growth at 37 °C. The plasmid, confirmed with digestion using BamHI and EcoRI and run on a 1% agarose TBE gel at 100 V for 60 mins, was named pGI1.

This new plasmid pGI1 was digested with NcoI and BamHI and ligated to the msfGFP. Electro-competent DH5α (Section 3.2.2.1) was transformed (Section 3.2.2.2) with this newly created plasmid. The plasmid, confirmed with digestion using NcoI and HindIII and run on a 1% agarose TBE gel at 100 V for 60 mins, was named pGI2.

The promoter for pGI2 was replaced with three variants with different expression levels. The plasmid pGI2 was digested with EcoRI and NcoI, ligated to the promoters placI,

placIQ and placIQ1 and transformed into DH5α as detailed above. These new plasmids were named pGI3, pGI4 and pGI5 respectively.

3.2.4.3 Creating Fluorescent Strains of UTI89

Electro-competent UTI89 (Section 3.2.2.1) was transformed (Section 3.2.2.2) with the plasmids pGI3, pGI4 and pGI5. To test the fluorescence, 5 ml cultures of LB broth, of each strain, were inoculated with a colony and incubated at 37 ºC at 250 rpm overnight. The next day a sample was taken and microscopy was performed using the Zeiss microscope (Section 2.5.1.1).

3.3 RESULTS

3.3.1 Replication of the UPEC Infection Cycle

The adhesion stage of infection was the first to be replicated using the static infection model (Section 3.2.1). Using 24-well plates, UTI89 was added to wells containing a monolayer of PD07i bladder cells alongside blank wells to test for any binding of the bacteria directly to the plastic wells. After incubating for 2 hours the wells were washed four times with PBS, the mammalian lysis solution was added and then the bacteria were plated out onto LB agar for counting. Initial adherence assays had a very high number of non-specific binding of the bacteria to the wells (data not shown). This appeared very similar and occasionally overshadowed the counts from the wells with the PD07i monolayer. To combat this, the amount of washes was increased from four to six and the vigour of the washes was also increased. This successfully reduced the non-specific binding. The plate counts still showed a high number of bacteria binding to the wells (Figure 3.2), however the plate counts from the wells with the bladder cell monolayer showed a significantly higher bacterial count than the bacteria only wells, with a p-value of <0.001 (Figure 3.2). This indicated that the bacteria were successfully adhering to the bladder cells. The K-12 *E. coli* strain MG1655 was also tested and the results suggested a very low adhesion count (data not shown). However, this could not be confirmed because the counts were not above the non-specific binding. These results showed that the modified protocol successfully modelled the adhesion stage of the UPEC infection cycle.

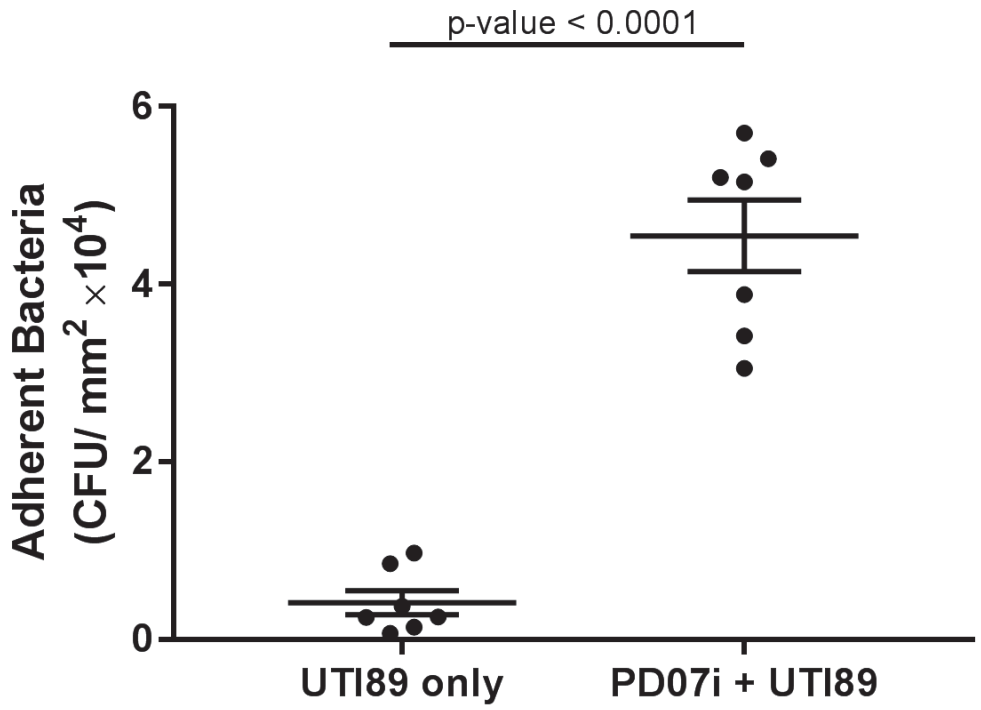

FIGURE 3.2: The number of attaching UTI89 bacteria in 24-well plates. In the presence of a confluent layer of PD07i bladder epithelial cells, there is a significantly higher degree of attachment. N = 7, each is average of n = 3; unpaired t-test showed a p-value <0.0001; error bars are SEM.

The bacterial internalisation and intracellular growth stages were the next to be established, also using 24-well plates. After the 2 hour incubation to allow for bacterial adhesion, the EpiLife media was removed and replaced with EpiLife containing 100 μg/ml of gentamicin to kill all extracellular bacteria. This was allowed to incubate for a further 1 hour to test for internalisation or 24 hours to test for intracellular growth. The wells were washed four times with PBS, the bladder cells lysed and the bacteria plated out onto LB agar. Both MG1655 and UTI89 were tested alongside each other to compare their ability of infect bladder cells.

The expected results would show that the internalisation of the UPEC strain UTI89 would be more efficient and be able to grow internally and colonise the bladder cells unlike the non-pathogenic MG1655. However, these results showed that there was no significant increase in internalised bacteria between MG1655 and UTI89 (p-value = 0.16) (Figure 3.3 blue). The same was also seen for the intracellular growth where a significant increase was not seen (p-value = 0.18) (Figure 3.3 red).

For both strains, a drop in the bacterial count was observed from the internalisation assay to the intracellular growth assay (Figure 3.3). This would be expected for MG1655 due to its non-pathogenic nature, however was unexpected for UTI89. For the intracellular growth assay in Figure 3.3, gentamicin exposure was for 30 hours rather than 22 hours as written in the literature [1]. The notion behind this was that by extending the intracellular growth stage it would have allowed more bacteria to grow inside the bladder cells and thus potentially increased the yield of infecting bacteria. However, as seen in Figure 3.3, this led to a decrease in the bacterial counts from the internalisation stage to the end of the intracellular growth stage. This decrease in number of bacteria after the extended gentamicin exposure may have been due to infected bladder cells rupturing, due to the bacterial burden, and allowing gentamicin into the cell, killing the bacteria before they could be counted. Reducing the time back to the 22 hours may be adequate time for the bacteria to grow intracellularly but not enough time for the bladder cells to rupture. Therefore from the results obtained, this infection model, although successful for modelling adhesion, required further optimisation to successfully reproduce the bacterial internalisation and intracellular growth infection stages.

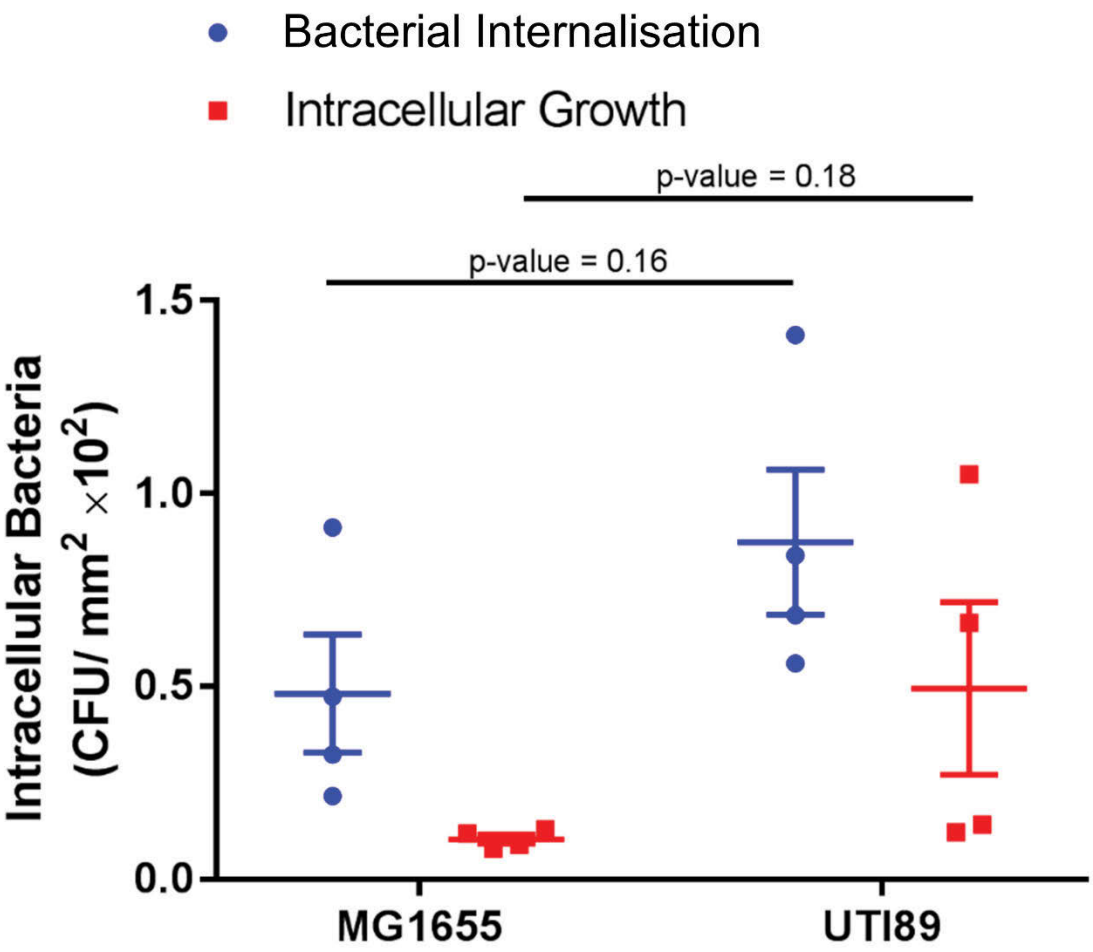

FIGURE 3.3: The number of intracellular bacteria after incubation with EpiLife media containing 100 µg/ml gentamicin for 1 hour (Bacterial Internalisation, blue) and 24 hours (Intracellular Growth, red). There were no significant differences between UTI89 and MG1655 in both infection stages, and there is a drop in the number of bacteria between the internalisation and intracellular growth stages for both strains. N = 4, each is average of n = 12; unpaired t-test to obtain p-values; error bars are SEM.

To attempt to improve upon the static infection model, the PD07i bladder cells were treated to promote their differentiation from intermediate cells towards the fully differentiated umbrella cells, which exist on the bladder surface. The rationale behind this was to improve the infection efficiency and improve the resemblance of the model to what occurs *in vivo*; umbrella cells contain uroplakins, which the UPEC bind to, as described in Section 1.2 [13], whilst intermediate cells have fewer uroplakins [87].

The bladder cells were grown to full confluency and exposed to E Medium (Table 2.4) for 10 days. After the ten days, microscopy images were taken to compare the difference (Figure 3.4). Bacterial internalisation and intracellular growth assays (Section 3.2.1) were then performed using UTI89 as previously mentioned. MG1655 was not used given the preliminary nature of this experiment and to decrease the variables. The bacterial plate counts showed no statistically significant improvements in the internalisation assay or the intracellular growth assay in E Medium exposed cells compared to EpiLife exposed cells (Figure 3.4). This was supported by the p-values as for both the internalisation and intracellular growth assays the p-values were 0.35 and 0.67 respectively (Figure 3.4). Again a high variability was observed, especially in the internalisation assay using E Medium exposed PD07i bladder cells.

The results showed that the infection load did not significantly improve (Figure 3.4), which suggested that the PD07i cells were either as efficiently infected as differentiated cell *in vitro*, or the differentiation medium used (E Medium, including $CaCl_2$) did not result in complete differentiation of these cells. Consistent with this, there have been no previously published observations indicating that differentiating bladder epithelial cells would improve infection events *in vitro*. Although the E Medium exposed cells appeared morphologically different (Figure 3.4), no methods, such as Mass Spectrometry, were used to detect the proper markers used to confirm differentiation such as cytokeratin or uroplakins [87]. A detailed look into this differentiation would be out of the scope of the aim of this experiment, which focused on improving the infection numbers. Microscopy was solely used to determine the effect of the E Medium and searching for the presence of large umbrella cells, of which none were obvious. Therefore, it was possible that the bladder cells were not efficiently differentiated.

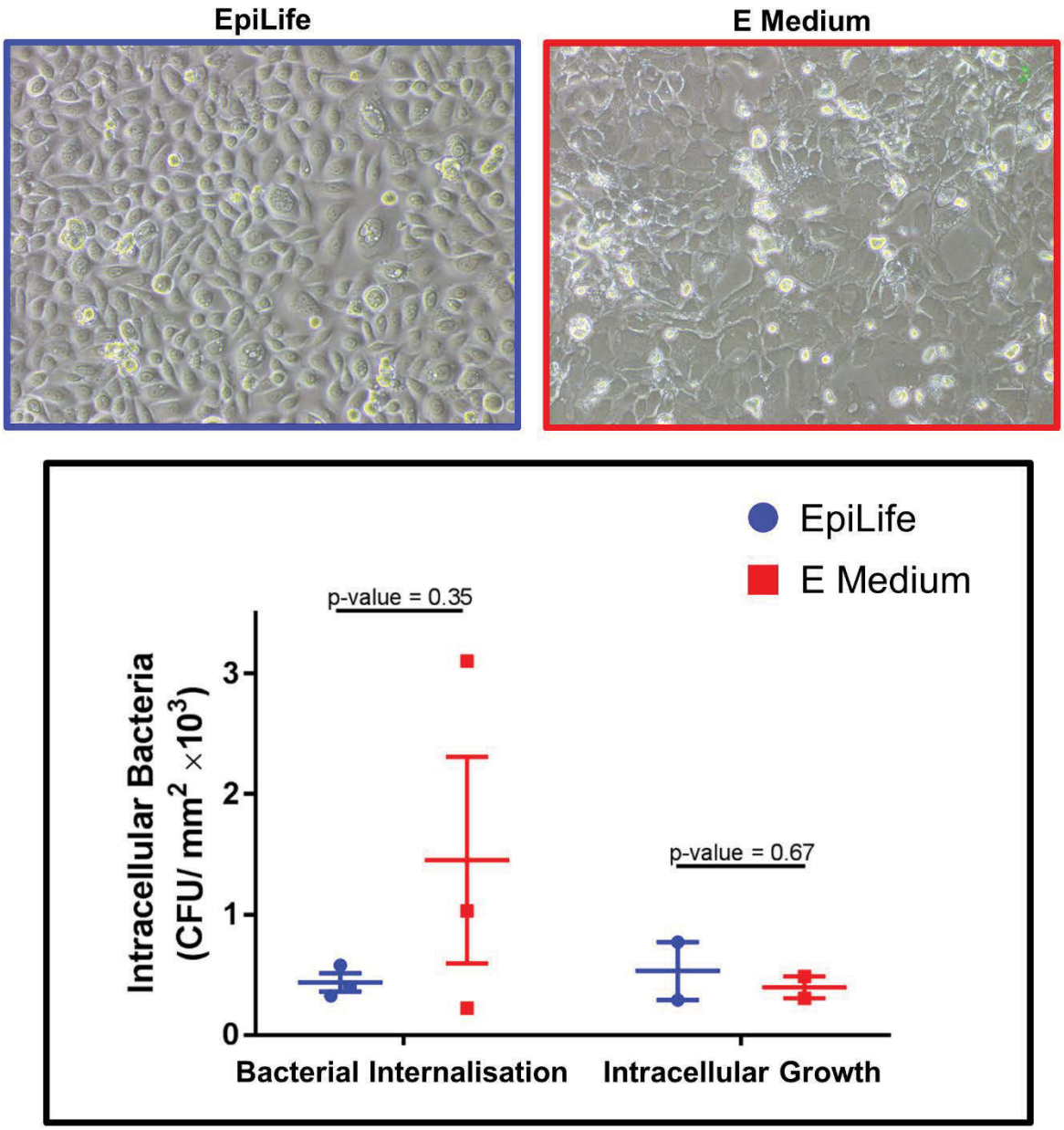

FIGURE 3.4: PD07i bladder cells exposed to EpiLife and E Medium. Microscopy showed a different morphology in PD07i cells exposed to E Medium compared to EpiLife. Bar graph comparing the number of intracellular UTI89 at both the Bacterial Internalisation and Intracellular Growth stages in a static infection using PD07i bladder cells exposed to EpiLife (blue) and E Medium (red). No significant differences were observed. N = 3 for Bacterial Internalisation and N = 2 for Intracellular Growth, each is average of n = 12; unpaired t-test to obtain p-values; error bars are SEM.

3.3.2 Application of the *In vitro* Static Infection Model to Investigate Genes Involved in Infection

The static infection model successfully modelled adherence of bacteria, however due to the problem of outliers, the bacterial internalisation and intracellular growth stages required some further optimisation. Further uses of this model reduced the technical replicates but increased the biological replicates. This reduced the occurrence of outliers and the results appeared more consistent (Figure 3.5).

Potential genes involved in infection have been identified through genetic screens and bioinformatic analysis. The static infection model is an effective tool to investigate the role of these genes, by confirming their role in the infection cycle of UPEC. This would further the understanding of how the bacteria progress through an infection. One such identified gene is *ytfB*, which has an unknown function in UPEC however was identified in a genetic screening of filamentous *E. coli* [80]. Given its homology to an adherence gene in *H. influenzae*, it raised the question as to whether it could be performing a similar role in UPEC infection.

3.3.2.1 The Role of *ytfB* in Infection

The gene *ytfB* was deleted from UTI89 and run through the static *in vitro* infection model alongside wild type UTI89 in 24 well plates. This strain was made by Amy Bottomley from the ithree Institute at UTS. Adherence, internalisation and intracellular growth assays were all used to determine if the deletion possessed the same capabilities as the wild type to progress through the stages of the infection cycle. The results showed that there was no significant difference in bacterial counts between UTI89 and UTI89Δ*ytfB* in the attachment, internalisation or intracellular growth of PD07i bladder cells (Figure 3.5 A, B and C).

To further investigate the role of this gene, the PD07i bladder epithelial cells were replaced with human embryonic kidney (HEK293) cells, as the kidneys are the next site of infection in an ascending UTI. An adherence assay was performed and the bacterial counts for UTI89Δ*ytfB* were shown to be much less than UTI89 suggesting a decreased ability of UTI89Δ*ytfB* to bind to HEK293 cells (Figure 3.5 D).

Therefore, this static infection model can be effectively used to study the function of different genes involved in the infection cycle of UPEC. In addition, this model was shown to work with both bladder and kidney epithelial cells allowing studies into different sites of infection in a UTI.

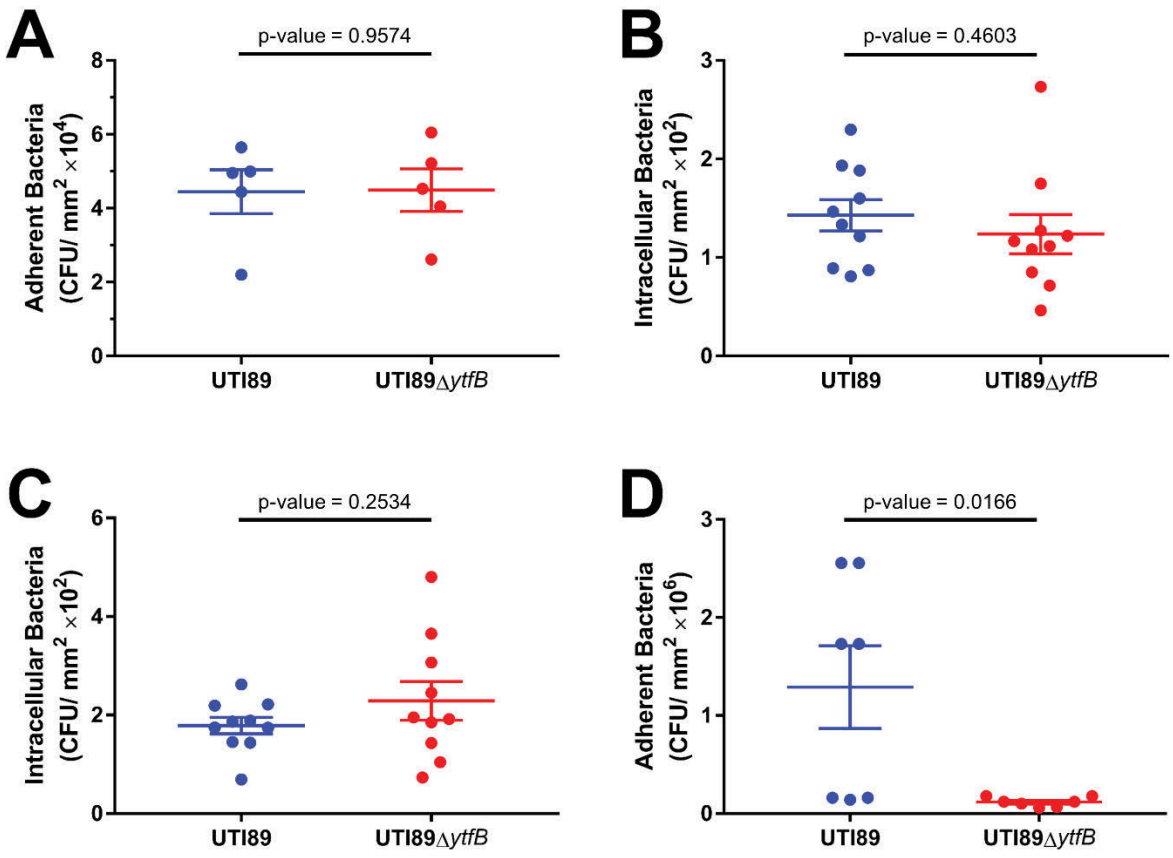

FIGURE 3.5: (A, D) Adherence, (B) Bacterial Internalisation and (C) Intracellular growth assays showing the bacterial counts for UTI89 and UTI89Δ*ytfB* using both PD07i bladder epithelial cells (A, B, C) and HEK293 cells (D). The only significant difference observed was the decreased binding of UTI89Δ*ytfB* to the HEK293 cells (D). N = 5 for (A), N = 10 for (B and C), N = 7 for (D), each is average of n = 2; unpaired t-test to obtain p-values; error bars are SEM.

3.3.3 Visualisation of the Bacteria in the Infection Model

So far, the earlier infection stages of adhesion, bacterial internalisation and intracellular growth have been replicated using plate counts, with adhesion successfully replicated and the other stages requiring further optimisation to reduce variability. However, this method does not accurately reflect what is occurring in the infection cycle. For the intracellular growth phases, plate counts cannot determine the true frequency of infection of individual bladder cells, the morphology of the bacteria or the distribution of bacteria in an infected bladder cell. For example, it cannot differentiate whether there was a large IBC in a single bladder cell or a few bacteria in multiple bladder cells. It would be more useful if the infection could be viewed in real time. Other studies [1, 42, 43, 51, 54] have used fluorescent strains to visualise IBCs and attaching and internalising bacteria, hence using fluorescently labelled bacteria would be a good approach to visualise live bacteria during infection in the *in vitro* infection models, and observe how they change over time.

3.3.3.1 Plasmids for Making Fluorescent Bacteria

Fluorescent strains of UTI89 were initially made by transforming electro-competent *E. coli* UTI89 cells with a plasmid encoding GFP under control of the *lac* promoter, pEGFP (J. Moller-Jensen, unpublished). This plasmid has a high copy number and so bright fluorescence of GFP was expected.

When these strains were grown up to log phase, in LB medium with 0.5mM IPTG, and viewed under the microscope, all of the bacterial cells expressed the GFP and appeared bright green (Figure 3.6). However, when the bacteria reached stationary phase, not all cells appeared green, with only a minor subpopulation showing fluorescence, while the majority of bacterial cells in the field did not (Figure 3.6). This inconsistent and unreliable fluorescence prompted a comparison with another GFP expression plasmid that utilises a different promoter.

Another GFP plasmid, pXG-10 [88], was used and had a low copy number meaning less GFP would be produced resulting in lower fluorescence detected. Upon viewing under the microscope, the fluorescence appeared consistent cell-to-cell, with every cell showing faint green fluorescence (Figure 3.6). However, it was considered too faint and similar to the background fluorescence of the UTI89 wild type that was used as a control (Figure

3.6). Therefore, this plasmid was considered unsuitable for use in an infection, as the bacteria would not be clearly visible.

The first GFP fluorescent plasmid that was tested, pEGFP, was bright (Figure3.6), but appeared to negatively affect the growth of the bacteria (data not shown), and gave a highly heterogeneous fluorescence of cells in the culture. The reason behind the variegated expression was not further investigated, whereas the bacteria may have struggled to grow due to the burden of the high copy number of the GFP expression plasmid. The other plasmid trialled, pXG-10, was not bright enough to be seen above the background fluorescence (Figure 3.6); likely due to the low copy number producing less GFP.

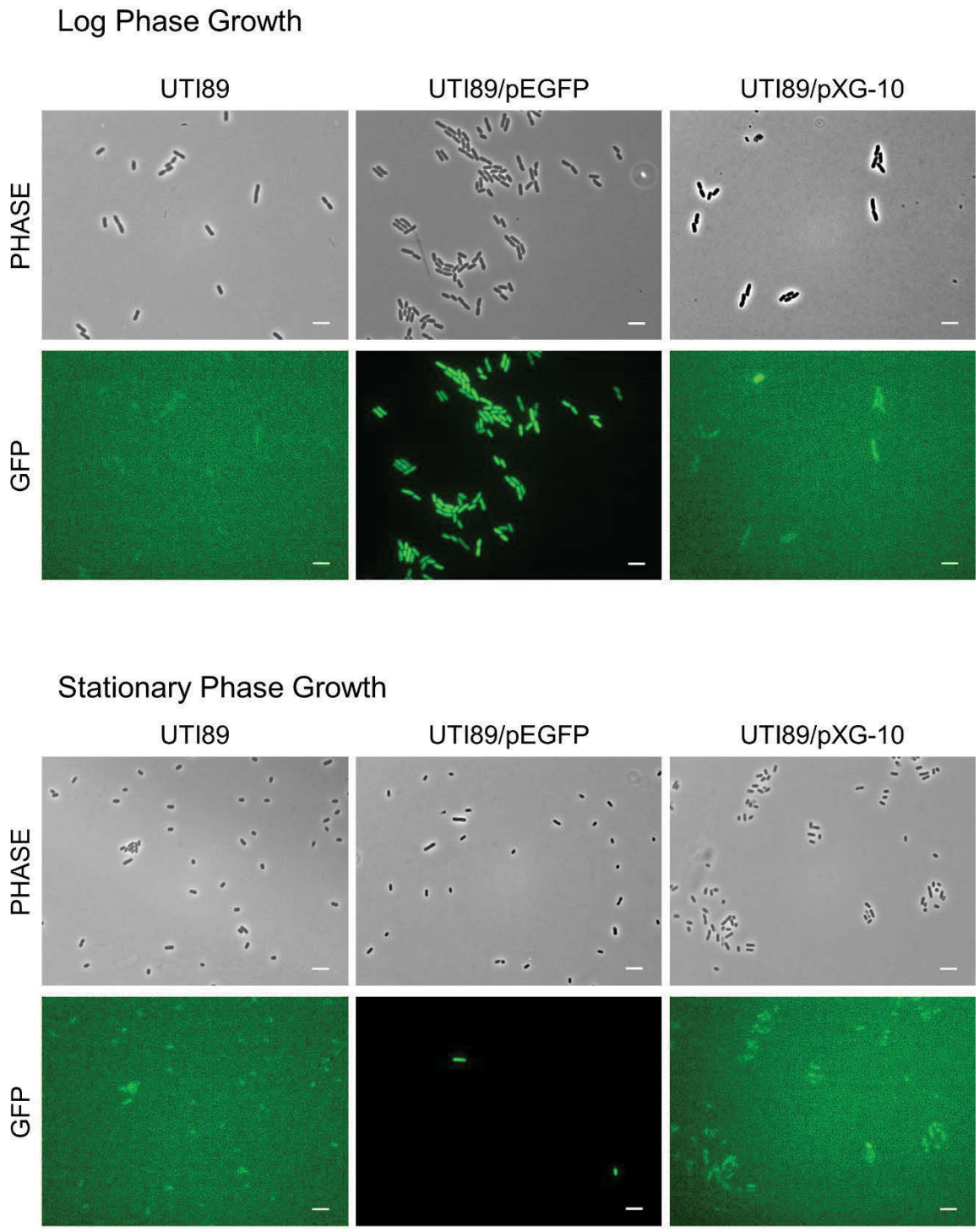

FIGURE 3.6: Phase contrast and fluorescence microscopy showing the GFP fluorescence of the plasmids pEGFP and pXG-10 at both log and stationary phase growth in UTI89. Scale bar is 5 µm, GFP exposure was 500 ms (Section 2.5.1.1).

3.3.3.2 Incorporation of Fluorescent Reporters at Chromosomal LacZ in UTI89

Given the issues encountered with introducing fluorescence on plasmids in the previous section, an attempt was made to insert the fluorescent genes directly onto the *E. coli* chromosome using Lambda Red Recombination. This had been reported to provide a bright and stable location for fluorescence reporters in UPEC (M. Schembri, personal communication). More specifically, the *lacZ* gene was exchanged with a cassette containing a fluorescent gene and the antibiotic resistance marker Kanamycin. This would result in an inducible fluorescence controlled by IPTG. The cassette was created by separately PCR amplifying the fluorescent genes of GFP and mCherry and the Kanamycin resistance gene and joining the fragments using an overlap extension PCR (Section 3.2.3).

Fluorescent strains expressing mCherry were created for both *E. coli* strains MG1655 and UTI89 (Figure 3.7). The strains were grown overnight in the presence of 0.5 mM IPTG and viewed under the microscope. Although it appeared faint, the level of fluorescence did appear above the background levels seen in the wild type for both strains (Figure 3.7). The GFP strains that were created were not fluorescent and after several subsequent attempts, still no GFP fluorescence was detected by microscopy, for reasons unknown, and so the mCherry strains were used.

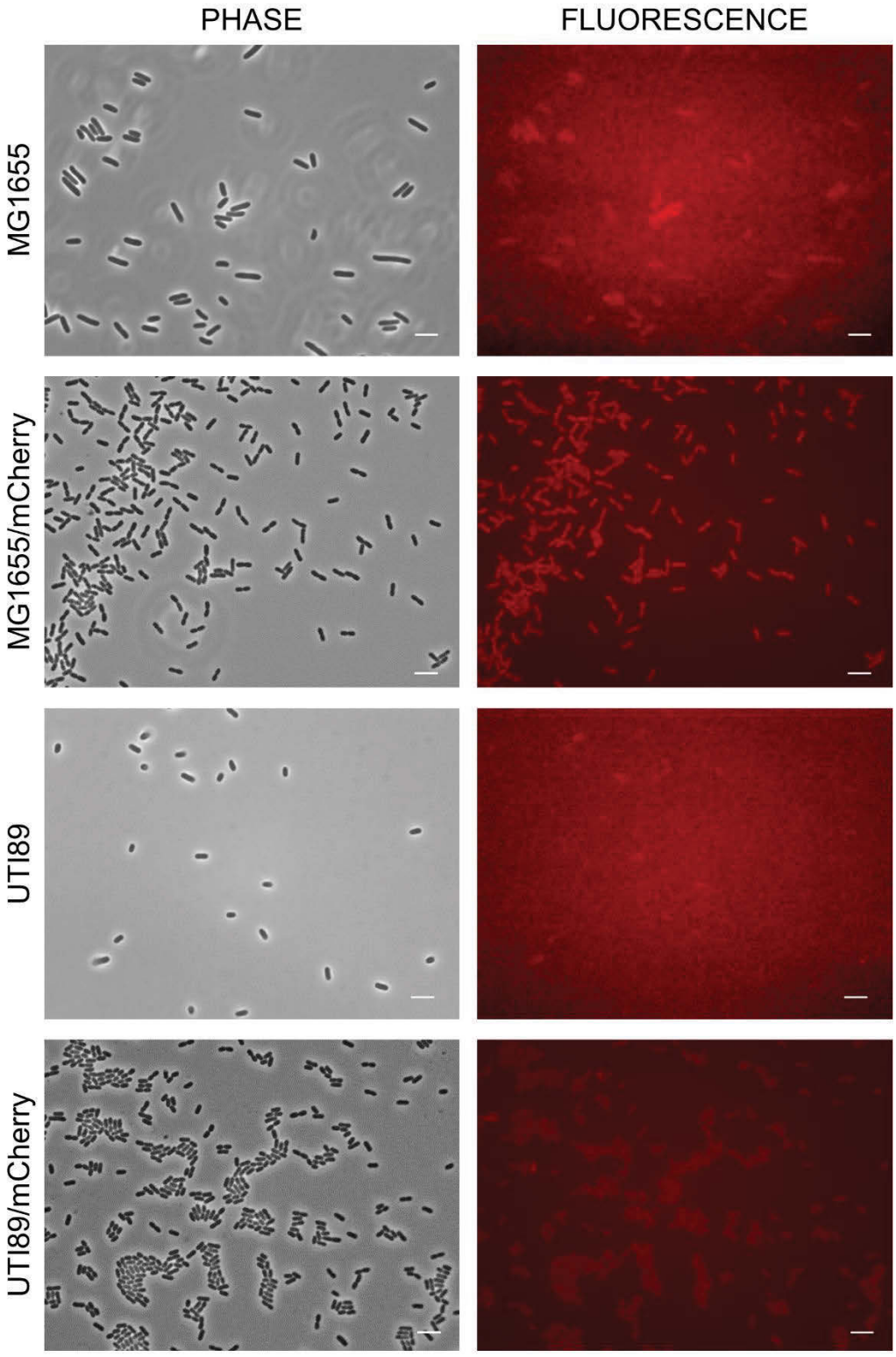

FIGURE 3.7: Phase contrast and fluorescence microscopy comparing wild type MG1655 and UTI89 with the mCherry fluorescent MG1655 and UTI89. The fluorescence appears higher than any auto fluorescence in both strains. Scale bar is 5 µm, TRITC exposure was 2000 ms (Section 2.5.1.1).

The mCherry fluorescence proved successful in visualising the bacteria in the intracellular growth stage using the static infection model; they were clearly visible amongst all of the bladder cells (Figure 3.8). However, with these images, it was difficult to distinguish intracellular and extracellular bacteria. It was also possible to see bacteria binding to the plate (Figure 3.8 blue arrowhead) as well as on the bladder cells. Also potential IBCs appeared visible amongst all the bladder cells, as the bacteria seemed to take the shape of the bladder cell and were grouped together (Figure 3.8). Without this fluorescence it would have been almost impossible to see any bacteria in amongst all of the bladder cells.

Although this fluorescence was successful in visualising UTI89 in the infection, the expression level was still too low as the exposure time was significantly longer. This would not be ideal for microscopy running over an extended time. In addition, the inducible fluorescence could require the addition of more IPTG during the course of the infection process. Therefore, a plasmid with constitutively and highly expressed fluorescence would prove more beneficial to use to monitor the bacteria over the course of the entire infection cycle.

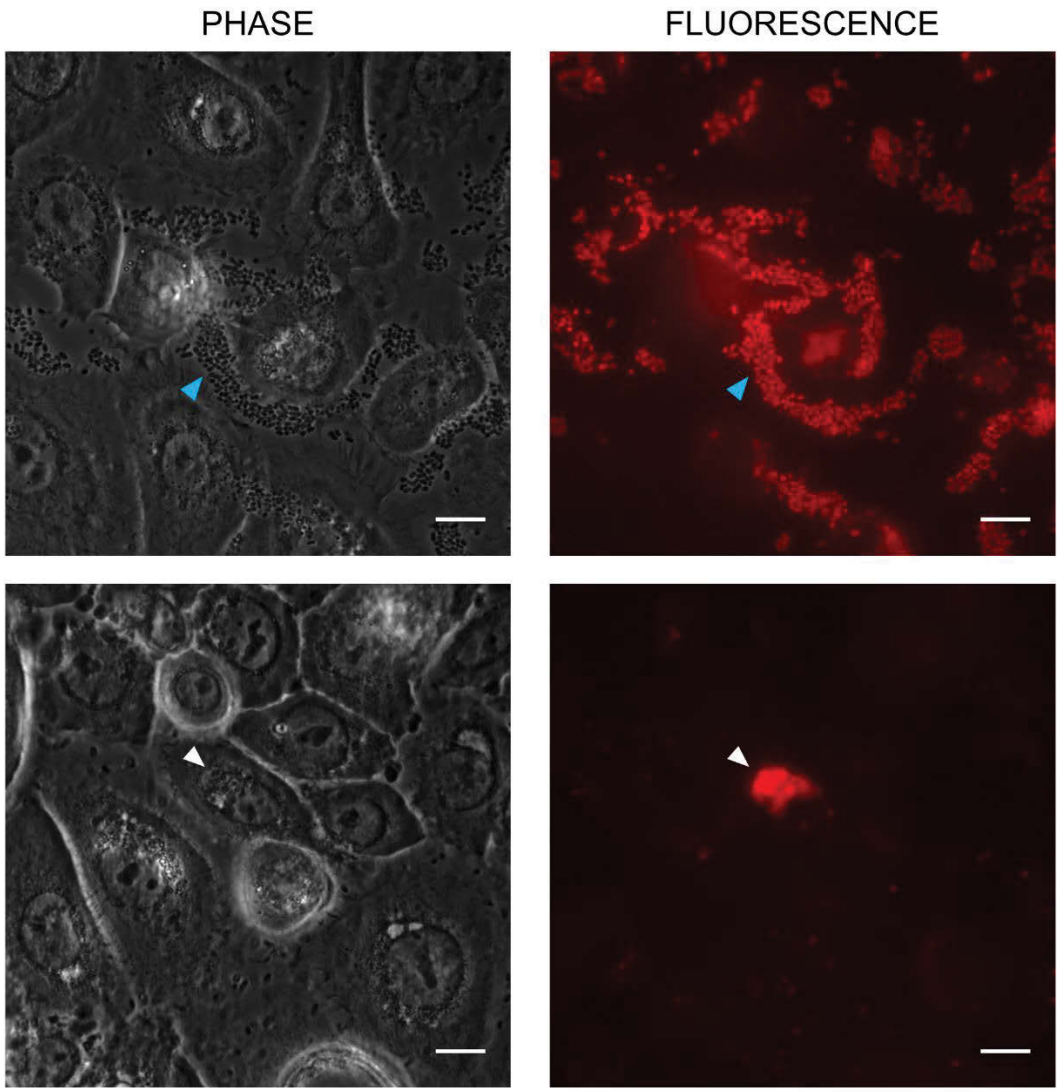

FIGURE 3.8: Phase contrast and fluorescence microscopy depicting mCherry fluorescent UTI89 amongst the PD07i bladder epithelial cells. An infected bladder cell appears to contain an IBC (white arrowhead). Bacteria also bound to spaces between the bladder cells where the plate surface was exposed (blue arrowhead). Scale bar is 5 µm, mCherry exposure was 1000 ms (Section 2.5.1.2).

3.3.3.3 Creation of a Fluorescent Plasmid for Constitutive Expression of GFP

To allow for easier visualisation of the bacteria in the infection, a plasmid was created that allowed for a brighter and constitutive fluorescent expression on the low copy number plasmid backbone pSC101. UTI89 were transformed with the plasmid pGI2 (Section 3.2.4.2) and viewed under the microscope only to find that there was no fluorescence detected. Therefore, the current promoter was replaced with three different promoters each allowing for constitutive expression but had varying expression levels. These were placI, placIQ and placIQ1, which formed part of the plasmids pGI3, pGI4 and pGI5 respectively (Figure 3.9).

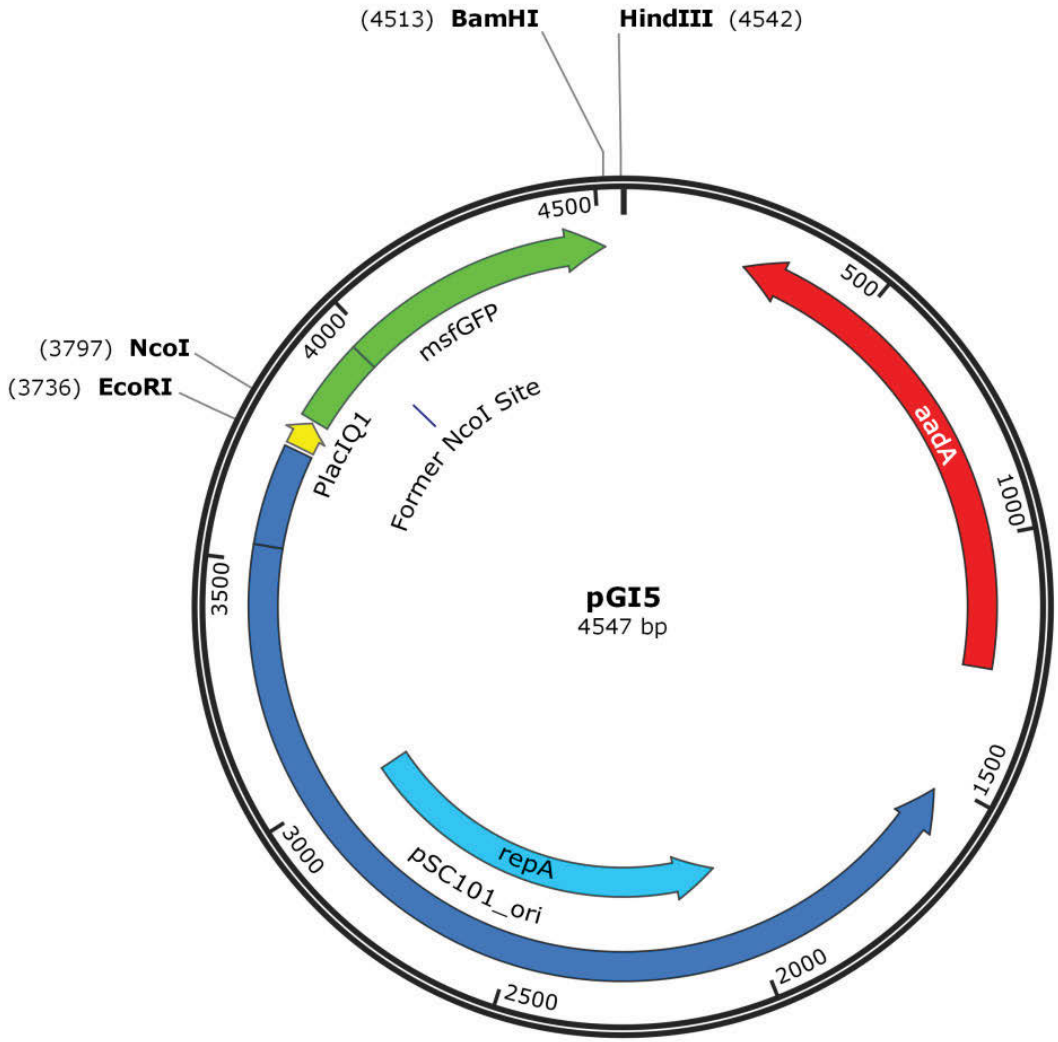

FIGURE 3.9: Plasmid map for pGI5 showing the restriction enzymes used to combine the plasmid and replace the promoter region. The plasmid map for both pGI3 and pGI4 is very similar except with a different promoter region.

Electro-competent UTI89 was transformed with these plasmids, grown to stationary phase and viewed under the microscope (Section 3.2.2). The pGI3 (placI) and pGI4 (placIQ) strains showed a low expression of fluorescence (Figure 3.10, C and D, E and F, respectively), both only slightly above the background shown by the wild type UTI89 (Figure 3.10, A and B). The strain containing pGI5 (placIQ1) was the brightest of the three by far, showing fluorescence much higher than background (Figure 3.10, G and H). The new strain UTI89/pGI5, showing bright and uniform bacterial fluorescence, was then used from this point forward.

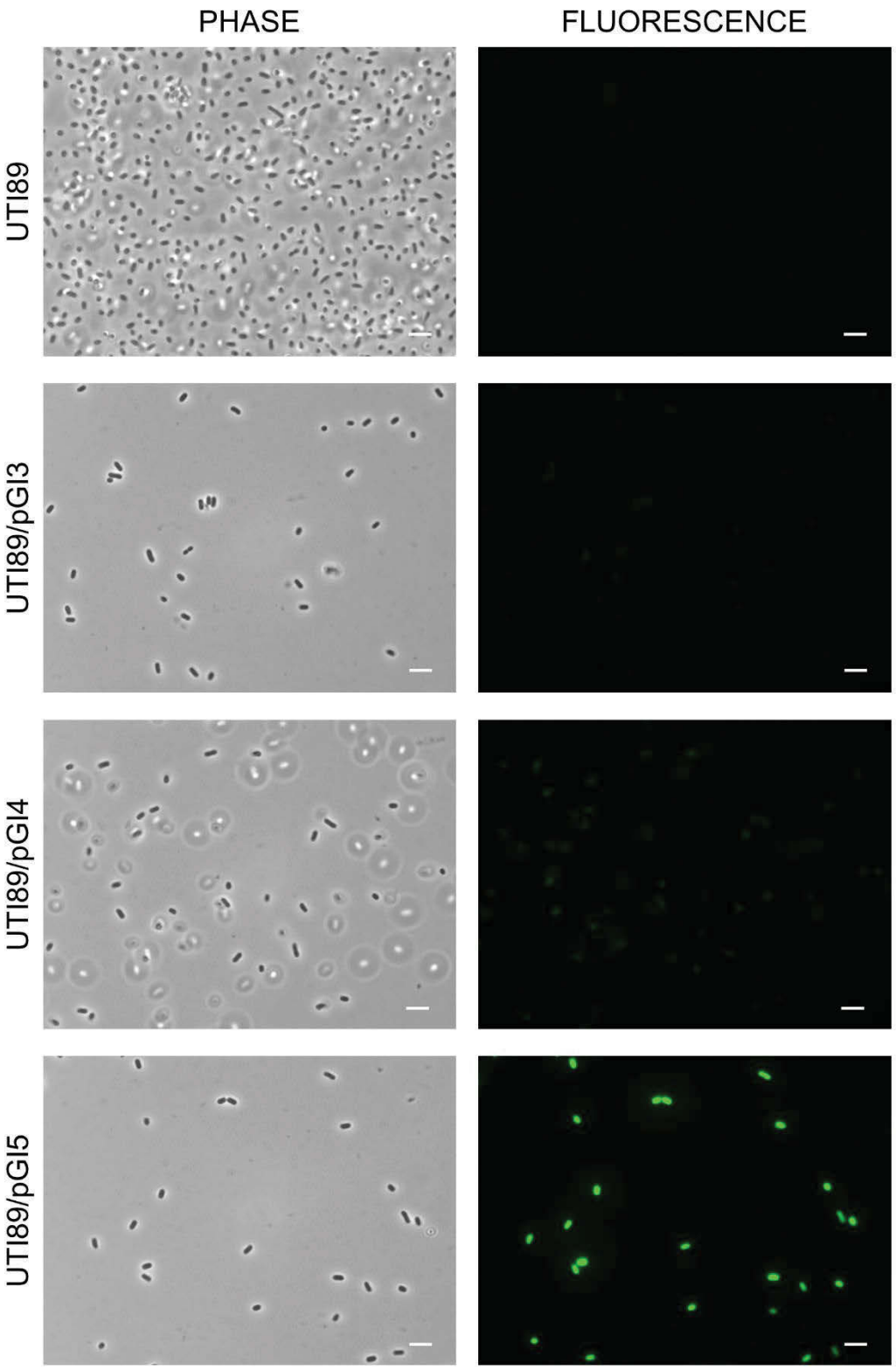

FIGURE 3.10: Phase contrast and fluorescence microscopy showing the GFP expression of the plasmids pGI3, pGI4 and pGI5 compared to the wild type UTI89. The strain containing pGI5 appeared the brightest while the other two plasmids appeared very faint. Scale bar is 5 μm, GFP exposure was 500 ms (Section 2.5.1.1).

3.3.4 Replication of the Later Stages of the Infection Cycle and Achieving Filamentation using the Flow Cell Infection Model

In order to achieve bacterial filamentation in an *in vitro* model of UPEC infection, research has shown that a flow cell system is required [43]. This method more closely resembled the *in vivo* bladder conditions as opposed to the static infection model. This published model was replicated and expanded upon to obtain both qualitative and quantitative results to measure the degree of filamentation.

During substantial preliminary work, reproducing this flow cell infection model was found to require careful use of a bubble trap system in the pump lines, and preheating of the culture media to avoid the formation of bubbles within the closed system, which otherwise lodge within the flow chamber. The published method reported a flow rate of 15 µl/min, yet with the flow chamber model used here, it was found that this resulted in unreliable flow using the same pump system reported. The solution to this problem was to increase the flow rate to 50 µl/min. With this optimisation, the flow cell model was successfully replicated as demonstrated in the following sections.

3.3.4.1 Intracellular Growth

To replicate the intracellular growth stage of the infection, UTI89/pGI5 cells were flowed over a monolayer of bladder epithelial cells and given enough time to attach and internalise, established by Andersen *et al.* (Section 2.3). Once the bacteria was internalised, the flow of EpiLife media was switched to a flow of EpiLife with 100 µg/ml gentamicin to remove all extracellular bacteria. After this time had elapsed, the flow chamber was viewed under the Nikon Ti Epifluorescence microscope to check for any signs of a successful infection. Multiple IBCs (1 – 3 per field of view) were observed throughout the monolayer of bladder epithelial cells. Upon analysing multiple microscopy images, it was determined that around 2 % of bladder cells contained an IBC, indicating a low frequency of infection events. Some examples of these IBCs were shown in Figure 3.11. It appeared as though the IBCs sometimes formed a rosette pattern with multiple lobes (Figure 3.11). One of the main advantages of the flow cell was that all other unbound and dead bacteria and debris were washed away in the flow. This was particularly important after the removal of gentamicin from the system, as it allowed for a much clearer visualisation of infected bladder cells.

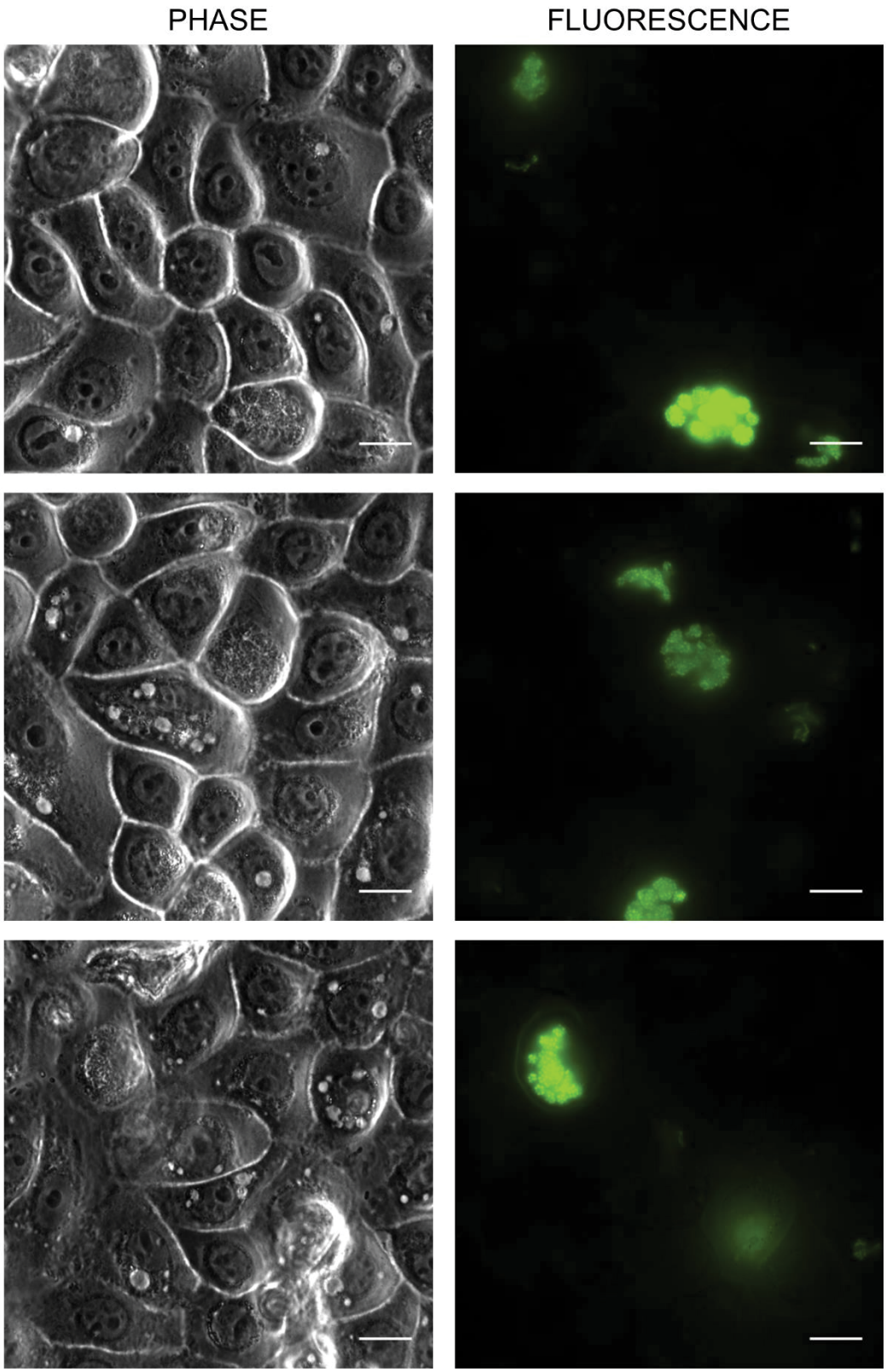

FIGURE 3.11: Phase contrast and fluorescence microscopy showing PD07i bladder epithelial cells infected with UTI89/pGI5 forming rosette like IBCs. Scale bar is 10 μm, GFP exposure was 500 ms (Section 2.5.1.2).

3.3.4.2 Achieving Filamentation with Concentrated Urine

Previous research has shown that bacteria filament when exposed to a flow of concentrated urine [43]. To induce this filamentation, after the 20 hour incubation with EpiLife and gentamicin, the flow was switched to concentrated urine for another 20 hours. After this incubation, the bacteria were harvested from the flow chamber for analysis using microscopy and flow cytometry (Section 2.3.3).

Figure 3.12 showed that when the bacteria were exposed to a flow of concentrated urine, a notable portion (46.2 %) of the population became filamentous while around half of the population remained short (approximately 2 μm). In comparison, in the presence of EpiLife media almost the entire population of bacteria (99.2 %) remained as short rod shaped cells (approximately 2 μm) (Figure 3.12). According to the flow cytometry analysis, nearly half of the bacterial population was longer in the urine exposed bacteria compared to the EpiLife exposed bacteria, as indicated by the peak located to the right of the histogram (Figure 3.12). The wider peak for the urine sample indicated bacteria of varying lengths compared to a tall sharp peak in the EpiLife sample, which indicated bacteria of very similar lengths (Figure 3.12).

Therefore, it was demonstrated that a flow of concentrated urine was able to induce a filamentous morphology change in the bacterial population. This modified model was effectively able to determine the degree of bacterial filamentation, which has not been previously quantified.

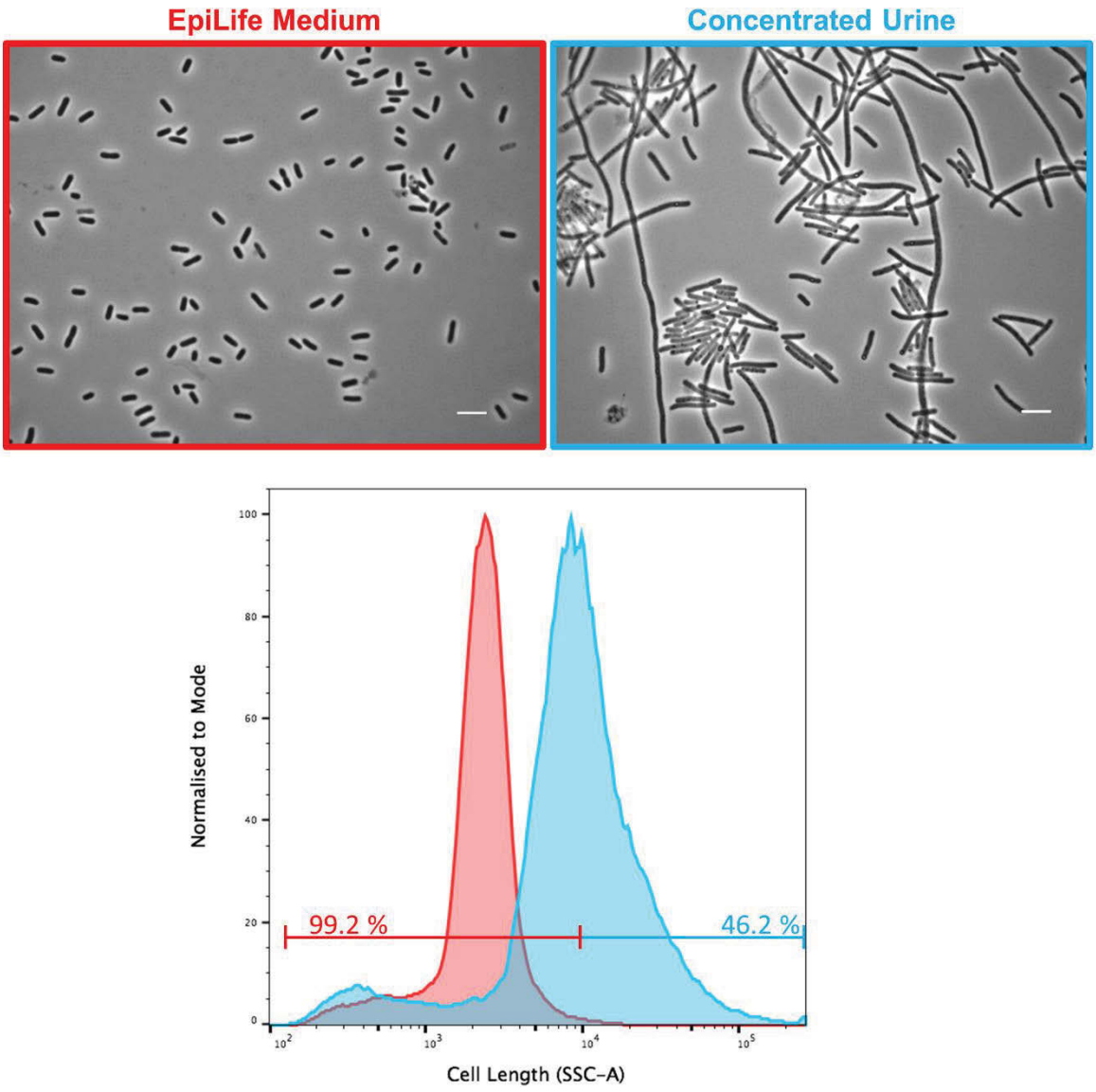

FIGURE 3.12: Microscopy and flow cytometry comparing UTI89/pGI5 exposed to EpiLife and concentrated urine. Phase contrast microscopy showed that filamentation occurred with UTI89/pGI5 in the presence of concentrated urine. In comparison, UTI89/pGI5 exposed only to EpiLife media did not filament and remained as short cells around 2 µm in length. Flow cytometry showed that 46.2 % of the bacterial population exposed to urine were longer than the bacteria exposed to EpiLife, where 99.2 % of the population were short. Scale bar is 5 µm (Section 2.5.1.1).

3.4 DISCUSSION

The main aim of the work described in this chapter was to establish in our laboratory, and improve on, current *in vitro* UTI models in order to quantify bacterial filamentation. UPEC are very adherent, due to the many types of pili present, as observed previously (Section 1.3.1). This adherence is magnified with the tissue culture treated surfaces of polypropylene multi-well plates that promote cell attachment. This resulted in non-specific adherence of the bacteria to the plastic surfaces of the plates in addition to the bladder cells, as shown in the results (Figure 3.2). This extra binding was not expected to be a problem for the bacterial internalisation or intracellular growth assays due to the addition of gentamicin to kill all extracellular bacteria. The adhesion assay detected external bacteria that have attached to the bladder cells but cannot differentiate whether the bacteria have attached to the bladder cells or the wells. Increasing the amount and vigour of washing reduced the number of non-bladder cell binding bacteria (Figure 3.2). The bacteria did appear to have a stronger binding to the bladder cells than to the plastic wells, and so the washing steps could be utilised to remove as much of the non-bladder cell binding bacteria as possible.

In Figure 3.3 (Section 3.3.1), there was a high variability in the bacterial counts due to the variability in the infection process. There is much to consider such as number of bacteria attached to the bladder cells, number of attached bacteria taken up by the bladder cells and number of bacteria growing intracellularly forming IBCs. These factors all contributed to variable results, which was highlighted by a larger number of technical replicates. Although the biological replicates were four, each consisted of 12 technical replicates. The only sample with a low variability was the intracellular growth of MG1655 (Figure 3.3 red). This was most likely due to the non-pathogenic nature of MG1655, which could prevent this strain from developing into IBCs within the bladder cells, keeping the bacterial counts consistent.

Microscopy cannot be used at the adhesion stage of infection either as it cannot be readily determined in this assay format if the bacteria are sitting on top of the bladder cells or have been internalised. 3D imaging of these cells (Z-stacks) may be used to determine the exact location of the bacteria in relation to the bladder cell, however may not be completely reliable. It would be difficult to determine with certainty whether the bacteria are attaching to the bladder cell or just resting on top. High-resolution microscopy and

fluorescent dyes could be used to highlight the bacterial pili and other bacterial and mammalian surface structures to confirm whether the pili have engaged with the host cell.

The established static infection model used filipin to boost the intracellular growth of UPEC. Filipin is an antibiotic, which sequesters cholesterol and induces a significant change in the surface membrane of mammalian cells [89, 90]. When this was tested, as a means to optimise the static infection model, no major improvements were noted in bacterial counts in intracellular growth (data not shown). Due to the instability of preparing and long term storage of filipin and its artificial effects on the bladder cells, filipin was not included in the static infections.

Fluorescent strains of the bacteria were developed in order to allow their visualisation within the infection. Considerations when choosing the best fluorescent markers include ensuring there is no toxicity to the bacteria and that the fluorescence is bright enough to show above autofluorescence or background [91]. Section 3.3.3.1 demonstrated that the plasmids used did not meet the criteria for a reliable expression of GFP and therefore further optimisation was required.

Lambda red recombination is widely used to replace genes with linear DNA fragments obtained from PCR. This method has been performed numerous times in *E. coli* and in other bacteria and yeast [92, 93]. The system uses three genes *gam*, *bet* and *exo* to inhibit the RecBCD exonuclease (*gam*) and allow for the linear DNA to be recombined (*bet* and *exo*) [94, 95]. Bet anneals the single stranded DNA into double stranded DNA and exo recombines it into the chromosome. Bacterial strains without RecBCD have been created, some with this region replaced with the lambda genes. In other cases, the lambda genes are introduced into a wild type *E. coli* on a plasmid, such as in this case with the recombinase plasmid pKD46 [94]. The construct designed in Section 3.3.3.2, was intended to fuse with the native *E. coli lac* promoter using recombinase expressed from a plasmid.

As shown in Section 3.23, the *lacZ* gene in *E. coli* was replaced with a cassette containing a fluorescent protein, GFP or mCherry, and an antibiotic resistance marker for selection, the gene encoding Kanamycin resistance from the plasmid pKD4. The *lacZ* gene in *E. coli* has been targeted for gene replacement in previous studies [95], and may be considered a neutral site for insertion under most conditions. While the mCherry strains were constructed successfully and gave rise to significant fluorescence, they appeared too

faint for robust detection of the bacteria within the cytoplasm of infected bladder cells (Figure 3.7 and 3.8). This may have been attributed to there being only a single copy of the gene on the bacterial chromosome, or weaker than expected expression from this site. The GFP strains did not appear to fluoresce at all, despite confirmation by PCR and DNA sequencing showing that the cassette had been properly inserted into the chromosome for both strains. The reason for this was not investigated further, but may have resulted from a genotypic extra-genic suppression of GFP function in the strain analysed. Taken together, the faintness of mCherry and lack of expression observed for GFP, suggested that a new custom approach to designing of a suitable fluorescent strain was warranted.

As the previous attempts to create a fluorescent bacterial strain resulted in minimal or no fluorescence, a constitutively expressed bright GFP, carried on a low copy number plasmid, so as to provide minimal disturbance to UPEC during infection or growth, was developed. A UTI89 compatible low copy number plasmid, pSC101, was used as the backbone along with GFP under the control of a constitutive promoter, PlacIQ1, which induces a high level of expression. Together these factors allowed the plasmid to express GFP to produce bright uniformly-labelled UPEC that could grow and infect bladder cells normally. As the goal was to label the entire bacterial cell with GFP, constitutive expression was favoured over inducible expression. It eliminated the need to include IPTG and should keep the level of expression consistent. As shown in Section 3.3.3.3, these goals were successfully accomplished and have resulted in the generation of a new strain (UTI89/pGI5) that may be used for ongoing infection studies.

A recent study has developed a model where the bacteria were grown on silicon surfaces without bladder cells and still became filamentous when exposed to a flow of concentrated urine [96]. This suggested that UPEC filamentation is not directly related to interactions with the bladder cells but may be associated with surface binding, such as biofilm growth, and the flow of urine. It has also been shown that the ability of the bacteria to filament is not due to urine solely, because suspension growth of UPEC in urine alone does not induce filaments. Rather, the biofilm mode of growth or a flow of urine are required for filamentation. Although removing bladder cells from the *in vitro* model would help to simplify it, the current bladder cell model used in this project was more clinically relevant to infections as the bacteria were growing, as they would be *in vivo*, inside a bladder cell rather than made to grow on a synthetic surface. The presence of

bladder cells would also allow the triggers of bacterial filamentation to be investigated specifically in response to host cell infection.

To observe the intracellular growth stage of the infection using the flow cell model, microscopy was essential. It allowed the size, shape and structure of the intracellular bacterial communities to be visualised, as shown in Figure 3.11. It also provided confirmation that successful infection of the bladder cells had occurred. The IBCs that were observed showed some to contain intracellular structures that had not been previously reported; a single bladder cell contained multiple IBCs and IBC lobes. The reasons for this are still unknown however it could be attributed to a bladder cell becoming infected by multiple bacteria or that a single IBC formed multiple compartments as it developed from a loosely packed early stage IBC to a tightly packed middle stage IBC, which appeared to be encapsulated within the cells (Figure 3.11) in discrete regions. Such a mode of intracellular growth might assist the bacteria from being detected by the host cell innate immune response and warrants further investigation.

To measure the degree of filamentation of the bacteria collected from the flow cell model, both microscopy and flow cytometry were used. Microscopy alone is largely qualitative and results may be biased if not done rigorously. For example, the images taken need to be randomly selected and enough bacterial cells need to be captured to accurately reflect the entire population. Flow cytometry support these results and can provide a relative measurement of the lengths of a much higher number of bacteria than microscopy alone, providing an accurate representation of a much larger sample of the population. The data is represented as a histogram, with longer bacteria appearing to the right (higher scatter signal per cell) and shorter bacteria to the left (lower scatter signal per cell). The shape of the histogram is representative of the degree of filamentation. When the bacteria were all typically rod-shaped and non-filamentous, the histogram showed a narrow peak indicating a high proportion of bacteria being the same length, representing short rod-shaped cells (Figure 3.12). However, in a filamentous sample the main peak was wider as there were varying lengths of filaments as well as bacteria that had remained short, as not all the bacteria in a population were observed as filamentous (Figure 3.12). Thus using this combined approach allowed for a more accurate measurement of the degree of filamentation.

As part of a collaborative study with Dr Amy Bottomley (ithree institute, UTS), the function of the UPEC *ytfB* gene was investigated, as these genes had indirectly been

implicated in filamentation [80], and was also a putative adhesion related protein by homology to other bacterial adhesins. The early stages of the infection cycle were initially tested to determine if this gene had an effect early on in the infection process using the static infection model. As shown in Section 3.3.2, there was no effect seen in the adherence, bacterial internalisation or intracellular growth assays on the PD07i bladder cells. However, when the kidney-derived cell line HEK293 was used, there was a clear effect shown in adherence, the very first stage of infection. The results suggest that *ytfB* may not have any effects on bladder infections but could be involved in kidney infections, when the bacteria continue to ascend the urinary tract. The later infection stages of bacterial internalisation and intracellular growth were not tested using HEK293 cells as any decrease in bacterial counts at these stages could have been attributed to the initial decrease in adherence. To further confirm the role of this gene in adhering to HEK293 cells, a complementation strain was used where *ytfB* was introduced back into UTI89Δ*ytfB* on a plasmid essentially making it behave like the wild type UTI89. This complementation experiment, carried out by Dr Amy Bottomley (personal communication), was used to successfully verify that the phenotypic effects seen were due to the absence of the *ytfB* gene. Therefore, this *in vitro* infection model can be effectively used to investigate the role of genes in the infection process before using more laborious models such as *in vivo* mouse models.

The bacteria used in these infection models, and in previously established models [1], were cultured statically to promote the expression of the type 1 fimbriae on the bacterial surface. Theoretically, growing the bacteria dynamically might inhibit the expression and proper formation of these surface adhesins therefore reducing the ability of the bacteria to attach to the bladder cells. However, Andersen *et al.* [43] made a bacterial suspension from colonies on an agar plate to use in their infections, which could have potentially disrupted any formed type 1 pili and reduced the attaching bacteria. There was no mention in their results of decreased bacterial counts suggesting no effect on the binding abilities of the bacteria.

A recent study has shown that type 1 pili expression in UTI89 and other UPEC strains was affected by different environmental conditions [97]. Growth in liquid culture in broth or human or mouse urine yielded bacteria with very little expression of type 1 pili, however when allowed to colonise bladder cells or form a biofilm on a silicon surface in a flow cell model, harvested bacteria had increased levels of type 1 pili expression [97].

In addition, UTI89 with and without type 1 pili expression were grown on a silicone surface in a flow cell model and showed no significant difference in attaching bacteria [97]. This suggested that type 1 pili are not essential for initial UPEC attachment. Therefore, it is possible that there would also be no significant impact to the infection process if bacteria were grown dynamically instead of statically before being introduced into an infection model. More research is required to understand this and consider the potential role of the other surface adhesins present in UPEC.

In summary, the work described in this chapter has established an appropriate method to measure the degree of bacterial filamentation in a UTI, and several improvements and ammendments to the procedure for *in vitro* infection of bladder cells by UPEC were tested and incorporated as appropriate. By using a modified *in vitro* flow cell model complemented with microscopy and flow cytometry, the results reported in this chapter have shown that the harvested bacteria can be analysed in a semi-quantitative manner to determine their morphological response. This model will be ulilised in Chapter 5 of this thesis, where it will be used to determine important features of the conditions required for filamentation in UTIs. Chapter 4 will build on the work described here and focus on the development of a new small-scale infection model that has been optimised for microscopy to visualise the stages in the infection cycle in real time.

CHAPTER 4

DEVELOPING A MICROFLUIDIC INFECTION MODEL FOR TIME-LAPSE MICROSCOPY OF THE INFECTION CYCLE

4.1 INTRODUCTION

There have been several *in vitro* infection models used to study the different stages of the UPEC infection cycle, detailed in Chapter 3, such as a static infection to quantify intracellular growth [1], and a flow cell model to look at the later infection stages of bacterial expulsion and re-infection [43]. Microscopy has been used with these models, especially the flow cell model, to capture snapshots of the UPEC morphology at the different stages in the infection cycle. Given that the UPEC show a complex pattern of morphological changes during the infection cycle, the ability to use time-lapse microscopy would be vital to investigate the transitions in morphology that occur. The currently used models have not been optimised for time-lapse microscopy and previous attempts during this project to set up the established flow cell model (Chapter 3) on a microscope proved inefficient and were ultimately unsuccessful. Previous studies have utilised video microscopy, with a complex setup, to observe the maturation of an IBC in mouse bladder explants [42], however the development of filamentous bacteria has yet to be observed in real time. Technology to enable this would provide further insights into the timing and conditions required for development of UPEC filaments and potentially other morphological transitions during their infection cycle.

The aim of the work described in this chapter was to develop a novel *in vitro* infection model to allow the real-time observation of the infection cycle using time-lapse microscopy. This would allow a closer examination of the different infection stages, specifically the growth and development of an IBC and the subsequent release of the bacteria from an infected bladder cell. In addition, the behaviour of the bladder cells and their role in the infection cycle could also be examined. The currently used models do not allow for visualisation and recording the dynamics of growth and behaviour of the bacteria after internalisation, factors that the development of this new model will address.

To achieve this aim, this new model was developed using a relatively new practice called microfluidics. Microfluidics involves the processing of tiny amounts of fluids, less than 1 ml, through small channels within dimensions in the micrometre range [98]. This technique, also referred to as ‘lab-on-a-chip’ technology, has been under continual development for several years but is only recently becoming widely applied to biological research. The main advantages of using microfluidics include the use of a lot less expensive reagents and media, its ability to be automated and it allows a higher degree of

control of conditions [98, 99]. It has been previously demonstrated that mammalian cells can be successfully cultured in a microfluidic environment and exposed to different solutions [100], thus building the foundation for the infection model that was established in this chapter.

The microfluidic infection model developed in this chapter was essentially a miniaturised version of the flow cell infection model (Chapter 3), and was established using the CellASIC ONIX Microfluidic System [101, 102]. This system uses a thin glass base plate (#1.5 coverslip), adhered to a cast set of microfluidic channels supplied by inlet wells that can be filled with the different media needed for each stage of the infection. These wells are connected to a culture chamber where the bladder cells are grown. The plate comprises four self-contained channels allowing up to four simultaneous experimental conditions to be run, meaning that the progress of four different UPEC infections can be monitored in real-time. The plate is connected to a manifold that uses pressurised air to pump the media from the wells into the chamber. Another advantage of this system is that it has been optimised for microscopy, which will allow the progress of the infection to be easily observed.

This chapter detailed the development of this novel microfluidic infection model. As this model relied on real time microscopy, the GFP fluorescent UPEC strain UTI89/pGI5, constructed in Chapter 3, was used to allow for the bacteria to be easily visualised.

4.2 MATERIALS AND METHODS

4.2.1 CellASIC Microfluidic Infection Model

This method is based on the operation of the CellASIC ONIX Microfluidics control unit and manifold with M04S-03 Microfluidic Plates [102]. To prepare a plate for an infection experiment, a sterile work environment was used. The PBS from the upper parts of wells 1 and 8 was first removed, as was the PBS from wells 6 and 7, including the bottom holes (Figure 4.1). A volume of 10 µl of EpiLife media was pipetted into the bottom hole of well 6 to initiate capillary flow and the plate was incubated at 37°C for 30 mins. The EpiLife media in the bottom of well 6 was then replaced with 10 µl of PD07i bladder cells at a concentration of 3×10^6 cells/ml. Well 7 was aspirated and the cell suspension was left for 10 mins to fill the culture chamber. The progress was monitored under a light microscope to check for a proper distribution of PD07i cells. If more cells were needed, to ensure complete coverage of the base of the chamber, another 10 µl of cells was added to the bottom of well 6 and well 7 was aspirated again to re-initiate capillary flow. Once enough cells had filled the culture chamber, 350 µl of EpiLife media was added to well 1 and 50 µl was added to well 7 to initiate gravity driven perfusion. The plate was left at 37°C for 2 days to allow the bladder cells to grow and reach confluency.

Static cultures of the required bacterial strains were set up the day before infection and incubated overnight at 37°C. The culture was centrifuged at 4000 rpm for 10 mins and gently resuspended in PBS to an absorbance (600 nm) of 0.2. Wells 6 and 7 were aspirated including the bottom hole. A volume of 10 µl of bacteria was pipetted into the bottom hole of well 6 to initiate capillary flow and pull the bacteria into the culture chamber. The bacteria were allowed to flow for 20 mins. Well 6 was then aspirated and the bottom hole filled with 10 µl of PBS (0 hours post infection).

The PBS from wells 2 – 4 was aspirated. To well 2, 110 µl of EpiLife media was added, well 3 had 210 µl of EpiLife with 100 µg/ml gentamicin and well 4 had 210 µl of sterile urine. For experiments observing the behaviour of the mammalian cells, 100nM SYTOX Orange stain (TEXAS RED filter set) was included in the urine. The upper part of wells 1 and 7 were aspirated. The plate was sealed to the microfluidic manifold [101, 102], and placed on an inverted microscope (Nikon Ti Epifluorescence). Using the ONIX control software, the flow pressure was set to 1 psi for all wells, well 2 was set to flow for 9 hours

(9 hours post infection) and then wells 3 and 4 were each set to flow for 20 hours in sequence (29 hours and 49 hours post infection respectively).

The culture chambers were viewed at 40x magnification, unless specified otherwise. Multiple points within each chamber were selected and brought into focus using the Nikon PFS system. For fluorescence microscopy, the GFP filter set was used, typically with an exposure time of 50 ms. The overall duration of the time-lapse imaging for the supplementary videos was 22 – 24 hours with an image recorded every 10 - 20 minutes. Images were taken using Nikon DS-Qi2 camera and analysed using the software FIJI.

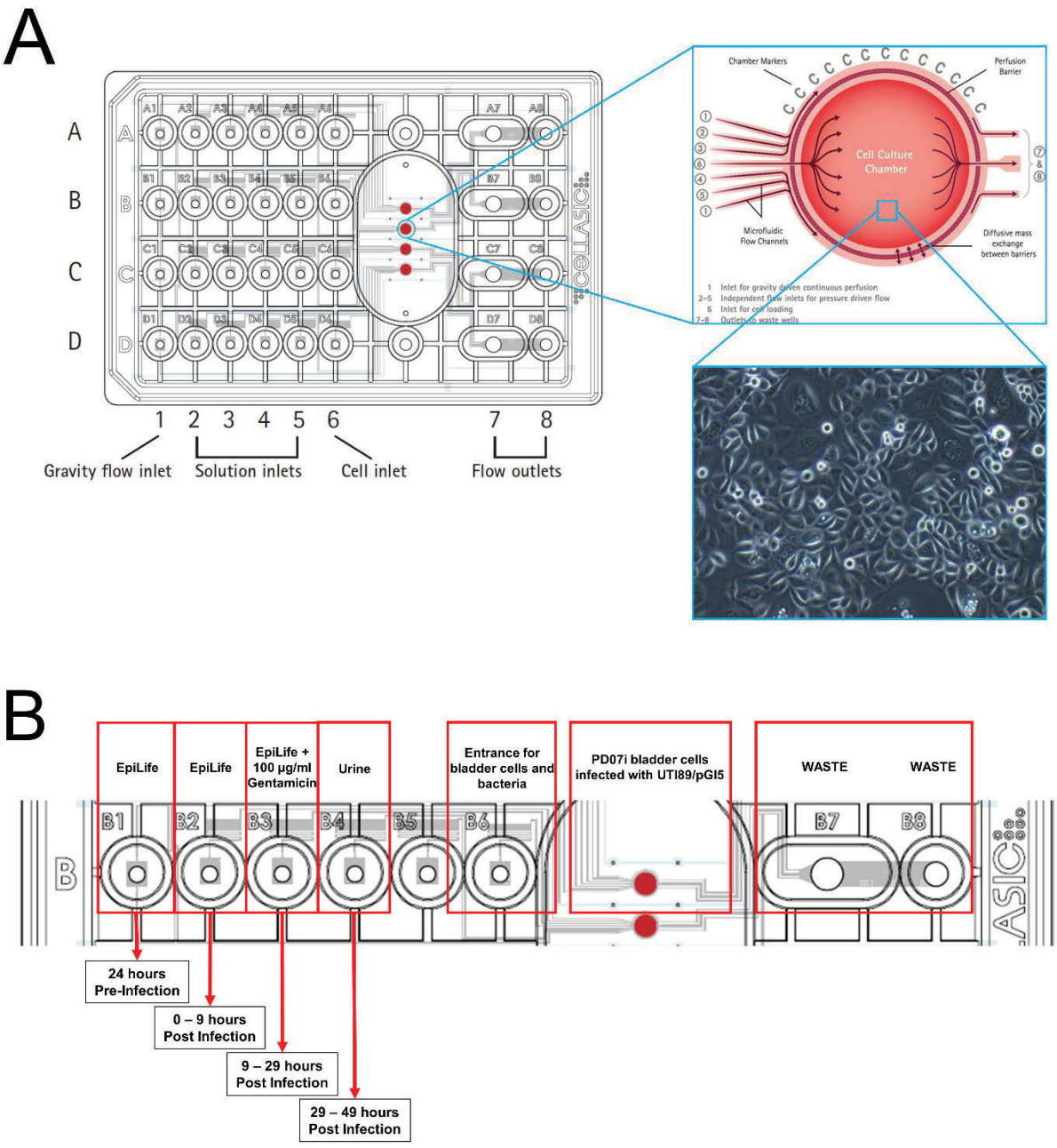

FIGURE 4.1: (A) Diagram of the CellASIC Microfluidic Plate containing four sets (A – D) of the inlet wells, culture chambers and the outlet waste wells. A magnified diagram of the culture chamber shows how the inlet channels enter and diffuse through the chamber. (B) Magnified diagram of a single channel set up showing the different media placed in each well and the timing of each step in the protocol. Adapted from [101, 102].

4.3 RESULTS

4.3.1 The Microfluidic Infection Model Produces Similar Infection Results to the Flow Cell Infection Model

Once the protocol for the microfluidic model was established, it was compared to the flow cell, utilised in Chapter 3, to determine whether this newly established model was able to replicate a UPEC infection to the same extent as the flow cell model. Microscopy images taken of IBCs formed in the microfluidic model appeared similar to those that developed in the flow cell model (Figure 4.2), and a similar infection efficiency of approximately 2% was observed (Section 3.3.4.1). The magnification was lowered to 40X for the microfluidic model to capture a wider field of view to attempt to capture close to the entire culture chamber area. The Nikon Ti microscope provided a high enough resolution to allow for this; however, the fine details of the IBC, such as the individual bacteria, were not as evident.

The microfluidic model also successfully reproduced bacterial filamentation during urine exposure (Figure 4.2). The filamentous bacteria were evident amongst the bladder cells; however, the bacteria could not be removed from the culture chamber. Therefore, it has been demonstrated that the microfluidic model successfully replicated the UPEC infection of bladder cells. With this new model established, the infection process could be closely monitored to observe the activities of the bacteria and host bladder cells during the course of an infection.

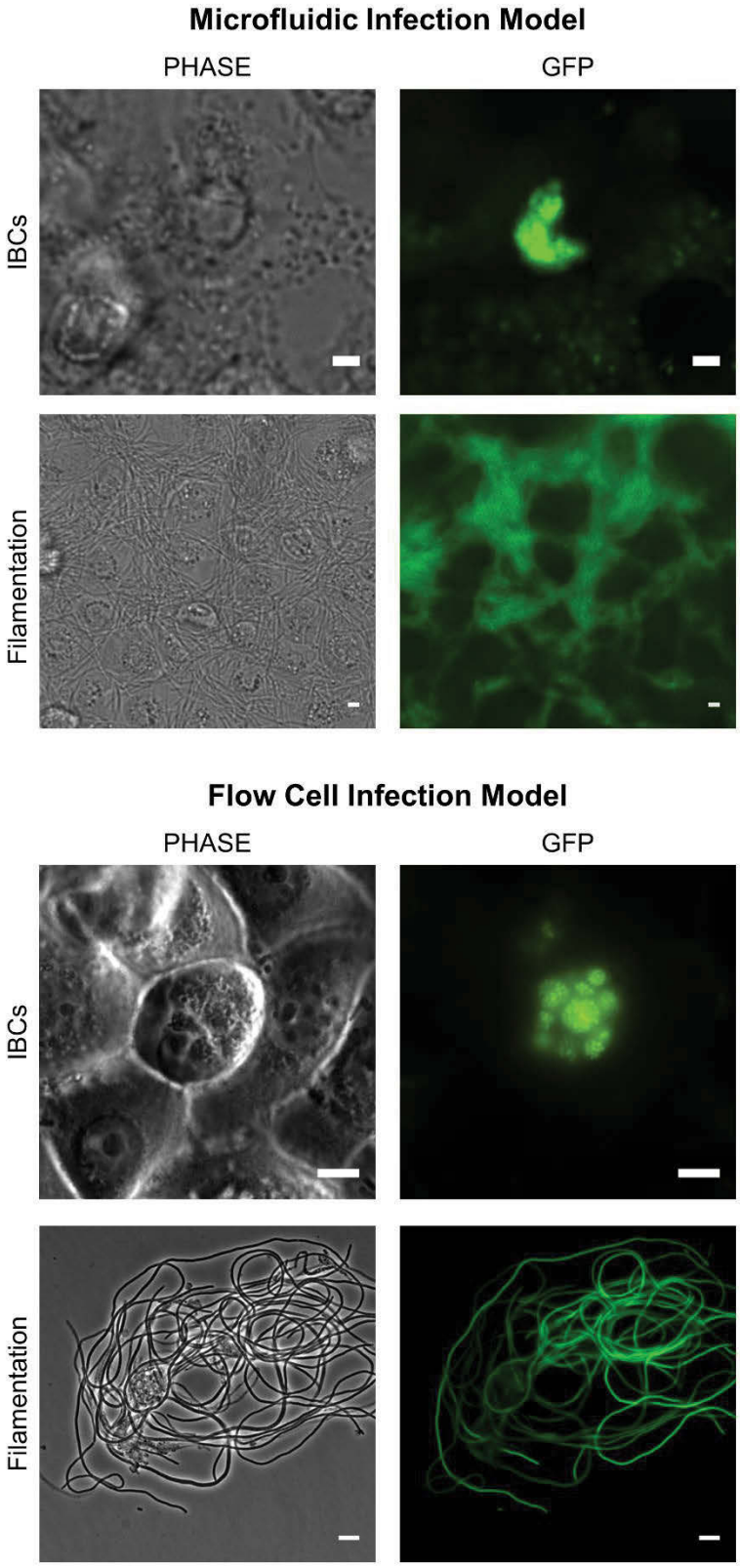

FIGURE 4.2: The microfluidic model produced similar results to the flow cell model. Microscopy of UTI89/pGI5 showed that the microfluidic model produced IBCs and filamentous bacteria similar to the flow cell model. Microfluidic microscopy was 40 X and flow cell microscopy was at 100X. Scale bar is 5 µm, GFP exposure is 50 ms (Section 2.5.1.2).

4.3.2 Infected Bladder Epithelial Cells are Mobile

Initially, the bladder cells were observed during the gentamicin exposure stage (9 -29 hours post infection) to examine their behaviour before contact with the urine. As shown in Figure 4.3, the bladder cells appeared mobile and were seen to move very dynamically across the field of view, indicating that the bladder cells had not yet established a confluent layer under these conditions. Fascinatingly, it was observed that infected bladder cells, as indicated by the presence of fluorescent sub-cellular colonies, moved on the surface like uninfected bladder cells in the same field of view (Figure 4.3). Even bladder epithelial cells containing large IBCs were shown to move around the field of view (Figure 4.3, black arrowheads), and some infected bladder cells were observed to move out of the field of view during the time-lapse (Figure 4.3, blue and white arrowheads).

SYTOX Orange DNA stain was used to detect dead/permeable bladder cells to give an indication of cell death over the course of the infection (Figure 4.3, red arrowheads). These bladder cells appeared round, were frequently seen partially or fully detached from the monolayer surface and were suspended in the media (Figure 4.3, red arrowheads). These bladder cells were very strongly stained by SYTOX Orange (Figure 4.3). This was in contrast to the viable and mobile bladder cells in the monolayer, both infected and uninfected, which did not take up any detectable amount of the SYTOX Orange stain (Figure 4.3).

This indicated that the infected bladder cells were still alive and able to move around in a similar manner to the uninfected bladder cells. This suggested that the IBCs did not incapacitate the bladder cells while they were developing within. This observation was very interesting in that it appeared that the growing bacteria did not harm the bladder cells until the IBC occupied a large portion of the cell causing it to burst. It would seem the bacteria did not harm their host immediately as they use it for nutrients and protection against factors such as antibiotics or the immune system [45].

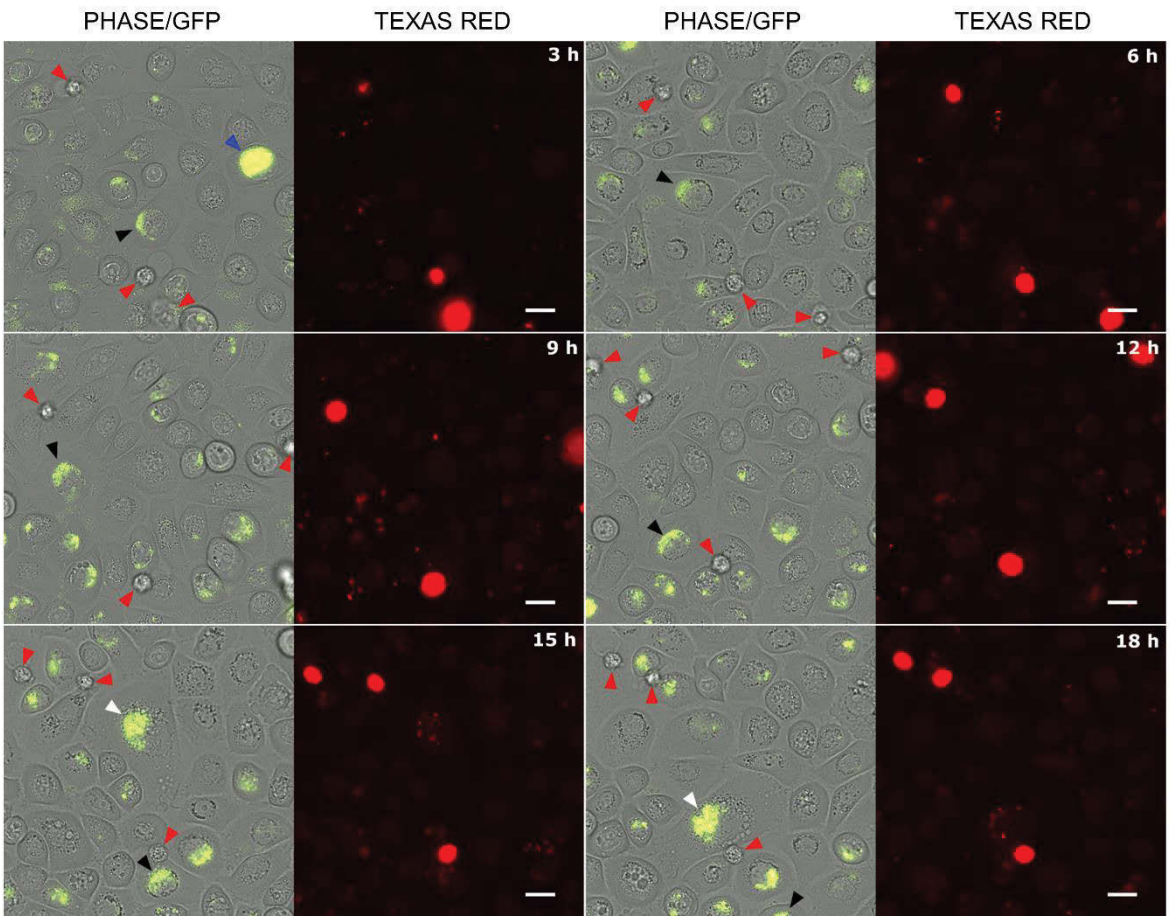

FIGURE 4.3: Infected bladder cells were mobile. Time-lapse microscopy showed time points every 3 hours during the 20 hour gentamicin exposure. PHASE showed the PD07i bladder cells in phase contrast images, GFP showed the fluorescence from UTI89/pGI5 shown as a green overlay on the phase contrast images, whereas TRITC showed the cell permeability using SYTOX Orange fluorescence. Infected bladder cells (examples indicated by black, white and blue arrowheads) appeared at different positions at each time point. SYTOX Orange indicated that infected and uninfected bladder cells were not permeable. Dead and permeable bladder cells were indicated by the red arrowheads. Scale bar is 20 μm; 60X oil objective was used for this experiment; GFP exposure 100ms, TEXAS RED exposure 500ms (Section 2.5.1.2). Refer to Supplementary Video 1 (S1) for full time-lapse.

4.3.3 Bladder Cells Become Permeable After Urine Exposure

Figure 4.3 showed a time-lapse experiment with the inclusion of the live-dead stain SYTOX Orange. This fluorescent dye was included to indicate if and when the bladder cells became permeable and if this correlated with the onset of bacterial filamentation. The results showed that over several hours of exposure to concentrated urine (1.028 g/ml), essentially all of the bladder cells became permeable. The bladder cells were imaged 20 mins before the switch to urine, immediately after the switch to urine and then 10 hours into the urine exposure (Figure 4.4).

The SYTOX Orange staining indicated that before the urine exposure the bladder cells were all non-permeable, apart from a few dead cells depicted by the intense red fluorescent spots (Figure 4.4), similar to the dead bladder cells seen in the previous results (Figure 4.3, red arrowheads). The bladder cells remained non-permeable immediately after the flow was switched to urine (Figure 4.4); however after 10 hours of urine exposure the SYTOX Orange stain was taken up by the entire population of bladder cells, which signified that they had all become permeable (Figure 4.4). The morphology and location in the field of view of the bladder cells remained unchanged during the course of the urine exposure, indicating that the mobility of the cells on the chamber surface was arrested upon exposure to urine. Both observations suggested that the urine treatment incapacitates PD07i bladder cells grown in monolayers.

It was also observed that the background fluorescence in the entire field of view greatly increased as the urine was introduced into the culture chambers (Figure 4.4). This suggested that the urine had an auto fluorescence in the GFP channel, which was also observed in many instances even when there were no bacteria present in the field of view (data not shown). After 10 hours of urine exposure, the bladder cells also appeared to become autofluorescent suggesting they had taken up some of the urine and were showing elevated fluorescence as a result, after becoming permeable (Figure 4.4). The supplementary video (S2) taken every 20 mins over the entire 20 hours urine exposure (29 – 49 hours post infection) showed the individual bladder cells become permeable at different times during the first few hours of urine flow, and by 10 hours, essentially all had become permeable.

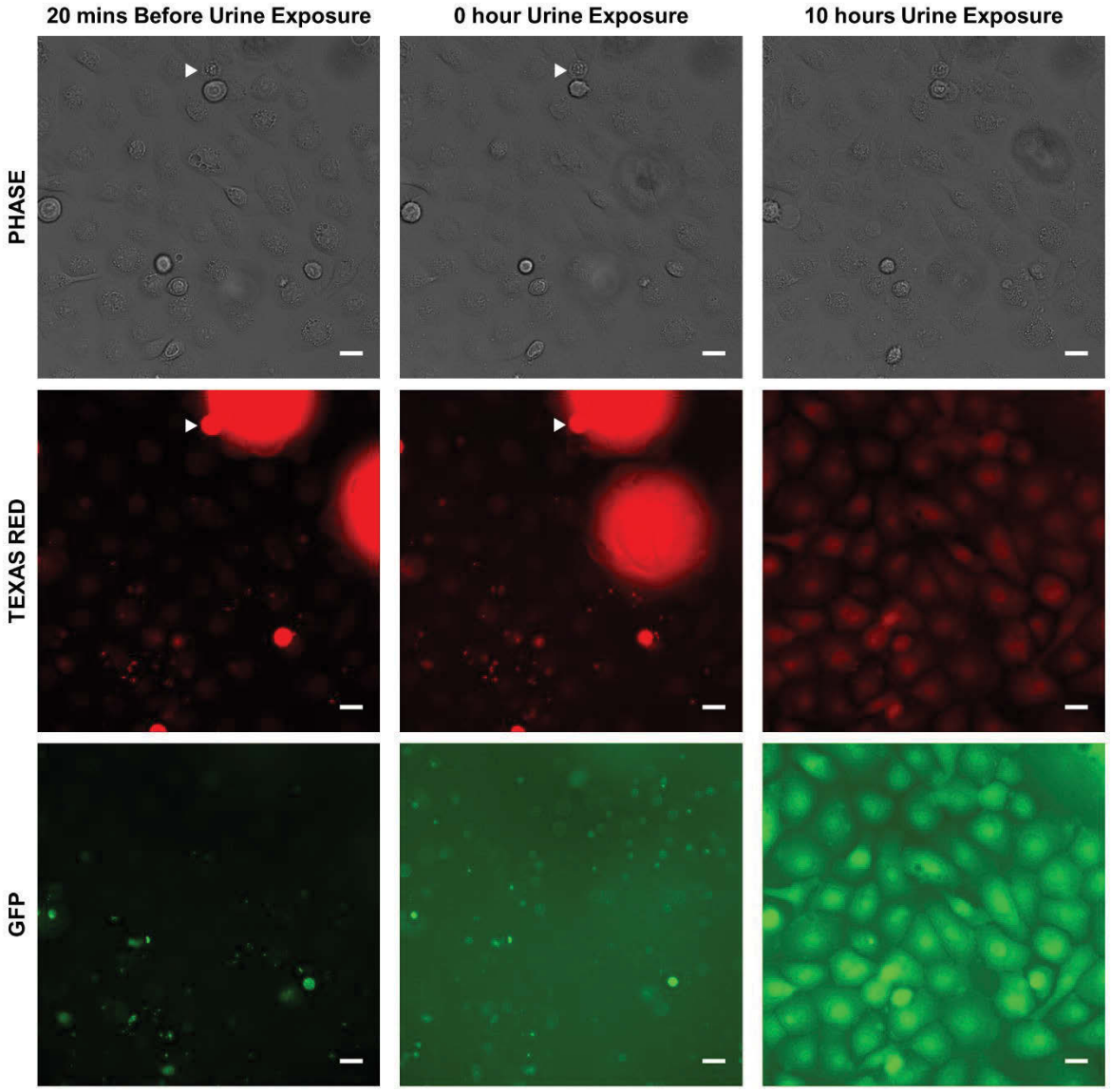

FIGURE 4.4: Bladder cells became permeable and stopped moving after exposure to urine. Microscopy images taken 20 minutes before urine exposure, 0 hours into urine exposure and 10 hours into the urine exposure. PHASE showed the PD07i bladder cells, GFP showed the UTI89/pGI5, TRITC showed the permeability using SYTOX Orange stain. SYTOX Orange staining indicated that the bladder cells were not permeable at the switch to urine but became permeable after 10 hours of urine exposure. Dead bladder cells have detached from the monolayer and taken up SYTOX Orange stain (white arrowheads). Urine appears to have a high background fluorescence in the GFP channel. Scale bar is 20 µm, 40X objective, GFP exposure 50ms, TEXAS RED exposure 100ms (Section 2.5.1.2). Refer to Supplementary Video 2 (S2) for full time-lapse.

4.3.4 Bacteria Emerge Filamentous from Infected Bladder Epithelial Cells

The time-lapse experiment was set up to capture both the Phase and GFP channels every 10 minutes for 24 hours. The 24 hours included the entire 20 hour urine exposure, preceded by the last 4 hours of the 20 hour gentamicin exposure. This was done to show the transition from EpiLife to concentrated urine, which was observed in the supplementary videos (S3 and S4).

By observing many replicates of the microfluidic infection model, numerous infected bladder cells were found to be almost entirely consumed from within by an IBC, followed by the eruption and expulsion of filamentous bacteria. Seven different biological replicates of time-lapse sequences were examined to identify developing IBCs and the release of bacteria from these IBCs. From these replicates, ten developing IBCs were observed of which approximately 70% resulted in the emergence of filamentous bacteria, while approximately 30% of IBCs resulted in short bacteria being expelled. One example is shown in Figure 4.5, which was recorded from the initial transition to concentrated urine (29 hours post infection) and recorded an image every hour until the end of the urine exposure after 20 hours (49 hours post infection). Filamentous bacteria began to emerge at the 7 hour mark after urine exposure in this cell, appearing initially in low numbers followed by a larger release of filamentous bacteria at around 15 hours after urine exposure (Figure 4.5).

As seen in Figure 4.6, not all infected bladder epithelial cells released filamentous bacteria. Figure 4.6 showed another infected bladder cell with a growing IBC. The infected bladder cell became overwhelmed by the internal bacteria and began to bulge and increase in size, as shown in hours 5 – 7 after urine exposure (Figure 4.6, 5h – 7h). The bacteria began to emerge at around 8 hours after urine exposure (Figure 4.6, 8h) followed soon after by sudden release of a high number of bacteria (Figure 4.6). The bacteria that were subsequently released from this cell appeared non-filamentous and rod-shaped (Figure 4.6). After 13 hours of urine exposure (Figure 4.6, 13h), the bacteria from the ruptured bladder cell had consumed the entire field of view so were not shown in Figure 4.6, however the entire 20 urine exposure (29 – 49 hours post infection) was seen in the supplementary video (S4). This showed that the filamentous response was variable; however, this model is still an effective tool to look for triggers of bacterial filamentation.

The infected bladder cells in both examples took up the SYTOX Orange stain variably after urine exposure (approximately 2 hours) but long before the release of the bacteria (data not shown).

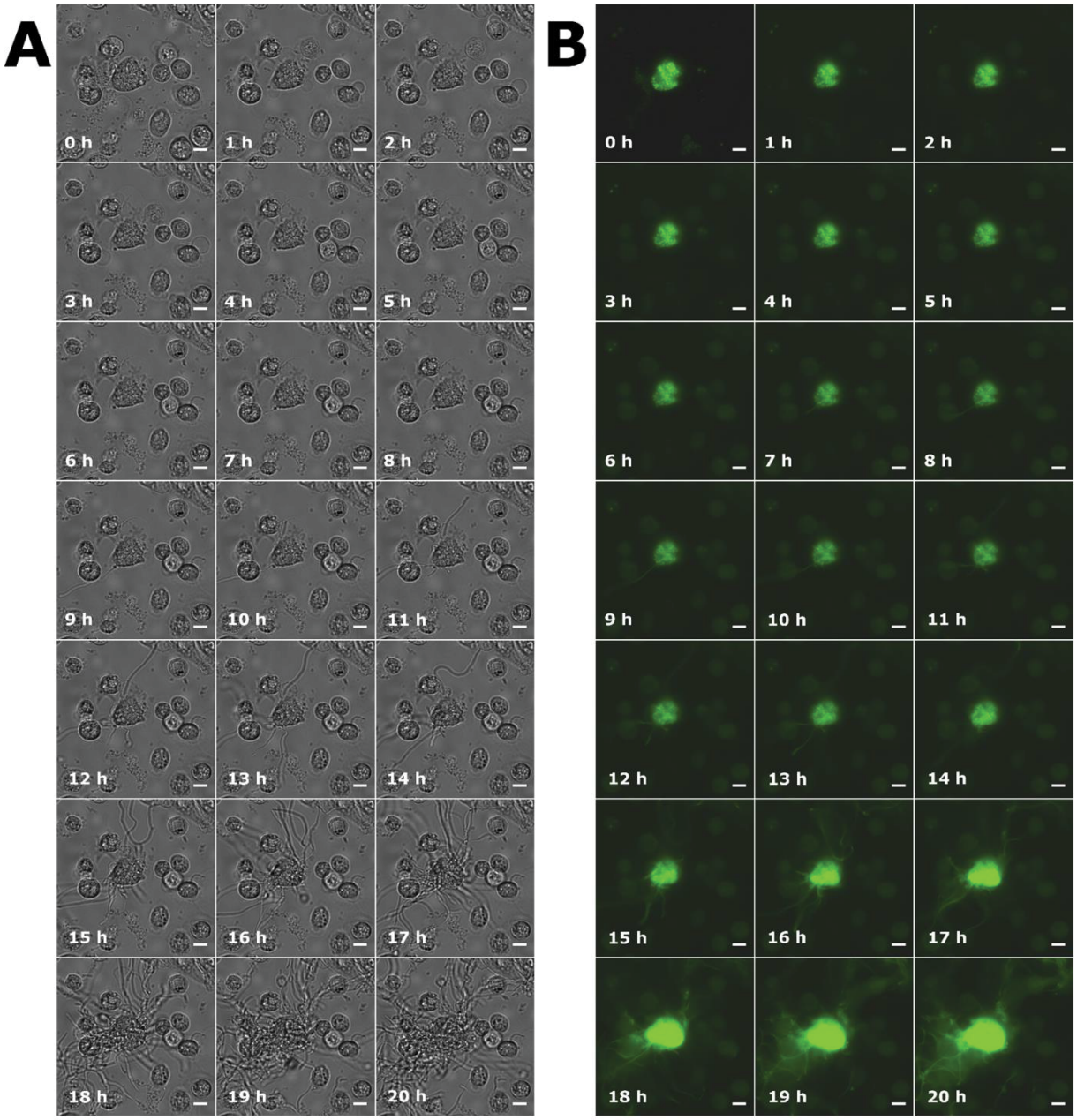

FIGURE 4.5: Filamentous bacteria emerging from an infected bladder cell. (A) Phase and (B) fluorescence time-lapse microscopy showed an IBC growing within an infected bladder cell during the 20 hour urine exposure (29 – 49 hours post infection). The bacteria overwhelmed the bladder cell causing it to rupture and release filamentous bacteria. Scale bar is 10 µm, 40X objective, GFP exposure 50ms (Section 2.5.1.2). Refer to Supplementary Video 3 (S3) for full time-lapse.

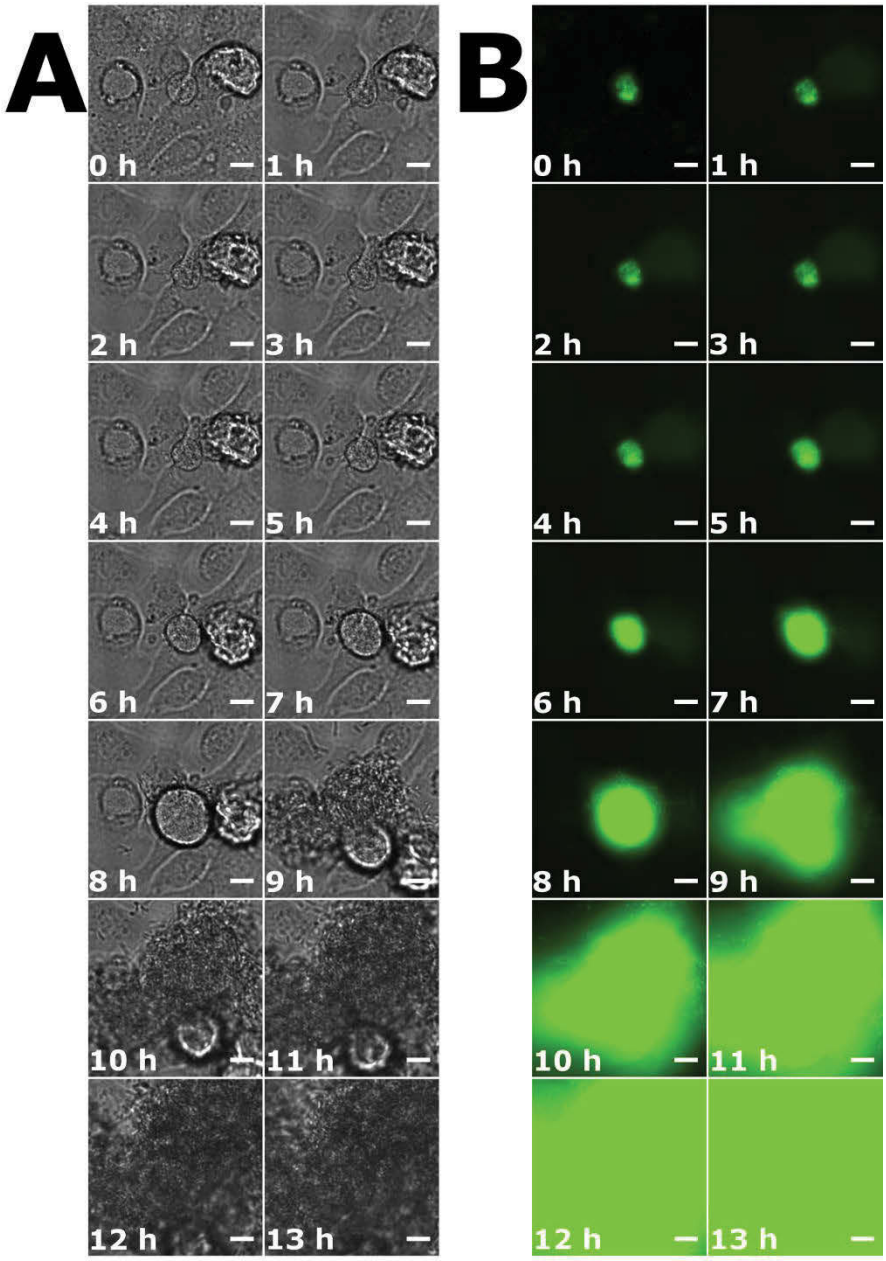

FIGURE 4.6: Short bacteria emerging from an infected bladder cell as a globular mass. (A) Phase and (B) fluorescence time-lapse microscopy showed an infected bladder cell where the bacteria have overcome the cell and been expelled, releasing shorter rod-shaped bacteria, during the 20 hour urine exposure (29 – 49 hours post infection). Scale bar is 10 µm, 40X objective, GFP exposure 50ms (Section 2.5.1.2). Refer to Supplementary Video 4 (S4) for full time-lapse.

4.4 DISCUSSION

Using this newly established microfluidic infection model, the real time progress of UPEC development within an infected bladder cell and the release of filamentous bacteria was observed for the first time. This has allowed a further understanding into the infection cycle and revealed some limitations of the *in vitro* infection models. Yet this has shown that a real time *in vitro* infection model can reproduce the main morphological characteristics of UPEC IBC and filament development during infection.

Section 4.3.2 showed that infected bladder cells behave in a similar dynamic manner to uninfected bladder cells. It would be expected that infected bladder cells, especially those containing a large IBC, would show signs of infection and die, however the results in Figure 4.3 and Supplementary Video 1 (S1) show a different outcome. The SYTOX Orange dye was not detected in any of these infected bladder cells (Figure 4.3 and S1), suggesting they had maintained their structure and integrity while the bacteria were growing within. This could also be the case for *in vivo* infection, where the host cells remain intact while the bacteria develop intracellularly. This could be a potential survival mechanism of the bacteria, where they do not cause any noticeable damage to their host until the bacterial population has dramatically increased in number. Currently this is only speculation and further studies would be needed to observe the behaviour of the bladder cells to confirm whether this does also occur *in vivo*.

Overall, the results of the preceding experiments in Sections 4.3.2 and 4.3.3 indicated that the bladder cells, whether infected or uninfected, became permeable and died when exposed to concentrated urine. This observation suggested a direct way in which the intracellular bacteria encountered the urine to trigger their morphology change into filamentous bacteria before their release into the lumen. The high permeability of the bladder cells, as shown in Figure 4.4, suggested that the urine was not able to support the growth or survival of these bladder cells in culture. This is expected to differ from the situation *in vivo* where the inner wall of the bladder is made of three layers of cells which are constantly being sloughed and regenerated via continual development of the transitional epithelium of the bladder [10, 13]. This *in vitro* model, and many others, has the bladder cells growing in a thin monolayer, which can easily be affected by the harsh conditions of the urine. In addition to this, the bladder cells infected in the bladder are larger umbrella cells whereas the bladder cell line PD07i resembles the intermediate cells

in the bladder. It could be that the umbrella cells react differently to the urine than the intermediate cells. In addition to the SYTOX Orange staining used in these experiments, the presence of the cell death marker lactate dehydrogenase could also be tested for by collecting the infection supernatant to confirm the death of the bladder cells.

Figures 4.5 and 4.6 depicted the developing IBC growing to fill the entire bladder cell and causing it to rupture, releasing the bacteria within. This model has allowed a timeframe to be placed on the progress of the infection giving approximate times for the development of an IBC and when the bacteria are released. The results shown (Figures 4.5 and 4.6) indicated that around 7 hours after urine exposure, the bladder cell began to rupture and release bacteria. This was also observed in other replicates of this model, which showed bladder cells rupturing at similar times (data not shown). However this still remained as a preliminary observation and required further investigation involving quantitative analysis of infected bladder cells and the proportion that produce filamentous vs rod-shaped bacteria. This observation was different to what was reported in the literature, which stated that filamentous bacteria were seen around 18 hours into the urine exposure [43]. However, this published observation was performed using the flow cell model, while these results were performed using the microfluidic infection model. This could account for the differences in time, being that the microfluidic model is smaller than the flow cell model. In addition, the published observation was performed without real time microscopy so was likely to be an estimate based on overnight observation of filamentous bacteria after urine exposure. Time-lapse microscopy has not yet been done using the flow cell infection model to compare the two *in vitro* models, although the more cumbersome nature of the larger scale apparatus was one of the reasons for developing the microfluidic model.

Section 4.3.4 demonstrated that the bacteria became filamentous before or during release from the bladder cell. This was consistent with earlier *in vivo* data from non-time-lapse approaches that showed filamentous bacteria emerging from within a bladder cell rather that forming after being released [44]. This suggested, and it has been hypothesised, that the bacteria encounter the urine while inside the bladder cell, which was further supported by the results in Section 4.3.3. Figure 4.6 showed rod shaped bacteria being released from a bladder cell, indicating that not all infection events resulted in filamentous bacteria. The underlying reason for this is still unknown, however may be attributed to the *in vitro* model itself. It is possible that within the culture chamber of the microfluidic plate, the

media and urine do not flow through evenly, for example, the top and bottom sections of the culture chamber might not be exposed as readily as the centre of the chamber. In addition, the trigger or signal that causes an IBC to form filamentous bacteria presently remains unknown. This trigger could potentially relate to these different morphological outcomes of UPEC being released from an IBC, as seen in Figures 4.5 and 4.6.

Although the microfluidic model revealed the progress of an infection, it was still unclear what was occurring inside the bladder cells as the IBC developed and the bacteria underwent morphological changes. This is mainly due to the tightly packed nature of UPEC within most of the infected bladder cells. The results presented here were captured using a high resolution inverted microscope and in future the method may incorporate higher (super) resolution systems and also greater temporal resolution, which may allow the study of the detailed development of an IBC, including when the bacteria begin to change shape from rods to filaments. The supplementary video (S3) accompanying Figure 4.5 showed a lot of movement within the bladder cell before the filamentous bacteria began to emerge (Figure 4.5, 1h – 7h). Therefore, a higher resolution (spatial and temporal) look within infected bladder cells in future could further elucidate how the bacteria develop into filaments from an IBC and provide quantitative measurements to record how the bacteria respond to the urine exposure.

Although it has been observed that the bacteria emerge filamentous from the bladder cells [44], this model has shed some light onto how this was possible. The results in Section 4.3.3 showed that bladder cells became permeable after urine exposure, and this permeability would be expected to allow the urine to directly contact the UPEC. Soon after this contact, the bacteria begin to alter their morphology within the bladder cell as shown by the time-lapse Supplementary Video 3 (S3), suggesting a link between the two events. To further support this possible link between bladder cell permeability and bacterial filamentation, the timing could be closely observed. The emergence of bacterial filaments from the bladder cell could be timed from when the bladder cell permeability is indicated by the SYTOX Orange staining to observe whether this timing is similar amongst many examples. Given that a random pattern of bladder cell permeabilsation was observed (Supplementary Video 2 (S2)), it would be interesting to note whether the bladder cells that become permeable later on than others release filamentous bacteria later on also. This would support the hypothesised link between these two events.

Given what we have observed from this microfluidic model, more research is required to better understand the bladder host cells and how they behave in *in vitro* models. Other studies using *in vitro* infection models have suggested that the bladder host cells are unaffected when exposed to urine [43]. However, it is unclear from this work how this conclusion was reached and the results presented in this chapter contradict this overall conclusion, as they appeared to show that the urine had a significant negative impact on the immortalised bladder cells. Therefore, while these models are considered adequate to investigate aspects of bacterial behaviour, they are unlikely to accurately reflect how fully differentiated bladder cells behave *in vivo*, particularly in response to urine exposure.

While the microfluidics-based model developed here allows real time observation, it has limitations for preparative analysis of bacteria in the infection. It was found to be impractical to harvest the bacteria from this model unlike the flow cell model where the yield of bacteria is considered sufficient for most modern analytical techniques. For example, the raw effluent during the urine exposure stage from the flow cell model contained a high proportion of bacteria, sufficient for direct analysis by flow cytometry and microscopy to determine the morphological profile of the bacterial population, i.e. the degree of filamentation. Therefore, the small volumes used, which is an advantage of this model, make the follow up analysis difficult.

On the other hand, the microfluidic infection model can be more suitable for screening purposes as this model allows up to four simultaneous infections to be run and uses minimal amount of media, and in this regards is significantly more cost effective. In previous cell culture research using a microfluidic-based system, the cytotoxicity of an anti-cancer drug was tested on HeLa cells [103, 104]. Similarly, one possible application for the microfluidic UTI infection model could be to screen the effectiveness of newly developed drugs on different stages of the infection cycle, such as the intracellular development of the bacteria. This could provide preliminary data towards developing new treatments against UTIs, and has the advantage over non-infection based growth assays of UPEC growth inside bladder cells, where many potential treatments may be directed.

This model has provided further insight into the progress of the UPEC lifecycle. It was demonstrated that infected bladder cells remained mobile as the UPEC grew and developed internally (Section 4.3.2). It was also shown that urine caused the permeability of the bladder cells growing in a monolayer (Section 4.3.3), suggesting a possible mechanism of urine contacting the UPEC. Following on from this, observations showed

that bacteria emerged from a ruptured bladder cell as preformed filaments and that not every infection event resulted in the development of filamentous bacteria (Section 4.3.4). However, there is still much more that remains to be discovered and understood. The exact signal or factor that induce the bacteria to filament is still unknown; however, this model has further demonstrated how the bacteria is exposed to the urine to possibly trigger the filamentation.

CHAPTER 5

INVESTIGATING THE CONDITIONS THAT INDUCE A FILAMENTOUS RESPONSE IN UPEC

5.1 INTRODUCTION

The ability of bacteria to filament provides them with many advantages that allow them to cause successful infection [39]. However, the mechanisms and host cues that trigger this bacterial response are currently unknown. As described previously in Section 1.6.1, the SOS response is one of the best characterised pathways of stress-induced filamentation in bacteria. It has been demonstrated to cause filamentation in cases of DNA damage such as by the release of oxidative radicals by the host immune system or contact with certain antibiotics [39], all of which could be potentially encountered by the bacteria during a UTI.

Using an *in vivo* mouse model of a UTI, where the bacteria were introduced into the bladder by transurethral inoculation, research has suggested that the SOS response played a vital role in bacterial filamentation during a UTI [54]. It was reported that when the cell division inhibitor SulA was deleted from UTI89, there was a complete lack of any filamentous response [54]. It was also noted that the SulA deletion strain was as competent as the wild type UTI89 in progressing through the earlier infection stages. However, the bacterial counts dropped off significantly during secondary infection, which results from bacteria being released from the first round of infected bladder cells. This suggested that SulA was required for the transition to the secondary infection, supposedly via its influence on filamentation, which was therefore considered important for the transition. Upon repeating this infection in innate immune deficient mice, which have a mutation in TLR-4 (Section 1.5.1), filamentation was not observed in the wild type or the SulA deletion UTI89 strains [54]. This suggested that filamentation might be a response to TLR-4 mediated immunity and used as a defence mechanism against the innate immune response of the host. A model was suggested, in which the host immune response causes an influx of neutrophils and other immune cytokines to the infection site, which release oxidative molecules that can damage the bacterial DNA and as a result cause the bacteria to follow the SOS response pathway. When the immune response is dampened in the TLR-4 mutant mice, there is no such signal or need for the bacteria to filament.

Recent research has contradicted this finding by presenting evidence that UTI89Δ*sulA* was able to filament as well as its wild type counterpart in an *in vitro* flow cell model of a UTI [43, 105]. Although this suggested that filamentation in UTIs is occurring independently of SulA, there are some factors that need to be considered. One such

consideration is that the *in vitro* model lacks a complete immune system, which was suggested previously to be required to trigger the SOS response [42, 54]. Therefore, a direct comparison between two studies utilising two different models may not be accurate. It is possible that the conditions that trigger UPEC filamentation are somewhat different in these two models, and further work is needed with thorough comparisons using equivalent host and bacterial strains in these two infection models.

Although the mouse and cell culture infection models represent significantly different infection conditions, there was one interesting observation that could be made when comparing both models. Justice *et al.* (2004) did not observe any filamentation in immune (TLR-4) deficient mice, but Andersen *et al.* (2012) and Khandige *et al.* (2016) did observe filamentation using their *in vitro* model [43, 105]. This may suggest potential differences in the features of intracellular infection with the *in vivo* and *in vitro* models as well as mouse bladder cells and human bladder cells. The common component between these two experiments was the lack of a complete immune response, and given that the recent studies observed filamentation without the presence of an immune system [43, 105], this suggested that there are other conditions by which bacteria can become filamentous during a UTI.

Alternatively, there may have been critical differences between the timing of observation, or the different bacterial strains compared in these studies. For example, the study by Justice *et al.* (2004) of *sulA* used bacteriophage P1 transduction to transfer the mutant allele of SulA from a K-12 background to UTI89 [42], which carried the danger of co-transduction of up to 100 kb of K-12 DNA into the UTI89 background. This may cause changes in pathogenicity that differ from the highly specific Lambda Red Recombination method used by Khandige *et al.* (2016) to delete *sulA* in UTI89 [105]. In summary, the host environmental factors that trigger bacterial filamentation in UTIs are still unclear. Therefore, this chapter further investigated the role of the UPEC SOS response as well as other potential external host triggers of bacterial filamentation to further our understanding of what might be inducing this advantageous bacterial morphological change.

One previously identified potential trigger is the urine itself [43]. It was observed that in an *in vitro* flow cell model of infection with relatively concentrated urine, the bacteria filamented extensively [43]. A correlation was shown between the concentration of urine and the degree of filamentation in their infections, that is the higher the concentration of

urine the longer the bacterial filaments [43]. However, it was noted that apparently not every batch of highly concentrated urine induced a high degree of filamentation [43]. This suggested that the bacteria may not directly respond to the urine concentration *per se*, but a particular constituent in the urine that varied in concentration between the batches. In addition, as discussed in Chapter 3, it was not only the presence of the urine that triggered this filamentation but also the bacteria growing in a biofilm-like mode [43] and potentially a response to the physical flow of the urine [96]. Urine is a complex biological fluid generated by the kidneys to remove waste from the body. The composition of urine is greatly affected by many factors including age, gender, diet and health status [106]. These findings hint at the possibility that there are one or more components of urine that trigger filamentation, possibly through a mechanism that is independent of the SOS response.

The pathways and mechanisms involved in bacterial filamentation remain relatively unknown, particularly the likely non-SOS modes of filamentation. As described above, evidence suggests that filamentation may be induced by multiple host environmental factors, such as the immune response, the bladder surface growth of bacteria (biofilms) and the urine, which combine to cause a bacterial filamentous response through an unknown pathway or multiple pathways. The aim of this chapter was to build on these initial observations and gain further insights into the conditions that trigger this bacterial filamentation in the *in vitro* model of infection that lacks the complete immune component of the mouse model. Based on the literature, it appeared likely that an unknown urine constituent is one of the requirments for triggering filamentation. By finding this urine trigger, and determining how bacteria respond, it may also uncover other new pathways used by the bacteria to undergo filamentation independent of the SOS response.

In this chapter, the *in vitro* flow cell infection model and the fluorescent UPEC strain UTI89/pGI5, both developed in Chapter 3, were used. Fluorescent UPEC strains have been used in many UTI studies, including both mouse and *in vitro* models [42, 43, 54]. UTI89/pGI5 was used in this chapter to allow the possibility to visualise the bacteria in the infection setting and allow for the use of an antibiotic, in this case spectinomycin, to help maintain sterility from extraneous bacteria throughout the duration of these experiments.

The literature has shown that SulA may not be required for filamentation of UPEC in a UTI [43, 105]. However, these previous studies do not entirely rule out the involvement

of the SOS response, as there are proposed to be two SOS inducible genes, *sulA* and *sfiC*, that independently cause filamentation after SOS induction [107]. The gene *sfiC* is another cell division inhibitor, like *sulA*, but it is not under the control of LexA, and instead is located in an SOS-inducible prophage called e14, which is also present in UTI89 [107, 108]. Recently, the *sfiC* locus has been identified to coincide with the open reading frame designated *ymfM* [80]. This observation has since been verified and extended in currently unpublished work by Shirin Ansari (UTS).

As detailed in Section 1.7.1, the SOS response involves a cascade of genes that are activated to repair damaged DNA, all initiated by RecA sensing of the DNA damage [39]. Therefore, in this chapter, *recA* was deleted from UTI89 and its effects on filamentation in the *in vitro* model from Chapter 3 were determined, with the aim of determining the effects of completely inactivating induction of the whole SOS response. In addition, the involvements of the *sulA* and *ymfM* genes, that are thought to independently block cell division in SOS conditions, were both investigated for their requirements in UPEC filamentation during *in vitro* bladder cell infection.

Building on these observations, this chapter also investigated the effects of different factors of urine, including urine concentration, molecular size and pH, on filamentation of UPEC during *in vitro* infection.

5.2 MATERIALS AND METHODS

5.2.1 Synthetic Human Urine (SHU)

The synthetic human urine was prepared as detailed in the publication Ipe, Horton and Ulett, (2016) [106]. A composite synthetic urine media was proposed based on urine media from multiple other studies. For this project, the SHU was prepared and the pH was adjusted with Hydrochloric acid to within the range of the real human urine used, which was 5 – 5.5. Table 5.1 lists the components and their concentration for the SHU media that was used for this work.

TABLE 5.1: The composition of the synthetic human urine media as based on [106].

COMPONENT	CONCENTRATION	SUPPLIER
Ammonium chloride (NH_4Cl)	20 mM	Sigma-Aldrich, USA
Calcium chloride ($CaCl_2$)	4 mM	Sigma-Aldrich, USA
Casamino acids	0.1 % (v/v)	Oxoid, USA
Creatinine ($C_4N_7H_3O$)	9 mM	Sigma-Aldrich, USA
Disodium hydrogen phosphate (Na_2HPO_4)	6.5 mM	VWR, Australia
Iron sulphate heptahydrate ($FeSO_4.7H_2O$)	5 nM	Merck Millipore, USA
Lactic acid ($C_3H_6O_3$)	1.1 mM	Sigma-Aldrich, USA
Magnesium chloride hexahydrate ($MgCl_2.6H_2O$)	3.2 mM	Sigma-Aldrich, USA
Magnesium sulphate ($MgSO_4$)	3.2 mM	Sigma-Aldrich, USA
Potassium chloride (KCl)	38 mM	Sigma-Aldrich, USA
Potassium hydrogen phosphate (KH_2PO_4)	16 mM	VWR, Australia
Sodium bicarbonate ($NaHCO_3$)	13.5 mM	Sigma-Aldrich, USA
Sodium chloride (NaCl)	100 mM	Sigma-Aldrich, USA
Sodium dihydrogen phosphate (NaH_2PO_4)	3.6 mM	VWR, Australia
Sodium oxalate ($Na_2C_2O_4$)	0.18 mM	VWR, Australia
Sodium sulphate (Na_2SO_4)	17 mM	Sigma-Aldrich, USA
Trisodium citrate ($Na_3C_6H_5O_7$)	3.4 mM	VWR, Australia
Urea (CH_4N_2O)	280 mM	Sigma-Aldrich, USA
Uric acid ($C_5H_4N_4O_3$)	0.6 mM	Sigma-Aldrich, USA

5.2.2 Fractionation of Urine to Obtain the Small Molecular Fraction

A single collection of concentrated urine, from a single male donor, was fractionated using the Vivaspin 20 columns with a 3000 dalton membrane filter (GE Healthcare). The urine was filtered through the column, via centrifugation, until approximately 75% had passed through the filter. The fractionated urine was then collected and used in the *in vitro* flow cell model.

5.3 RESULTS

5.3.1 The Role of the SOS Response in Filamentation

As seen in the literature, there are contradictory views on the role of the SOS response in bacterial filamentation in UTIs. However, as described above, this likely resulted from the preliminary and incomplete nature of analyses to date that have addressed the involvement of SOS effector genes. To test if this pathway was being utilised by the bacteria, the *recA* gene was deleted from UTI89 using lambda red recombination (Iain G. Duggin, UTS), and then the resulting strain was transformed with the fluorescent plasmid pGI5 (Chapter 3). Using the *in vitro* flow cell infection model (Section 2.3), UTI89Δ*recA*/pGI5 was compared to UTI89/pGI5, which was the wild type control. The bacteria were then harvested for microscopy and flow cytometry, to determine the cell length of the bacterial population and thus define the degree of filamentation in the absence of the SOS response.

Phase-contrast microscopy of bacteria eluting from the flow chambers at the standard time point for observing filamentation (20 hours post urine exposure) showed the majority of bacterial cells were short (approximately 2 μm) with some slightly elongated cells (< 10 μm) and relatively fewer much longer filaments (> 20 μm) for UTI89Δ*recA*/pGI5 (Figure 5.1). The wild type UTI89/pGI5 displayed a visibly larger amount of bacteria eluting from the flow chambers and a large proportion of them were seen as very long filaments (> 20 μm) (Figure 5.1). This observation indicated that the *recA* deletion strain showed a poor capacity to develop into elongated cells greater than 10 μm. A measure of the cell length using flow cytometry complemented this as UTI89Δ*recA*/pGI5 showed a peak towards the left, consistent with the population being a majority of shorter bacteria (96.60 %), while UTI89/pGI5 had a peak towards the right hand side of the histogram, indicating 8.69 % of the population were much longer bacteria (Figure 5.1).

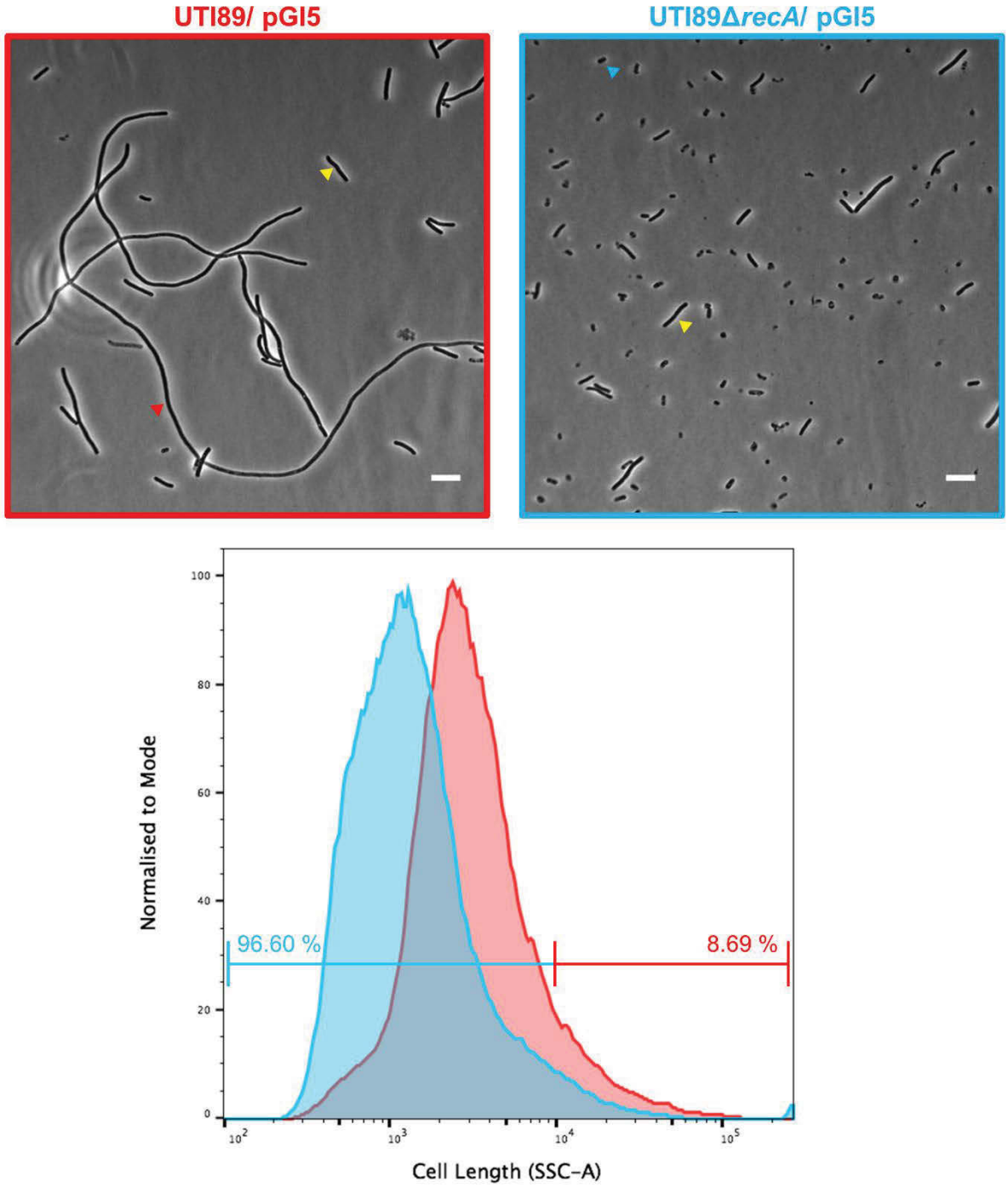

FIGURE 5.1: Phase microscopy and flow cytometry of UTI89/pGI5 (red) and UTI89Δ*recA*/pGI5 (blue), harvested from the *in vitro* flow cell infection model after exposure to concentrated urine. Microscopy of UTI89/pGI5 showed filamentous (red arrowhead) and some slightly elongated bacteria (yellow arrowhead), while UTI89Δ*recA*/pGI5 exhibited short (blue arrowhead) as well as slightly elongated bacteria (yellow arrowhead); scale bar = 5µm (Section 2.5.1.2). Flow cytometry showed a difference in peak position, with UTI89/pGI5 appearing towards the right corresponding to longer bacteria and UTI89Δ*recA*/pGI5 appearing towards the left corresponding to shorter bacteria; 96.60% of the population of UTI89Δ*recA*/pGI5 were short and 8.69% of the population of UTI89/pGI5 were filamentous; the y-axis was normalised to mode to clarify the different peak positions; x-axis depicted the side scatter measurement (SSC-A) which corresponds to length of the bacteria (Section 2.5.2).

Upon harvesting the bacteria after urine exposure from the flow chambers in the *in vitro* infection model, the yield of bacteria from UTI89Δ*recA*/pGI5 appeared much less than UTI89/pGI5, with absorbance readings from multiple replicates showing a notable decrease. This suggested that UTI89Δ*recA*/pGI5 had a greatly reduced growth rate or fitness in the infection model. The generally poor growth of *recA* deletion strains was also observed during static overnight growth in LB media consistently showing an absorbance reading less than half of UTI89/pGI5. To investigate the growth defect further, an intracellular growth assay was performed, using the *in vitro* static infection model described in Section 3.2.1. This was a simple method to quantify the bacteria, to investigate whether UTI89Δ*recA*/pGI5 may have been unable to form very long cells after urine exposure because it could not proceed adequately through the earlier infection cycle stages of adhesion, internalisation and intracellular growth. The results obtained from the bacterial counts showed significantly (p-value = 0.0029) lower numbers for UTI89Δ*recA*/pGI5 compared to UTI89/pGI5 (Figure 5.2). This showed that UTI89Δ*recA*/pGI5 had a drastically reduced ability to grow inside bladder cells compared to wild type UTI89, consistent with the slower growth in LB and the low yield of bacteria harvested from the *in vitro* flow cell model at the filamentation stage.

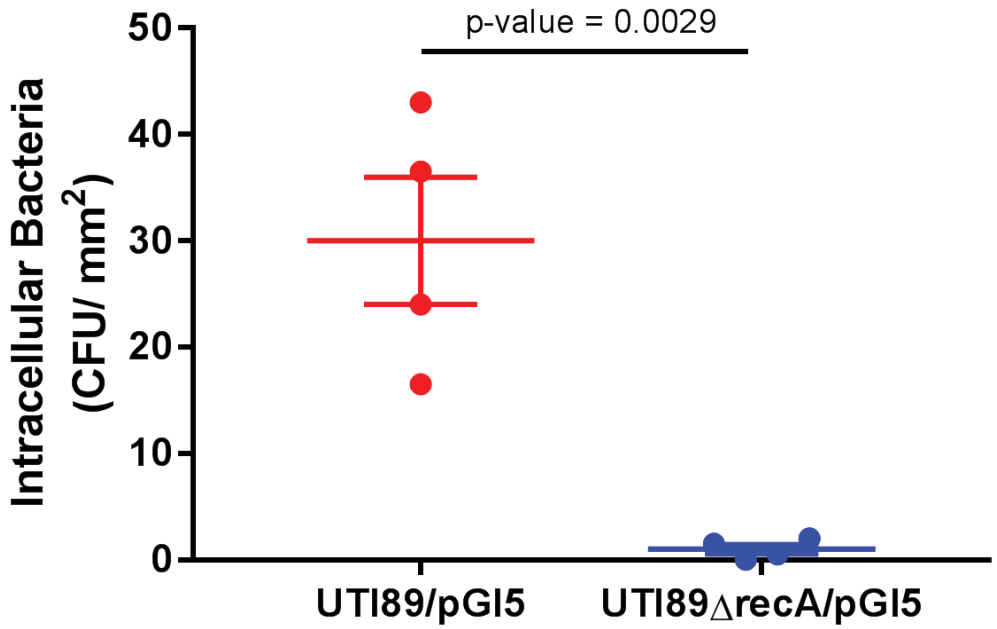

FIGURE 5.2: An intracellular growth assay comparing UTI89/pGI5 and UTI89Δ*recA*/pGI5 using the *in vitro* static infection model, described in Section 3.2.1. UTI89Δ*recA*/pGI5 showed significantly lower bacterial counts than UTI89/pGI5; significance is shown by the p-value = 0.0029 using Unpaired t-test; error bars are SEM; y-axis depicts the intracellular bacterial counts displayed as colony forming units per area in millimetres (CFU/mm^2). N = 2, n = 2, each point indicates each technical replicate (n).

Given that the *recA* experiments were inconclusive due to the growth defects observed in UTI89Δ*recA*/pGI5 (Figure 5.2), other potential SOS deletion strains of UTI89 were developed to investigate the role of the SOS pathway. These strains included individual deletions of *sulA* (J. Moller-Jensen, University of Southern Denmark) and *ymfM* (Shirin Ansari, UTS), as well as a double deletion strain of both *sulA* and *ymfM* (Shirin Ansari, UTS). Deletion of both *sulA* and *ymfM* (*sfiC*) was previously shown to prevent filamentation after SOS induction in E. coli K12, whereas the individual deletions did not [107]. The *sulA* only deletion was not tested in the present study as other studies previously observed filamentous bacteria with this strain in the flow cell model [43, 105]. If the SOS mediators of filamentation, *sulA* and *ymfM*, are responsible for UPEC filamentation, then UTI89Δ*sulA*Δ*ymfM*/pGI5 should not produce filamentous bacteria, similar to UTI89Δ*recA*/pGI5, however without the ambiguous growth defects of the *recA* deletion strain. Both strains were transformed with the fluorescent plasmid pGI5. These strains were tested alongside wild type UTI89/pGI5 in the *in vitro* flow cell model to observe their ability to form filamentous bacteria (Figure 5.3). Intracellular growth assays, using the *in vitro* static infection model, were also performed to determine if these genes affected the fitness (growth rate) of the bacteria (Figure 5.4).

Upon harvesting the bacteria from the flow cell model, phase-contrast microscopy showed that both UTI89Δ*ymfM*/pGI5 and UTI89Δ*sulA*Δ*ymfM*/pGI5 had high yields of filamentous bacteria (> 20 μm) present, indistinguishable from the wild type UTI89/pGI5 (Figure 5.3). This was complemented with flow cytometry, which showed similarly placed histogram peaks for all three strains, indicating that all three strains contained the same proportion of filamentous bacteria (Figure 5.3). This was supported by the quantification, which showed around 7 – 10% filamentous bacteria for all three strains (Figure 5.3). The bacterial counts obtained from the intracellular growth assay showed no growth defects in either UTI89Δ*ymfM*/pGI5 or UTI89Δ*sulA*Δ*ymfM*/pGI5 compared to UTI89/pGI5 (Figure 5.4). Together, these results demonstrated that the bacteria were still able to filament when exposed to urine in the absence of the two known SOS effector genes, which suggested that SOS is not involved in bacterial filamentation in a UTI.

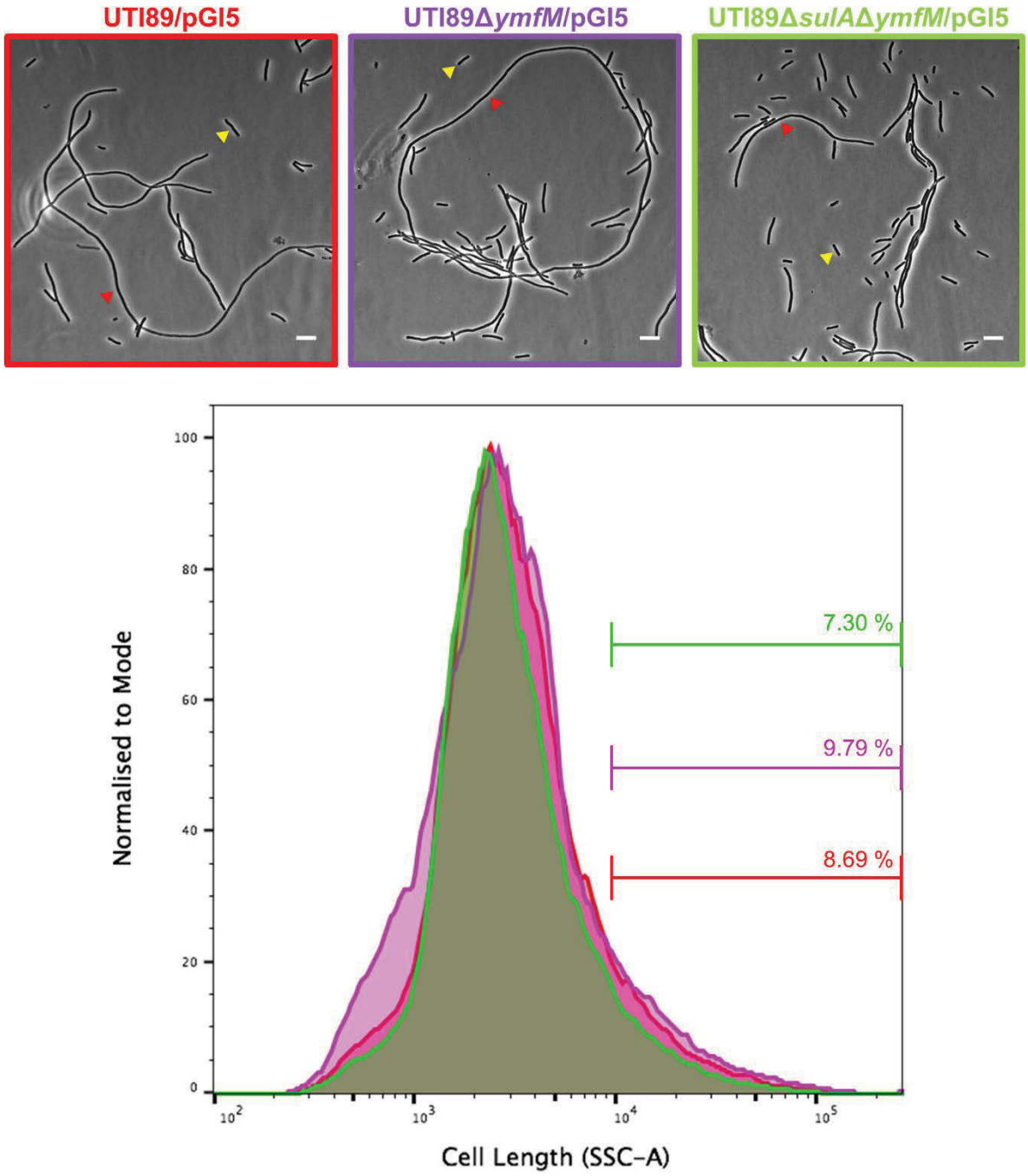

FIGURE 5.3: Phase microscopy and flow cytometry of UTI89/pGI5 (red), UTI89Δ*ymfM*/pGI5 (purple) and UTI89Δ*sulA*Δ*ymfM*/pGI5 (green), harvested from the *in vitro* flow cell infection model after exposure to concentrated urine. Microscopy showed all three strains showed filamentous (red arrowhead) and some slightly elongated bacteria (yellow arrowhead); scale bar = 5µm (Section 2.5.1.2). Flow cytometry showed all three stains had a very similar peak indicating a bacterial population with a similar morphology; 8.69% of UTI89/pGI5, 9.79% of UTI89Δ*ymfM*/pGI5 and 7.30% of UTI89Δ*sulA*Δ*ymfM*/pGI5 was filamentous; the y-axis was normalised to mode to clarify the different peak positions; x-axis depicted the side scatter measurement (SSC-A) which corresponds to length of the bacteria (Section 2.5.2).

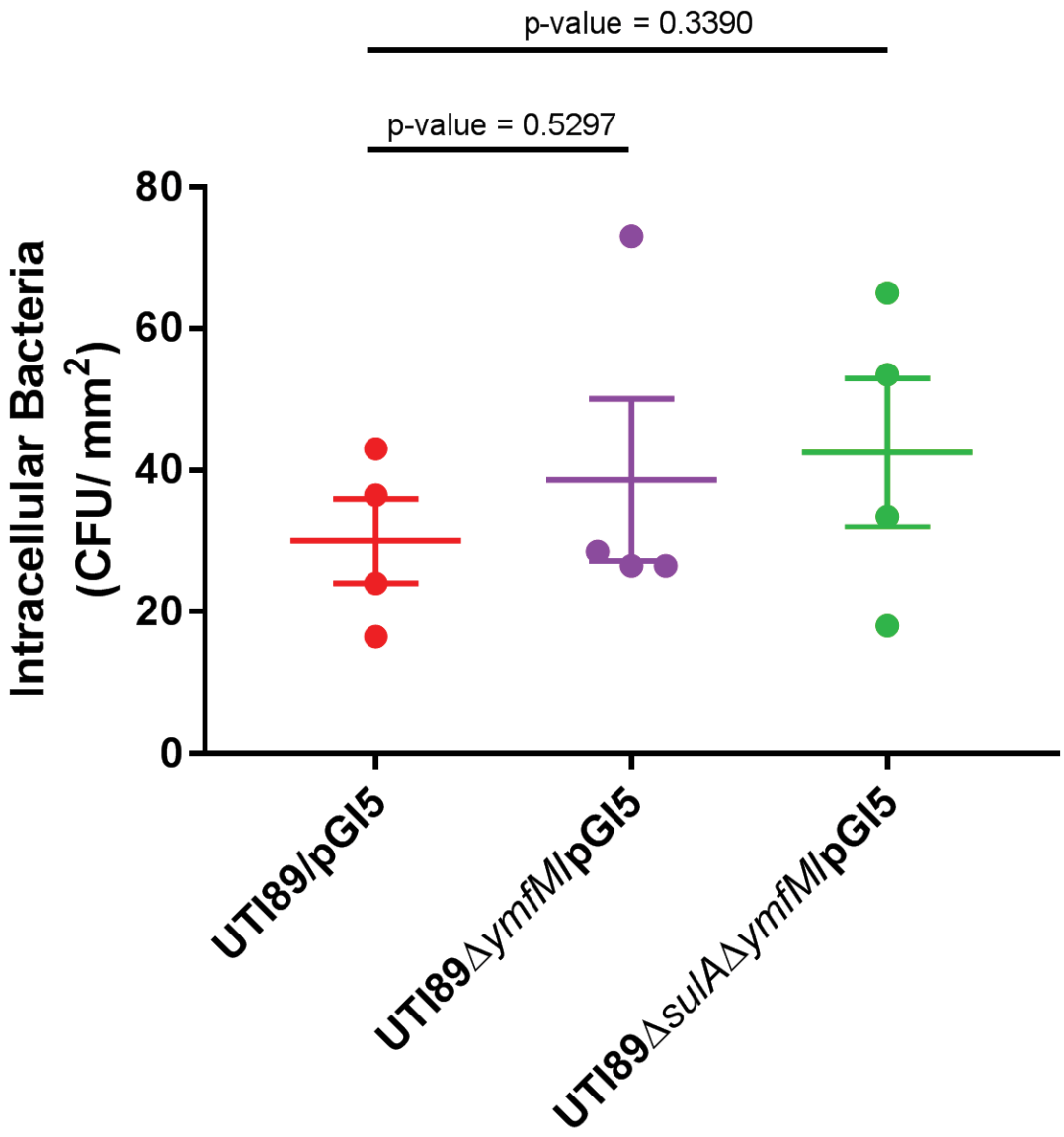

FIGURE 5.4: An intracellular growth assay comparing UTI89/pGI5 to UTI89Δ*ymfM*/pGI5 and UTI89Δ*sulA*Δ*ymfM*/pGI5 using the *in vitro* static infection model, described in Section 3.2.1. Similar bacterial counts were seen for both UTI89Δ*ymfM*/pGI5 and UTI89Δ*sulA*Δ*ymfM*/pGI5 compared to the control UTI89/pGI5. Unpaired t-test to obtain p-values; error bars are SEM; y-axis depicts the intracellular bacterial counts displayed as colony forming units per area in millimetres (CFU/mm^2). N = 2, n = 2, each point indicates each technical replicate (n).

5.3.2 Urine pH has an Effect on Filamentation

The literature has shown that urine concentration plays a pivotal role in inducing filamentation. To further investigate specific urine conditions that trigger this response, another general property of urine that was tested was the pH. Research has shown that pH can have an indirect effect on bacteria in a UTI, by reacting with certain host molecules that can control the growth of the bacteria [109]. Whilst urine has been documented to be between pH 5 – 7, the urine used throughout the present work consistently had a pH of 5.3 – 5.6. This slightly acidic urine was able to reproducibly induce bacterial filamentation, suggesting that acidic urine is more likely to induce filamentation.

To test the role of pH, a single batch of concentrated urine, at a specific gravity of 1.0253 g/ml and with a pH of 5.33, which was known to cause filamentation, was divided into four aliquots and the pH adjusted to approximately 1.5 units higher or lower in two of the samples to determine if there was any effect on the ability of the urine to induce filamentation. The pH was made acidic (pH 4) by the addition of hydrochloric acid and was neutralised (pH 7) by the addition of sodium hydroxide. Upon neutralising to pH 7, a precipitate was formed that was removed by centrifugation. When this was removed, it raised the possibility that the possible urine components that trigger filamentation had also been removed with the precipitate. Therefore, the fourth sample of urine was neutralised, the precipitate removed and then readjusted to the starting pH (pH approximately 5.3) using hydrochloric acid. If this sample were to trigger filamentation, then it could be ascertained that the component had not been removed with the precipitate.

Microscopy of the bacteria from *in vitro* flow cell infections sampled at the filamentation time point showed that the acidic urine and the neutralised urine had a population consisting mainly of short rod shaped bacteria suggesting that both batches were unable to induce filamentation of the bacteria (Figure 5.5). This was supported by the flow cytometry, which also suggested a population of short bacteria as histogram distributions of bacterial cell length (side scatter) were consistent with those of known short rod shaped populations (Figure 5.5). The quantification showed that the proportion of short bacteria in the acidic urine was 97.50% and the proportion of filamentous bacteria in the neutral urine was 1.29% (Figure 5.5). Some of the bacteria that were exposed to the acidic urine at pH of approximately 4 appeared shorter than typical *E. coli*. The microscopy showed short, almost coccoid, bacteria and the flow cytometry had a shoulder peak towards the

far left, suggesting the presence of a population of extremely short bacteria (Figure 5.5). In addition to this, the bacterial yield collected from the flow chamber appeared much lower than the other samples (higher pH values), suggested by a much lower absorbance reading. These observations suggested that the shorter bacteria observed might have been the coccoid bacteria present in a growing IBC [42]. When the urine exposure commenced in the flow cell model, it was likely that the bacteria were still growing as IBCs within the bladder cells. The bladder cells may have become permeable shortly after urine exposure and the bacteria may have encountered the urine while still developing in an IBC (Section 4.3.3). This suggested that the bacteria and bladder cells were highly susceptible to the acidic pH and were unable to survive. The viability was confirmed by inoculating LB broth with a small sample from the flow chamber and growing it for 3 hours, taking an absorbance reading at inoculation and after the 3 hours. The acidic sample showed no increase in absorbance reading, while the other samples (control, alkaline and readjusted) more than doubled in absorbance reading (data not shown), suggesting the bacteria exposed to the acidic urine were not viable.

The neutralised-then-readjusted (pH 5.3) urine was able to induce filamentation of the bacteria almost to the same degree as the normal urine, as the microscopy showed the presence of elongated bacteria in both urine batches (Figure 5.5). This was supported by the flow cytometry, which showed similar cell length distributions of the normal and readjusted urines that were consistent with highly filamentous samples – with a high proportion of bacteria towards the right hand side of the side scatter histogram (Figure 5.5). These histogram peaks corresponded to a population consisting of a high proportion of elongated bacteria with the quantification showing a filamentous population of 35.30% in the normal urine and 21.20% in the readjusted urine (Figure 5.5).

The results from Figure 5.5 showed that the pH of urine played a significant role in bacterial filamentation; when the pH was made more acidic or neutralised, the urine lost the ability to induce filamentation but when the pH was readjusted, the urine regained that ability. By neutralising the urine, removing the precipitate and then readjusting the pH this showed that the filamentation trigger(s) was still present in the urine. The lack of filamentation during pH 4 conditions appears to be the result of inactivation of the bacteria before the filamentation stage. However, it remains unclear as to whether this pH change is directly affecting the bacteria or whether it is affecting a secondary factor(s) present in the urine, which the bacteria directly detect.

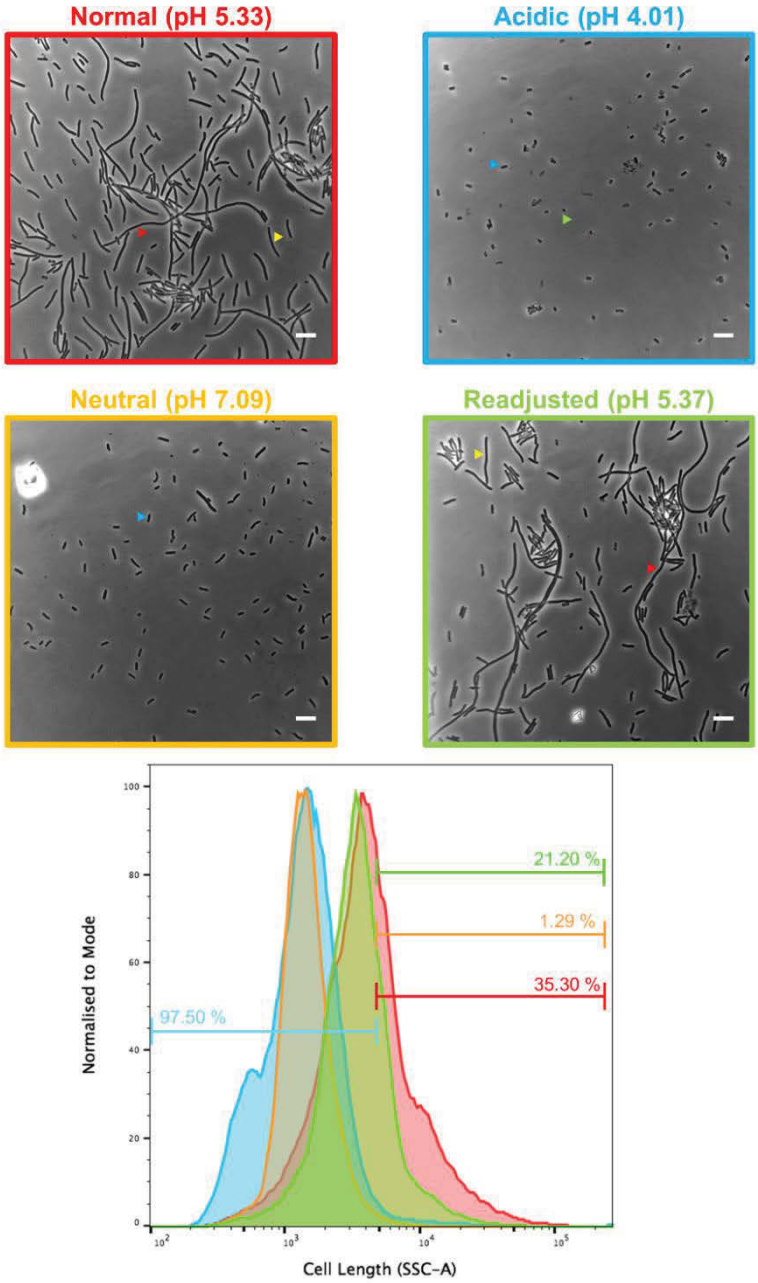

FIGURE 5.5: Phase microscopy and flow cytometry of UTI89/pGI5, harvested from the *in vitro* flow cell infection model after exposure to concentrated urine under different pH conditions; control (red), acidic (blue), neutral (orange), readjusted (green). Microscopy of the normal showed filamentous (red arrowhead) and some slightly elongated bacteria (yellow arrowhead); acidic urine exposure exhibited bacteria that were short rod shaped (blue arrowhead) as well as some tiny round bacteria (green arrowhead); bacteria exposed to neutral urine were shown to be all rod shaped (blue arrowhead); readjusted urine appeared to contain elongated (yellow arrowhead) and filamentous (red arrowhead) bacteria similar to the control; scale bar = 5µm (Section 2.5.1.2). Flow cytometry showed left hand peaks for both acidic (97.50% short bacteria) and neutral (1.29% filamentous bacteria) urine corresponding to a population of short bacteria; the peaks for the normal (35.30% filamentous bacteria) and readjusted (21.20% filamentous bacteria) urine showed right hand peaks representing longer bacteria; the y-axis was normalised to mode to clarify the different peak positions; x-axis depicted the side scatter measurement (SSC-A) which corresponds to length of the bacteria (Section 2.5.2).

5.3.3 Synthetic Human Urine does not Induce Filamentation

As the previous results showed that urine concentration and pH were involved in filamentation, these factors were tested with synthetic human urine (SHU), prepared with pure laboratory reagents, to observe whether the same filamentous response would occur in bacteria exposed to this SHU. A newly developed composite SHU was used, based on a study that reviewed previously developed SHU solutions and proposed a composite SHU based on these existing solutions and their applications [106].

Synthetic human urine (SHU) was made as detailed in Section 5.2.1 and consisted of a mixture of common salts and components found in real human urine. Using the *in vitro* flow cell infection model, UTI89/pGI5 was exposed to the SHU alongside real human urine. The pH of the SHU (pH 5.6) was matched to that of the batch of real urine for comparison. The concentration (specific gravity) of the real urine and the SHU was 1.021 g/ml and 1.026 g/ml respectively; urines with concentrations over 1.020 g/ml have been shown to be adequately concentrated to trigger filamentation. Thus, both urines had been matched as close as possible, with the main difference being their source.

The microscopy showed that the real urine induced bacterial filamentation, as seen previously, depicted by the elongated bacteria observed (Figure 5.6). The SHU did not induce any filamentation as the microscopy showed only short rod shaped bacteria (Figure 5.6). This was reinforced by the flow cytometry where the peak representing the SHU was narrower and towards the left of the histogram, representing a homogenous population consisting of 99% short bacteria (Figure 5.6). The flow cytometry curve representing the real human urine contained a peak towards the left of the histogram but also had a large shoulder towards the right of the histogram indicating a heterogeneous population containing short bacteria and 12.2% much longer bacteria (Figure 5.6). It should be noted that such moderate variation of the degree of filamentation between batches of real human urine was observed commonly throughout the course of this work.

The complete lack of filamentous bacteria after exposure to concentrated, slightly acidic SHU demonstrated that filamentation was not a general response to a high salt concentration or the pH *per se* but must have been due additionally to some other constituent or constituents found only in real urine. This also highlighted a limitation associated with using SHU – the lack of naturally occurring components [106].

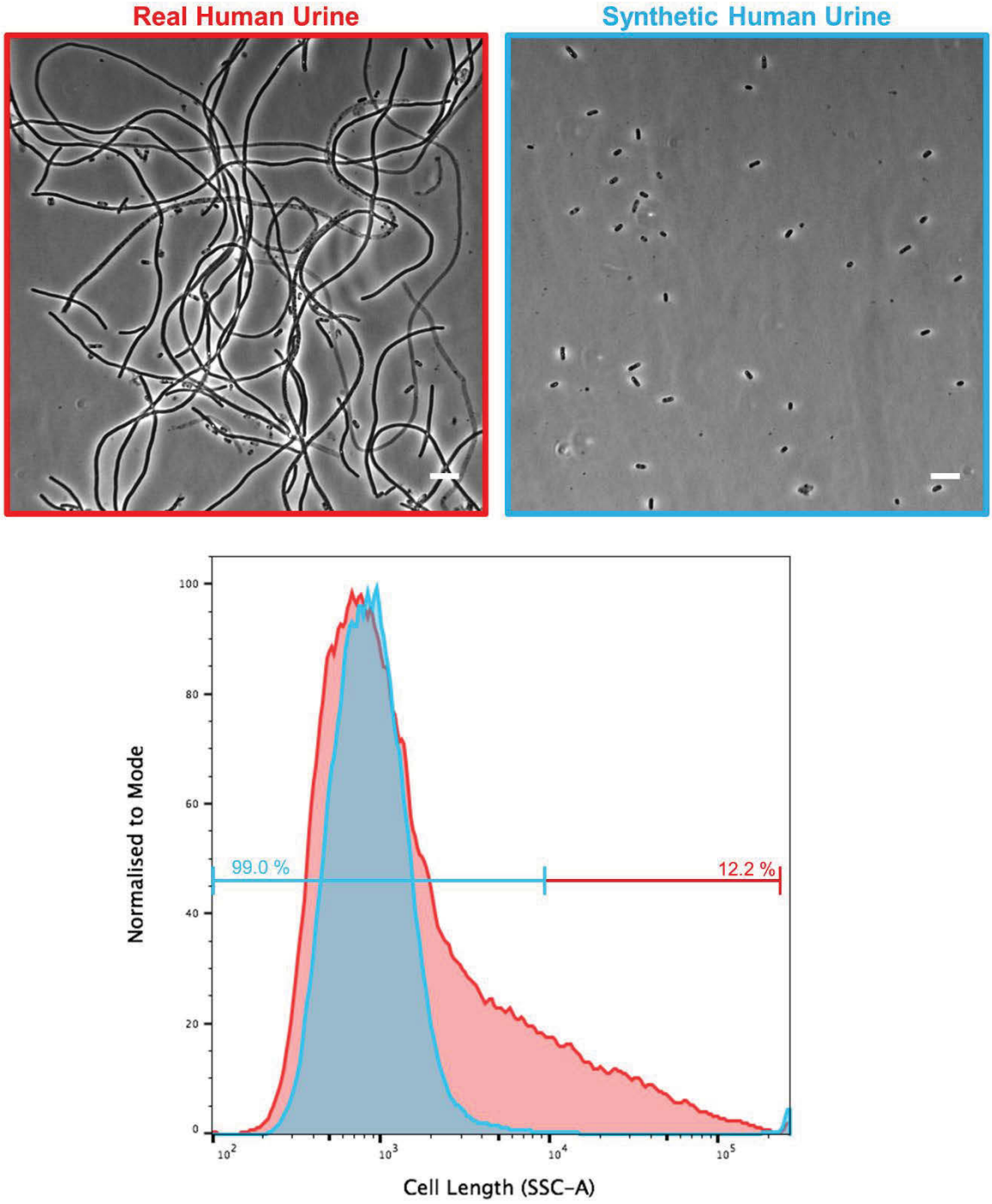

FIGURE 5.6: Phase microscopy and flow cytometry of UTI89/pGI5, harvested from the *in vitro* flow cell infection model after exposure to concentrated real human urine (red) or SHU (blue). Microscopy of the bacteria exposed to real urine showed some short bacteria in amongst a large proportion of filamentous bacteria; bacteria exposed to the SHU exhibited only short rod shaped bacteria; scale bar = 5µm (Section 2.5.1.2). Flow cytometry, for bacteria exposed to real urine, showed a left hand peak with a large right hand shoulder indicating a mixed population of short and filamentous bacteria (12.2% filamentous); the bacteria exposed to SHU were represented by a narrow left hand peak indicating a population of short bacteria of a similar length (99% short); the y-axis was normalised to mode to clarify the different peak positions; x-axis depicted the side scatter measurement (SSC-A) which corresponds to length of the bacteria (Section 2.5.2).

5.3.4 The Small Molecular Mass Fraction of Urine can Induce Filamentation

Literature has suggested differences in urine composition can affect the filamentous response of UPEC, and the results previously described in this chapter have revealed that filamentation was specific to real urine within a certain pH range. This pointed to the possibility that there is a constituent or multiple constituents of real urine that trigger bacterial filamentation, in addition to the pH of the urine as shown previously in Section 5.3.2.

To further investigate this, urine was fractionated through a membrane filter using a Vivaspin 20 column, as detailed in section 5.2.2, to remove all molecules of 3000 Daltons and higher. This small molecular mass urine fraction was used alongside whole urine, in the *in vitro* flow cell infection model, to observe whether it could induce a filamentous response in UTI89/pGI5.

The microscopy showed that bacteria exposed to both the whole urine and the small molecular urine were elongated, with only few short bacteria observed (Figure 5.7). The flow cytometry showed near identical histogram curves for both types of urine. There was a peak towards the left indicating short bacteria and a long shoulder peak towards the right indicating very long bacteria (Figure 5.7), representative of a heterogeneous bacterial population. Quantification showed a filamentous proportion of 12.2% in the whole urine and 12.7% in the small molecule urine (Figure 5.7). The short population control was the synthetic human urine used in the previous experiment (Figure 5.6).

The fraction of the urine that had not passed through the filter, containing the large molecules of 3000 Daltons and higher, was diluted using sterile water back to the starting volume, so the concentration of large molecules should still be very similar to the whole urine. This large molecular mass urine was also tested in the infection model to determine whether it too could induce a filamentous response in the bacteria. Microscopy showed that the bacteria remained short and rod shaped (data not shown), preliminarily suggesting that this portion of the urine was not able to induce filamentation.

These results proposed that the trigger of filamentation was a molecule or collection of molecules less than 3000 daltons. As urine is a product mainly consisting of metabolites

from the body, it consists of thousands of small molecules [110]. Although this has begun to narrow down a possible trigger, there is much more work that is required.

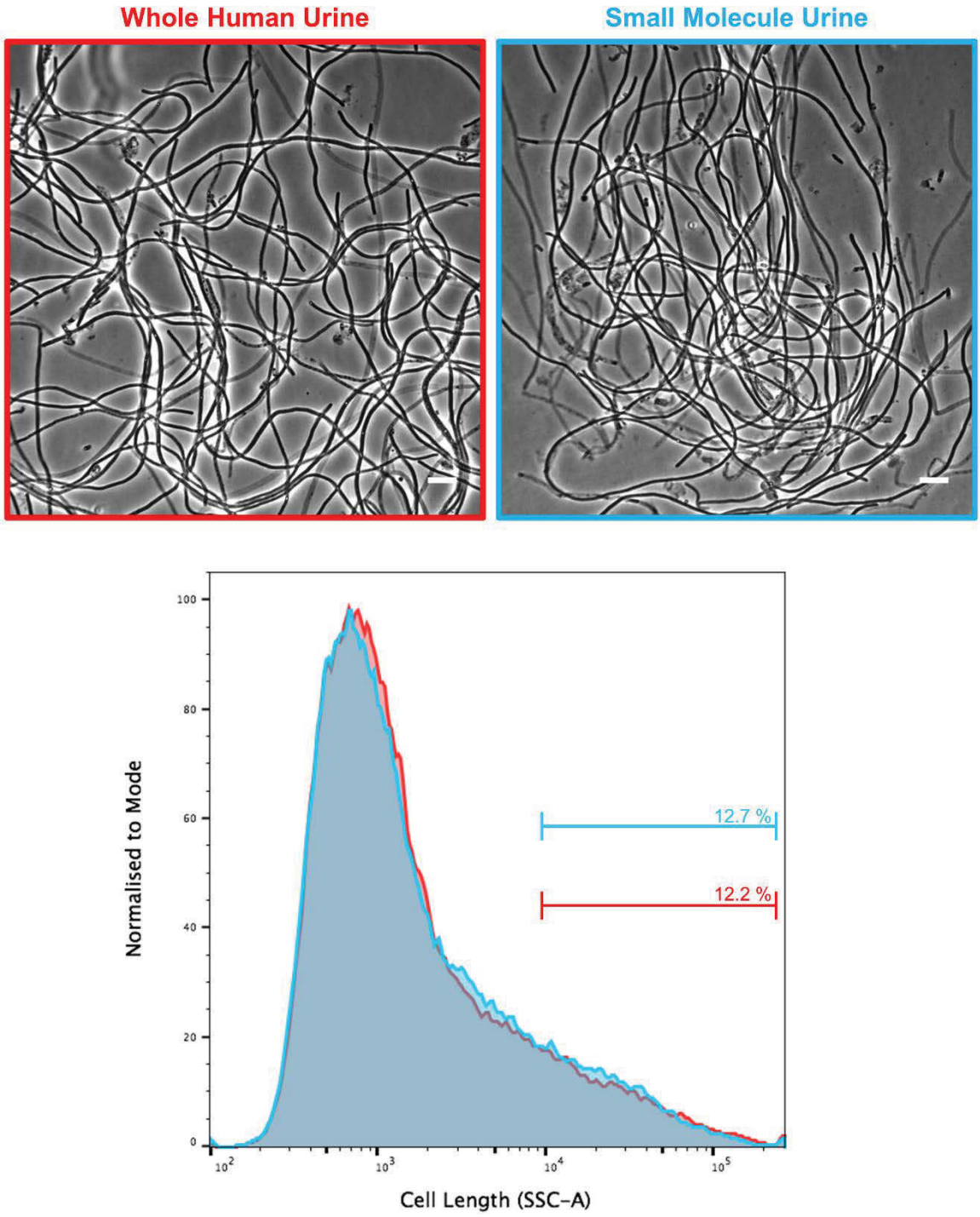

FIGURE 5.7: Phase microscopy and flow cytometry of UTI89/pGI5, harvested from the *in vitro* flow cell infection model after exposure to whole urine (red) or small molecule urine (blue). Microscopy showed elongated bacteria in both types of urine indicating a filamentous response; scale bar = 5µm (Section 2.5.1.2). Flow cytometry showed very similar curves for both urine types, a left hand peak with a large right hand shoulder indicating a mixed population of short and filamentous bacteria, 12.2% of bacteria for whole urine and 12.7% of small molecule urine were filamentous; the y-axis was normalised to mode to clarify the different peak positions; x-axis depicted the side scatter measurement (SSC-A) which corresponds to length of the bacteria (Section 2.5.2).

5.3.5 Small Urine Batches Induce a Differing Degree of Filamentation

As Andersen *et al.* (2012) had shown that different urine batches induced a different degree of bacterial filamentation based on concentration (specific gravity) [43], the same observation was also tested for small molecule urine, as the previous results demonstrated that small molecular urine was able to induce filamentation in UPEC (Section 5.3.4). Multiple urine batches were collected, each batch was from a single donor collection at different times (Batches A – E) and one batch from an independent second donor (Batch F), and the urine was fractionated to obtain the small molecule fraction. The concentration of each batch was measured to be 1.026 g/ml (A), 1.028 g/ml (B), 1.028 g/ml (C), 1.016 g/ml (D), 1.026 g/ml (E) and 1.029 g/ml (F). UTI89/pGI5 was exposed to the different batches of small molecule urine in the *in vitro* flow cell model to observe the ability of the urine to trigger filamentation of the bacteria.

The bacteria were harvested from the flow cell model at the filamentation stage, after 20 hours of urine exposure, and the degree of filamentation was quantified through flow cytometry and visually confirmed through microscopy. Through microscopy it was observed that three out of the six batches contained extremely elongated bacteria (> 20 μm) (Figure 5.8 A, C and F), two batches contained slightly elongated bacteria (3 – 20 μm) (Figure 5.8 B and E) and one batch (Batch D, with the lowest specific gravity 1.016 g/ml) contained all short rod shaped bacteria (approximately 2 μm) (Figure 5.8 D).

The flow cytometry results, in Figure 5.8 G, confirmed that batches A and F contained the highest population of very long bacteria (5.50% and 8.27% respectively), correlating to the long trailing right hand shoulder peak in their histogram profile, with F having the most longest bacteria of all batches as the histogram peak was shifted to the right. This supported the microscopy which showed extremely filamentous bacteria (> 50 μm) (Figure 5.8 A and F). The flow cytometry histogram profile for Batch D showed the population consisted entirely of short bacteria (99.70%), displayed by the left most peak of all the urine batches and again reinforced by the short rod bacteria seen in the microscopy (Figure 5.8 D). Batches B, C and E had similar flow cytometry histogram profiles, showing a moderate amount of elongated bacteria (0.43%, 1.50% and 0.39% respectively), with their histogram peaks falling between those of Batch F (highly filamentous) and D (no filamentous bacteria). This was supported by the microscopy, which showed a large proportion of bacteria between 3 – 20 μm (Figure 5.8 B, C and E).

This suggested that the large filament (> 50 μm) seen in the microscopy of Batch C was a rare occurrence for that bacterial population and that urine was not able to induce a consistent filamentous response.

From these results, it was shown that even in small molecule urine, inducing a filamentous response in the bacteria was highly dependent on the concentration of urine, as was also shown by Andersen *et al.* (2012) for whole urine [43]. Figure 5.8 showed the varying degree of filamentation with different urine batches; however, the highly concentrated batches consistently had a high degree of filamentation. Therefore, it was not necessary to standardise the urine batches, but by using batches that were only above a certain specific gravity (> 1.020 g/ml), this study was able to induce filamentation reproducibly.

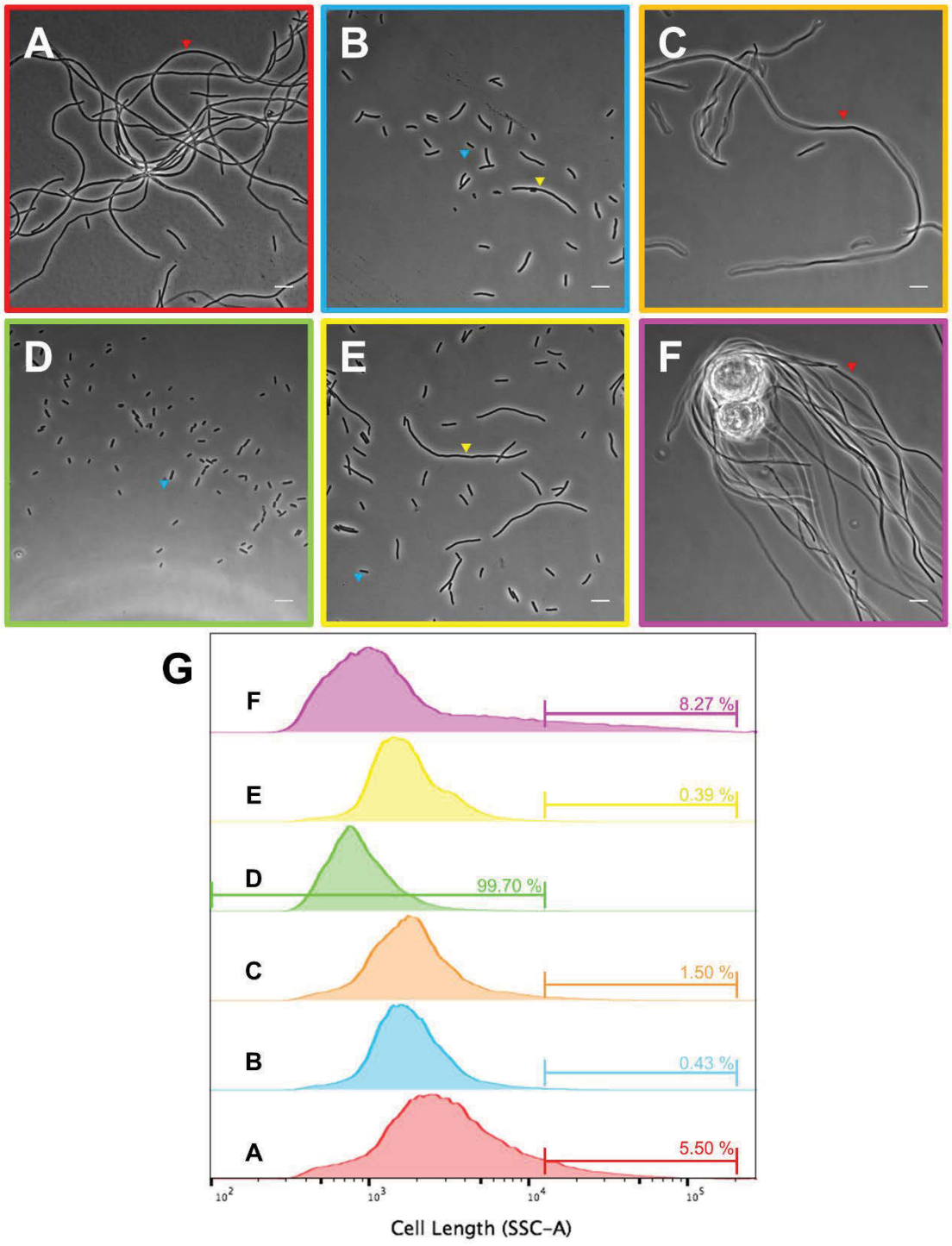

FIGURE 5.8: Phase microscopy (A – F) and flow cytometry (G) of UTI89/pGI5, harvested from the *in vitro* flow cell infection model after exposure to concentrated small molecular urine. Microscopy of UTI89/pGI5 showed that urine Batches A, C and F contained highly filamentous bacteria (red arrowheads) with few shorter cells; Batches B and E exhibited slightly elongated (yellow arrowheads) as well as short bacteria (blue arrowheads); Batch D only contained short bacteria (blue arrowheads); scale bar = 5µm (Section 2.5.1.2). Flow cytometry showed Batches A and F contained the highest proportion of long bacteria with their right hand histogram peaks (5.50% and 8.27% respectively); Batch D had a population consisting of short bacteria as depicted by the left most peak (99.70%); Batches B, C and E contained a population consisting of only a slight proportion of elongated bacteria (0.43%, 1.50% and 0.39% respectively); x-axis depicted the side scatter measurement (SSC-A) which corresponds to length of the bacteria (Section 2.5.2). Colours of the histogram correspond to the microscopy images.

5.4 DISCUSSION

Previously, there have been many hypothesised host triggers of bacterial filamentation in UTIs. One such hypothetical trigger, which was touched upon in Section 5.1, was a response to the host immune system, mainly TLR-4. TLR-4 recognises the lipopolysaccharides on the bacterial cell surface and is responsible for recruiting neutrophils to the site of infection. It has been shown that UPEC filament in the presence of TLR-4 and remain rod shaped without functional TLR-4 [42, 54]. This suggested that by removing the threat of neutrophils, the UPEC might not need to become filamentous. It was hypothesised that TLR-4 was externally signaling the immune system, which the bacteria detected and therefore become filamentous. In this instance, TLR-4 would be an indirect filamentation trigger, as the bacteria would still undergo filamentation through the SOS pathway due to DNA damage caused by the host immune cells.

Another hypothesised filamentation trigger was apoptosis of the host bladder cells, which arose during the course of this work. Apoptosis of bladder cells and bacterial filamentation have been observed to occur around the same time, suggesting a possible connection between the two events. The bacteria may have initiated bladder cell apoptosis due to overwhelming bacterial burden or the bladder cell may sacrifice itself by exfoliation to help rid the body of infection. It was hypothesised that the bacteria could respond to this by filamenting, as they will be released into the harsh external environment of the bladder lumen. Section 4.3.4 highlighted that UPEC became filamentous while still inside a permeable, hence dying, bladder cell. Therefore, apoptosis would also be an indirect link to triggering filamentation as it would allow the bacteria to be exposed to the main trigger and therefore filament.

Although these hypothesised host factors have been considered as indirect filamentation triggers, recent research has shown that filamentation can occur without the presence of host bladder cells [96], thus disproving the hypotheses of host factors as the sole triggers of filamentation. It was demonstrated that bacteria grown on an artificial silicon surface in a biofilm-like manner, as discussed in Chapter 3, were also able to filament when exposed to urine [96].

This chapter aimed to elucidate some of the conditions that trigger bacterial filamentation in UTIs. Although the literature has suggested that UPEC undergo the SOS response

during a UTI, the results of this chapter have suggested the SOS response is not the primary mechanism that triggers extensive filamentation during experimental infection *in vitro*. Furthermore, the results here show that features of human urine represent specific essential host factors required for inducing filamentation in UPEC. This chapter has demonstrated that a combination of certain properties of urine such as high concentration, a certain pH range, and possibly specific small molecules, whose activity relies of these conditions, were able to induce filamentation.

The SOS response is initiated by RecA and removing this protein would prevent the bacteria from activating this pathway. While this would be a simple method to determine if the SOS response is triggered in a UTI, the results in Section 5.3.1 of this chapter demonstrated that the UTI89*recA*/pGI5 struggled to grow in liquid culture and could not progress through the infection cycle (Figure 5.2), leaving it uncertain as to whether RecA and the SOS response is required for filamentation in UPEC. RecA has many functions aside from initiating the SOS response including DNA repair and homologous recombination [111], which may have resulted in the poor growth of the bacteria in culture and during infection.

Another means to inhibit the SOS response, without major growth defects to the bacteria such as in the *recA* experiments, could be to target the SOS gene *dinI*. This gene has been shown to inhibit the SOS response when overexpressed by preventing the degradation of LexA by RecA [111]. DinI was observed to bind to RecA preventing RecA from binding to single stranded DNA, which initiates the SOS response. DinI is able to bind to RecA, which affects the binding of single stranded DNA and RecA by either preventing the two from binding or displacing the single stranded DNA from RecA [112]. By developing a strain of UTI89 that could overexpress *dinI* and testing it using the *in vitro* flow cell model, it could be possible to determine whether the RecA-activated SOS response is triggered during a UTI to induce the observed filamentation.

There are two known SOS-induced cell division inhibitors that work independently of each other, *sulA* and *ymfM*, which are dependent on and independent of LexA degradation, respectively [107, 108]. The results showed that a single deletion of *ymfM* (UTI89Δ*ymfM*/pGI5) still produced filamentous bacteria in the flow cell model (Figure 5.3), which suggested that the bacteria were using an alternative pathway. Most interesting was the double deletion UTI89Δ*sulA*Δ*ymfM*/pGI5, which removed both of the known SOS cell division inhibitors and hence should have stopped any SOS induced

bacterial filamentation. The results from the flow cell infection showed that this double deletion strain still produced filaments similar to the control UTI89/pGI5 (Figure 5.3). This suggested that the filamentation observed was independent of the SOS response and was mediated by another bacterial response pathway, triggered by the urine.

Recent unpublished findings from collaborators (J. Moller-Jensen and colleagues, University of Southern Denmark), using the mouse model of UTI, have also found that deletion of any of the SOS genes (*recA*, *sulA*, *ymfM* or *sulA* and *ymfM*) does not prevent filamentation (J. Moller-Jensen, personal communication), consistent with the findings of the present study. As the infection proceeds significantly faster in the mouse model compared to the *in vitro* model, the development of significant filaments in the *recA* deletion strain may have been observed before the growth defects of the *recA* deletion became evident in the mouse (*recA* deletion growth defects are mainly observed in the latter stages of growth in culture). A complete understanding of the behaviour of the *recA* deletion strain awaits a full time course study of the infection; however, the observations show that the SOS response is completely dispensable for observing high-level filamentation in experimental UTI.

A recent study by Khandige *et al.* (2016) identified another gene involved in bacterial filmentation during a UTI [105], called *damX*. When deleted from UTI89 this strain grew well but showed no filamentous bacteria in both the *in vitro* and *in vivo* UTI models [105]. The SOS response was expected to be operational in this strain, so the lack of filamentation seen strongly supports the above results from the present study. This study introduced another pathway of UPEC filamentation independent of the SOS response, although the mechanisms remain to be elucidated. Together, the results shown in the literature and this thesis have strongly suggested that filamentation observed in a UTI is not due to the SOS response but some other pathway which has yet to be uncovered. Recent developments have implicated urine as a requirement to trigger this pathway.

Synthetic human urine was used to attempt to maintain consistency between experiments, which was a result of the variability in real human urine. In addition to its constant composition, it would also be easy to modify this composition and test the effects on the bacteria in an infection setting. Section 5.3.3 showed that SHU, with a matched concentration and pH to real urine, could not trigger filamentation. These results proposed that filamentation was not a general response to concentration or pH but that it was a response triggered by a component or multiple components naturally occurring in real

urine. A similar study was performed that found that UPEC did not filament in response to artificial urine [96]. This study used artificial urine formulated by [113], while the SHU used for this experiment (Section 5.3.3) was a newly formulated mixture based on previously developed artificial urine, including the urine used in the previously mentioned study [106]. This could eliminate the salt components in urine as the filamentation trigger and point towards components not found in SHU, such as proteins or metabolites.

Section 5.3.2 also demonstrated that these triggering components, whether it be one or many, were sensitive to pH changes. In many cases of pH sensitivity, molecules undergo irreversible structural changes that render them permanently inactive. This has been observed in the pore-forming toxin Listeriolysin O in *Listeria monocytogenes*. This toxin is active at a pH <6 and, due to a deprotonation brought on by a neutral pH, the toxin undergoes an irreversible conformational change that renders it inactive at a neutral pH [114]. In Section 5.3.2, the readjusted urine regained its ability to trigger filamentation, indicating that the trigger component might be rendered inactive at a neutral pH and active at a slightly acidic pH (approximately pH 5.3) (Figure 5.5). Interestingly, this change in activity was reversible as the pH of the same batch of urine was neutralised and then readjusted to mildly acidic and was still able to trigger filamentation (Figure 5.5). This points towards the urine trigger not being a protein, as it most likely would undergo an irreversible denaturation, such as the Listeriolysin O. Instead, this trigger appears to lose its activity when it is deprotonated and regains its activity when protonated, suggesting the pH is affecting the filamentation trigger through charge and not conformational change. Alternatively, separate receptors on the bacteria that sense the pH and other components, respectively, may need to be activated in order for a filamentation response to be triggered.

The pH of the urine also has an effect on the activity of siderocalin, a molecule that is released by the host to obstruct iron acquisition of UPEC by enterobactin [109]. Siderocalin was more active at a higher pH and helped restrict bacterial growth, while a low pH decreased the activity. Siderocalin contains a positively charged binding site, which binds the iron molecules. It appears that in an acidic pH, this binding site may become protonated reducing its positive charge and affinity for iron. Therefore, urine pH appears to be able to affect the charge of many different molecules to affect their activity. These results support the idea that a naturally occurring urine component is responsible for inducing filamentation. It is known that pH affects the activity of different molecules

and to further understand what is occurring in the urine, the specific triggers need to be identified.

Given that the results have pointed towards a urine component or components, an initial urine fractionation began to narrow down the scope of molecules (Section 5.3.4). These results showed that urine was still able to trigger filamentation when large molecules were removed (Figure 5.7). Although this urine fractionation has narrowed down the size range to molecules less than 3000 Daltons, it is still difficult to comment on the components that are responsible for filamentation as this fraction still encompasses a large number of molecules. An extensive human urine metabolome database recently compiled and developed by Bouatra *et al.* (2013) includes thousands of urine metabolites, a large majority of which has a molecular weight less than 3000 [110].

This chapter has only begun the investigation into the urine trigger and has paved the way for further research. To pinpoint the size of this urine trigger, the small molecule urine fraction can be further fractionated using size exclusion chromatography. This technique is capable of fractionating molecules as small as 100 daltons. One technical limitation of this technique is the initial low sample volume that can be loaded onto the chromatography columns making it near impossible to use the flow cell infection model. Making use of the microfluidic infection model, described in Chapter 4, is possible; however, this would only yield microscopy observations of bacteria in the infection setting. Mass spectrometry could also be used to create a profile of the components in the small molecule urine fraction, similar to what was performed by Bouatra *et al.* (2013) who used this technique to create the extensive metabolome of human urine [110]. This would allow comparisons between urine that does and does not induce filamentation and reveal any differences. This chapter has established the general conditions in urine that trigger filamentation, such as concentration and pH, and the techniques mentioned above would allow for a more comprehensive analysis of the urine components. By creating a profile of different urine samples the varying components can be accurately identified, which could reveal potential pathways undertaken by the bacteria to trigger the filamentation during a UTI.

Determining the expression profile of different bacterial genes, using RNA sequencing, is another technique that can be utilised to uncover the intracellular pathway that bacteria use to induce filamentation. By pinpointing the genes involved, it could direct towards an external urine trigger. Comparisons could be made again between urine that does and

does not trigger bacteria to filament, to highlight any genes involved in blocking cell division. Figure 5.5 has also shown a link with urine pH and so comparing the genome expression of bacteria exposed to urine with a pH of 5.5 compared to a pH of 7 could offer some insight into how the bacteria behave. Analysis of gene expression has already identified one cell division gene, *damX*, as being involved in filamentation due to its upregulation during this phase [105]. In addition, multiple genes involved in metabolism were also found to be upregulated, offering a potential link between filamentation and bacterial metabolism [105]. Furthermore, this supports the idea that one or more small molecule urine metabolites could be involved in triggering the filamentous response.

The work in this chapter can be further expanded by using urine from different donors to investigate any differences between gender, age and other biological factors, however, this will become much clearer once the key component(s) of urine are identified. By using proteomic, transcriptomic and metabolomic techniques and analyses, the complex nature of urine and the UPEC signal-transduction and cell division responses that it triggers can be understood, with the long term aim of developing therapeutic interventions in these processes, which could help in treating these very common infections by increasingly antibiotic resistant strains of *E. coli*.

CHAPTER 6

GENERAL DISCUSSION

UTIs caused by UPEC are one of the most successful and persistent infections in the world. These infections are becoming more difficult to treat with the emergence of antibiotic resistant bacteria. Given this is such a common infection, there is a need for new treatment options. The infection cycle is a complex multi-stage process with much research being conducted on the different stages of this cycle. Some is focused on the initial stage of attachment, seen to be one of the most important steps. Other research, such as the work described in this thesis, has looked at the later stages of infection, particularly bacterial filamentation, which is thought to be a vital part of the infection cycle of UPEC, as it enables the bacteria to survive and reinitiate the infection cycle in the harsh environment of the urinary tract.

Filamentation is an intriguing response to conditions, such as those that arise during a UTI, where rod shaped bacteria grow to many times their typical length. Initially, filamentation was assumed to be the response of sick and dying bacteria in a population; however, evidence suggests that this is a survival mechanism to combat different stresses or promote growth and dispersal in various environments. The observation of successful growth and re-division of filaments, to reproduce viable rod shaped UPEC, demonstrate that the filamentation response is a deliberate mechanism that confers a survival advantage. Filamentation has been observed in studies including *in vivo* and *in vitro* infection models, however there has been little research done on the underlying mechanisms behind filamentation making it a relatively poorly understood process. As described previously in this thesis and the literature, filamentation can be instigated by many sources. These include antibiotics, larger organisms and the host immune system. Many of these external sources have been shown to trigger the bacterial DNA damage (SOS) response.

The overall focus of this thesis was to investigate the conditions that trigger the filamentous response in UPEC in order to identify the bacterial response pathway that is occurring during a UTI. This thesis addressed a series of objectives, which involved improving current models to reproduce the infection cycle and assess the extent of the filamentous response to different external conditions. These tools were then utilised to investigate the conditions required for filamentation during *in vitro* bladder cell infection and to test the potential involvement of the bacterial SOS response in UPEC filamentation during these infections.

6.1 Development of a Flow Chamber UTI Model

To begin to investigate bacterial filamentation, an appropriate model was required that could quantify filamentation and create a UPEC cell length distribution that reflected an overall assessment of the filamentous response to certain conditions. Chapter 3 examined the efficacy of currently established *in vitro* bladder cell infection models in modelling the UPEC infection cycle, especially filamentation. The first model to be tested was the static infection model, which was originally designed to look at the adherence, internalisation and growth of UPEC within the host bladder cells [1]. Although this method successfully showed a statistical difference between pathogenic UPEC and non-pathogenic *E. coli* in adherence, the following stages were less obvious and further optimisation was required. Furthermore, this model was not suitable for modelling filamentation as it had been shown that the bacteria do not adopt a filamentous morphology when grown in a static culture of urine [43, 96], as they are required to grow on a surface in a biofilm-like manner. Instead, the UPEC required an exposure to a flow of urine [43, 96], which provided another stress of force which could wash the bacteria away. Although this static model proved effective in modelling the early infection stages, another model was required to reproduce filamentation in the later infection stages to investigate the underlying triggers of bacterial filamentation.

The next model to be looked at was the recently established flow cell infection model, which appeared to better mimic *in vivo* bladder conditions. The static infection model promoted bacterial adherence by centrifugation, whereas this flow cell model had the bacteria attach to the bladder cells through the hydrodynamic flow of the urine [43], which was considered more representative of *in vivo* conditions. This model was designed to study the later infection stages of bacterial release, filamentation and then secondary infection. By developing the flow cell infection model in this study, using a new improved fluorescent UPEC reporter strain combined with microscopy and flow cytometry, it was demonstrated that the filamentous response could be measured reproducibly. Flow cytometry was able to measure the relative length of a high number of bacterial cells, which gave an indication of the proportion of filamentous bacteria. Although microscopy was used to visually confirm the presence of bacterial filaments, it can also allow accurate cell lengths to be measured. However, this method relies on clearly distinguishable outlines of individual bacterial cells, which was very difficult to obtain from these

experiments due to the extensive lengths of the filamentous bacteria obtained, which, when mounted on microscope slides, resulted in tangled and overlapping bacteria. More work is required to determine an effective method to accurately measure the lengths of very filamentous bacteria. Although a microscopic method was developed to capture clear images of filaments using focus-stacked microscopy [96], this still required the bacteria to be separated and not contacting neighbouring cells. Therefore, although flow cytometry cannot produce absolute length measurements, it is still an effective technique to observe morphological changes in a large number of bacteria.

By implementing this method with the established flow cell model (Section 2.4), a clear difference between filamentous and short bacteria was observed in the cell length distributions obtained from flow cytometry. This allowed for clear differences in the filamentous response to be observed when the UPEC was exposed to different external conditions, paving the way for further research into the causes of filamentation in UTIs.

By developing new fluorescent strains of UPEC, the bacteria were uniformly labelled under different conditions and could be readily visualised inside cultured human bladder cells. An interesting observation, which had not been seen previously, was the appearance of multi-lobed rosette-like morphologies of the IBCs within the infected bladder cells (Section 3.3.4.1). Previous studies had only reported IBCs as a single large globular mass within an infected bladder cell [16, 42, 44, 51]. As discussed in Section 3.4, the reasons for this morphology are unknown however; they might be attributed to multiple internalised bacteria or result from a stage of initial intracellular UPEC growth and division prior to IBC cluster formation. The latter could be more likely as the first hypothesis would require multiple bacteria to become internalised in the same part of the bladder cell. This demonstrated that there was still much more to discover about how UPEC behave during their infection cycle and how they establish infection within bladder cells.

6.2 Real Time Microscopy of the Infection Cycle

To further understand how filamentation occurred during an infection, microfluidics and real time microscopy were utilised to develop a novel *in vitro* UPEC infection model. While time-lapse microscopy had been previously used to observe the infection progress in mouse bladder explants, including IBC development [42], the dynamic behaviour of

the host bladder cells *in vitro* and the direct observation of the development of filamentous bacteria had not.

Initially, it was demonstrated that infected bladder cells, even those containing rather large IBCs, showed similar mobility characteristics compared to uninfected bladder cells in the same experiment (Section 4.3.2). This supported the idea that the bacteria in IBCs did not kill their hosts and therefore could effectively use the bladder cells for protection and survival against the harsh external environment. Justice *et al.* (2004) showed that polymorphonuclear leukocytes (PMNs) were able to distinguish and were attracted to infected bladder cells, however could not immediately access the internalised bacteria [42]. This allowed the bacteria sufficient time to increase numbers in an IBC, so when the PMNs did enter the bladder cell they were unable to clear all of the bacteria. This demonstrated that the intracellular environment offers protection to the bacteria from external factors such as the host immune system and some antibiotics that cannot penetrate mammalian cells; therefore, it would be in the best interest of the bacteria to keep their host alive. The results presented here are consistent with these observations and indicated that IBCs do not immediately kill their host cells in the *in vitro* infection models.

The real time microscopy also directly revealed that the bacteria emerged filamentous from the bladder cells (Section 4.3.4). This had not been previously demonstrated and it had remained unclear whether the bacteria filamented within or after expulsion from their host. Observing the behaviour of an IBC exposed to a flow of urine showed that the bacteria emerged from the bladder cell whilst generating filaments concurrently or by having already become filamentous inside the bladder cells. It was known that concentrated urine could induce filamentation [43], but the exact mechanism by which the bacteria sensed the urine was unknown. The permeability of the bladder cells during urine exposure, observed in the real time microscopy (Section 4.3.3), suggested a way in which the bacteria could directly sense the urine from their intracellular locations. This would provide a survival advantage for the bacteria as they emerged from the safe haven of the bladder cell and disperse into the harsh environment of the bladder, where they were immediately exposed to many factors that aimed to eliminate them, including the flow of urine and host immune response.

The above observations raise the question of how urine or the host environment is sensed and induces filamentation in a real UTI or an *in vivo* mouse model of UTI. The results

presented here would suggest that infected bladder cells become permeabilised prior to the onset of significant filamentation and dispersal. However, it remains a possibility that the permeability of the bladder cells in response to urine may be an artefact of the *in vitro* infection model. This would be most likely due to the non-fully differentiated state of the immortalised bladder cells, which would be expected to make them more sensitive to lysis after urine exposure compared to the fully differentiated umbrella cells of the bladder, which accommodate a wide range of osmotic forces *in vivo*. How and when lysis or permeabilisation occurs *in vivo* is therefore currently less clear, although it might instead require extensive IBC development that physically overwhelms and permeabilises the host bladder cell. In support of this hypothesis, *in vivo* UTI models have reported the development of extremely large IBC pods, which have yet to be observed *in vitro*. Therefore, more research is required to understand how the bladder host cells behave during *in vitro* and *in vivo* infections and how they respond to urine. Nevertheless, the results reported here suggested a plausible mechanism by which direct exposure to urine, after the bladder cell becomes permeable, can provide the signals that UPEC respond to for initiating the filamentation response. Precisely how and when this permeabilisation occurs may differ between the *in vitro* and *in vivo* UTI models. However, *in vitro* models are still a valuable tool to study UPEC infection as they can effectively show any effects on the degree of bacterial filamentation brought on by different factors such as urine.

Microfluidic tools have been previously used for drug screening purposes as they can be high throughput and cost efficient [99, 103, 104]. As discussed in Section 4.4, this microfluidic model can be implemented as a screening tool to discern the effectiveness of drugs on the development of UPEC. As this model can visualise the development of the bacteria directly, any effects can be more accurately attributed to certain points in the infection cycle.

At the conclusion of Chapter 4, time-lapse microscopy provided further insight into the later stages of the infection cycle using a novel microfluidic infection model. It highlighted a possible pathway that externally triggered filamentation in UPEC and suggested possible limitations with *in vitro* models that needed to be addressed. For future studies into the lifecycle of UPEC, the microfluidic infection model developed here can be used to directly observe any changes or effects to the infection progress as a result of introducing any drugs or altering any external factors. In addition, fluorescence microscopy and staining of cell components, both bacterial and mammalian, could be

used to reveal the changes that occur during different processes such as the re-modelling of the mammalian cell to house the developing IBC. By viewing the effects in real time, it is anticipated that the microfluidic model can help further the understanding of the underlying mechanisms of the UTI cellular infection cycle, and help new therapies develop for the future treatment of recurrent and antibiotic resistant UTIs.

6.3 Conditions that Trigger Bacterial Filamentation

As established in the literature [43, 96], bacteria appeared to be sensing an external trigger in urine, during infection of bladder cells, and responded by becoming filamentous, however the exact mechanisms underlying this morphology change remain largely unknown. Studies have reported contradictory results regarding the involvement of UPEC genes, such as *damX* [105] and *sulA* [54]. The gene *sulA* forms part of the SOS response, which, as mentioned previously, is responsible for many cases of experimentally induced filamentation.

External triggers such as the immune response and antibiotics are known to trigger the SOS response; however, investigations ([43, 96] and Chapter 5) have implicated the urine as another external trigger, but it was not known whether this triggers the SOS response or another pathway leading to filamentation. While the SOS response has been the widely accepted mode of filamentation, the work presented in this thesis has suggested the potential for alternative pathways independent of SOS that could be employing metabolism. It is very likely that UPEC possess multiple pathways that result in them adopting a filamentous morphology and the urine may be involved in one such pathway.

This was supported by the results presented in Section 5.3.1, which showed that filamentation occurred in the absence of the two known SOS induced cell division inhibitors *sulA* and *sfiC*. This strongly suggested that the block in cell division observed was not due to the SOS response but through another means. These results are consistent with Khandige *et al.* (2016) who proposed that UPEC filamentation occurs via *damX*, although the exact pathway is yet to be elucidated.

Results presented in Chapter 5 demonstrated that UPEC filamentation during *in vitro* bladder cell infection was a response to certain constituents of urine that are yet to be uniquely identified. Comparing the effect of synthetic human urine (SHU) to real human urine showed that filamentation was not a response to general urine properties such as

concentration or pH *per se*, but that UPEC appeared to be sensing a specific urine component (Section 5.3.3 and [96]). In addition, this urine component appeared to be sensitive (reversibly) to changes in urine pH (Section 5.3.2) and had a size less than approximately 3000 Daltons (Section 5.3.4). These observations suggested that the component or components of urine triggering bacterial filamentation were most likely pH sensitive metabolites.

A published transcriptome study performed on the later stages of the UPEC infection cycle found that multiple genes, many involved in metabolism, were upregulated during the filamentation stage [105]. This supported the studies in Chapter 5, which suggested a metabolite component of urine responsible for filamentation. If a metabolite in the urine were being sensed by the UPEC, then most likely it would affect bacterial metabolism genes, or affect a stress response, which could in turn affect cell division genes resulting in filamentous bacteria. The present study has laid out the foundation and made the first steps towards identifying and understanding precisely what component(s) of urine are triggering filamentation of UPEC. Knowing these components will be a major advance in the understanding of UTIs and will in turn allow us to understand why UPEC respond in a filamentous manner during the late stages of bladder cell infection. This in turn will also help identify the important bacterial genes that contribute to signalling, establishing and maintaining the block to bacterial division that occurs during filamentation.

6.4 Experimental Limitations

For the research conducted in this thesis a single urine donor was used, except in Section 5.3.5 which compared different urine batches and their ability to induce filamentation. Although using a single donor can introduce some bias, previous research has shown filamentation occurring in human urine from different urine donors both *in vitro* (Andersen *et al.* 2012) and *in vivo* (Rosen *et al.* 2007). Urine is a complex fluid with high variability and as briefly mentioned in Section 2.3 a single donor was used to attempt to reduce this variability. Therefore, as the novel research in this thesis focused on narrowing down the component in human urine that induces this filamentation, a single donor reduced the large variability in urine composition between individuals and removed a significant variable in this experimental work. As mentioned at the end of Section 5.4, once the relevant urine components have been identified, different urine donors can be implemented to begin comparing the differences in the urine components and their effect

on bacterial filamentation to begin to understand this bacterial behaviour in relation to human urine in general.

The quantification of the proportion of filamentous bacteria in a population was made simple using flow cytometry, which allowed a large number of bacteria to be analysed to provide a better reflection of the bacterial population. Analysis of microscopy images would have been impractical and not accurate in this work due to the tangled nature of the filaments harvested from the flow chamber. For the work in this thesis, the control used was the sample that appeared to yield the shortest bacteria in each experiment, based on the overlay of the flow cytometry histograms. To improve this quantification, the control sample should have been short bacteria obtained from culturing in liquid LB broth, which would yield uniform rod shaped bacteria. This control would better distinguish between typical rod shaped bacteria and any filamentous bacteria. The control samples used in this thesis could have potentially underestimated the proportion of filamentous bacteria. This is due to the stresses applied to the bacteria in the flow chamber that require the bacteria to progress through the infection cycle, which could lead to a non-uniform population of bacteria that may be slightly longer than the typical rod shape, even in conditions that do not promote filamentation. However, the trends observed in the flow cytometry are still accurate showing that the urine has a clear effect on the bacteria and induces filamentation through a still unknown inducer.

6.5 Implications for Understanding UPEC

UPEC is responsible for causing one of the most common infections worldwide and the alarming rise in antibiotic resistance will only worsen this growing problem. Alternatives to antibiotics are being actively sought to treat these infections. By further understanding bacterial filamentation in UPEC, it is possible to further understand the pathogenesis and attenuate the virulence of these infections. Current research is attempting to develop treatments that are specific to UPEC such as targeting vaccines to certain virulence factors including siderophores, toxins and adhesins [2]. Other studies have shown that extracts of cranberries can impede the adhesion of *E. coli*, mainly through P fimbriae, to kidney uroepithelial cells by affecting the bacterial cell surface [115-117]. Recently, it was found that inactivating FimH on Type 1 pili of UPEC could promote their removal from the gut and therefore reduce the incidence of a UTI, a technique that has minimal effect on the other bacterial flora in the gut [118].

Determining the external factors that control the infection cycle of UPEC could also help researchers introduce a whole array of new age treatments for UTIs that do not rely on antibiotics. For example, the general properties of urine could be altered during a UTI to restrict the growth and development of UPEC, such as altering pH towards alkali to promote the activity of the siderophore siderocalin [109] or inhibit the ability of the bacteria to become filamentous (Section 5.3.2). Since host nutrition and metabolism can affect the composition of the urine, this could be therapeutically modulated in order to inhibit the development of UPEC. Indeed, a well-established treatment for UTI is the thorough hydration of patients usually by advice to increase water intake. It is therefore possible that a significant reason behind the effectiveness of this treatment is in the prevention of filamentation and UPEC dispersal because of more dilute urine and greater flushing of urinary tract surfaces through micturition.

It has been demonstrated that certain metabolites have been shown to promote siderocalin activity [109]. Furthermore, this thesis has suggested that certain metabolites may trigger filamentation during a UTI (Section 5.3.4). With further research, it could be possible to establish certain urinary compositions that could promote the clearance of UPEC or even develop drug treatments that do not directly target the bacteria but factors in the host that could impede bacterial growth. This could remove the side effects that arise with antibiotic use and ameliorate the problem of antibiotic resistance.

APPENDIX

The supplementary data can be found on the accompanying USB along with a digital copy of this thesis.

Supplementary Video 1 (S1): Accompanying Figure 4.3

Time-lapse microscopy of infected PD07i bladder cells moving around the field of view. Image captured every 10 mins for 21 hours. Scale bar is 20 μm, 60X oil objective, GFP exposure 100 ms, TEXAS RED exposure 500 ms.

Supplementary Video 2 (S2): Accompanying Figure 4.4

Time-lapse microscopy of infected PD07i bladder cells becoming permeable during exposure to a flow of urine. Image captured every 20 mins for 20.5 hours. Scale bar is 20 μm, 40X oil objective, GFP exposure 50 ms, TEXAS RED exposure 100 ms.

Supplementary Video 3 (S3): Accompanying Figure 4.5

Time-lapse microscopy depicting filamentous bacteria emerging from an infected bladder cell. Image captured every 10 mins for 24 hours. Scale bar is 10 μm, 40X oil objective, GFP exposure 50 ms.

Supplementary Video 4 (S4): Accompanying Figure 4.6

Time-lapse microscopy depicting short bacteria emerging from an infected bladder cell. Image captured every 10 mins for 24 hours. Scale bar is 10 μm, 40X oil objective, GFP exposure 50 ms.

REFERENCES

1. Berry RE, Klumpp DJ, Schaeffer AJ: **Urothelial cultures support intracellular bacterial community formation by uropathogenic Escherichia coli**. *Infection and immunity* 2009, **77**(7):2762-2772.
2. Flores-Mireles AL, Walker JN, Caparon M, Hultgren SJ: **Urinary tract infections: epidemiology, mechanisms of infection and treatment options**. *Nature reviews Microbiology* 2015, **13**(5):269-284.
3. Ulett GC, Totsika M, Schaale K, Carey AJ, Sweet MJ, Schembri MA: **Uropathogenic Escherichia coli virulence and innate immune responses during urinary tract infection**. *Current opinion in microbiology* 2013, **16**(1):100-107.
4. Hunstad DA, Justice SS: **Intracellular lifestyles and immune evasion strategies of uropathogenic Escherichia coli**. *Annual review of microbiology* 2010, **64**:203-221.
5. Ikaheimo R, Siitonen A, Heiskanen T, Karkkainen U, Kuosmanen P, Lipponen P, Makela PH: **Recurrence of urinary tract infection in a primary care setting: analysis of a 1-year follow-up of 179 women**. *Clinical Infectious Diseases* 1996, **22**(1).
6. Bien J, Sokolova O, Bozko P: **Role of Uropathogenic Escherichia coli Virulence Factors in Development of Urinary Tract Infection and Kidney Damage**. *International journal of nephrology* 2012, **2012**:681473.
7. Trautner BW, Hull RA, Darouiche RO: **Escherichia coli 83972 inhibits catheter adherence by a broad spectrum of uropathogens**. *Urology* 2003, **61**(5):1059-1062.
8. Darouiche RO, Donovan WH, Del Terzo M, I. TJ, Rudy DC, Hull RA: **Pilot trial of bacterial interference for preventing urinary tract infection**. *Urology* 2001, **58**(3).
9. Chang A, Hammond TG, Sun TT, Zeidel ML: **Permeability properties of the mammalian bladder apical membrane**. *The American Journal of Physiology* 1994, **267**.
10. Lewis SA: **Everything you wanted to know about the bladder epithelium but were afraid to ask**. *American Journal of Physiology Renal Physiology* 2000, **278**(6).

11. Martini FH, Nath JL: **The Urinary System**. In: *Fundamentals of Anatomy and Physiology.* 8 edn: Pearson Benjamin Cummings; 2009: 965-1008.
12. Ross MH, Pawlina W: **Urinary System**. In: *Histology: A Text and Atlas.* 5 edn: Lippincott Williams and Wilkins; 2006: 646-685.
13. Apodaca G: **The uroepithelium: not just a passive barrier**. *Traffic* 2004, **5**(3):117-128.
14. Truschel ST, Ruiz WG, Shulman T, Pilewski J, Sun T-T, Zeidel ML, Apodaca G: **Primary Uroepithelial Cultures**. *Journal of Biological Chemistry* 1999, **274**(21):15020-15029.
15. Pak J, Pu Y, Zhang ZT, Hasty DL, Wu XR: **Tamm-Horsfall protein binds to type 1 fimbriated Escherichia coli and prevents E. coli from binding to uroplakin Ia and Ib receptors**. *The Journal of biological chemistry* 2001, **276**(13):9924-9930.
16. Rosen DA, Hooton TM, Stamm WE, Humphrey PA, Hultgren SJ: **Detection of Intracellular Bacterial Communities in Human Urinary Tract Infection**. *PLoS Medicine* 2007, **4**(12).
17. Johnson JR, Russo TA: **Extraintestinal pathogenic Escherichia coli : "The other bad E coli "**. *Journal of Laboratory and Clinical Medicine* 2002, **139**(3):155-162.
18. Oelschlaeger TA, Dobrindt U, Hacker J: **Pathogenicity islands of uropathogenic E. coli and the evolution of virulence**. *International Journal of Antimicrobial Agents* 2002, **19**(6).
19. Schwan WR: **Flagella allow uropathogenic Escherichia coli ascension into murine kidneys**. *International journal of medical microbiology : IJMM* 2008, **298**(5-6):441-447.
20. Mulvey MA, Schilling JD, Martinez JJ, Hultgren SJ: **Bad bugs and beleaguered bladders: interplay between uropathogenic Escherichia coli and innate host defenses**. *Proceedings of the National Academy of Sciences of the United States of America* 2000, **97**(16).
21. Tarchouna M, Ferjani A, Ben-Selma W, Boukadida J: **Distribution of uropathogenic virulence genes in Escherichia coli isolated from patients with urinary tract infection**. *International journal of infectious diseases : IJID : official publication of the International Society for Infectious Diseases* 2013, **17**(6):e450-453.

22. Klemm P, Christiansen G: **Three fim genes required for the regulation of length and mediation of adhesion of Eschericha coli type 1 fimbriae**. *Molecular and General Genetics* 1987, **208**(3).
23. Busch A, Phan G, Waksman G: **Molecular mechanism of bacterial type 1 and P pili assembly**. *Philosophical transactions Series A, Mathematical, physical, and engineering sciences* 2015, **373**(2036).
24. Martinez JJ, Mulvey MA, Schilling JD, Pinkner JS, Hultgren SJ: **Type 1 pilus-mediated bacterial invasion of bladder epithelial cells**. *The EMBO Journal* 2000, **19**.
25. Jones CH, Pinkner JS, Roth R, Heuser J, Nicholes AV, Abraham SN, Hultgren SJ: **FimH adhesin of type 1 pili is assembled into a fibrillar tip structure in the Enterobacteriaceae**. *Proceedings of the National Academy of Sciences of the United States of America* 1995, **92**.
26. Russell PW, Orndorff PE: **Lesions in two Escherichia coli type 1 pilus genes alter pilus number and length without affecting receptor binding**. *Journal of bacteriology* 1992, **174**.
27. Klemm P: **Two regulatory fim genes, fimB and fimE, control the phase variation of type 1 fimbriae in Eschericha coli**. *The EMBO Journal* 1986, **5**(6).
28. Abraham JM, Freitag C, S., Clements JR, Eisenstein BI: **An invertible element of DNA controls phase variation of type 1 fimbriae of Escherichia coli**. *Proceedings of the National Academy of Sciences of the United States of America* 1985, **82**.
29. Costerton JW, Stewart PS, Greenberg EP: **Bacterial Biofilms: A Common Cause of Persistent Infections**. *Science* 1999, **284**.
30. Hancock V, Ferrieres L, Klemm P: **Biofilm formation by asymptomatic and virulent urinary tract infectious Escherichia coli strains**. *FEMS microbiology letters* 2007, **267**(1):30-37.
31. Allsopp LP, Totsika M, Tree JJ, Ulett GC, Mabbett AN, Wells TJ, Kobe B, Beatson SA, Schembri MA: **UpaH is a newly identified autotransporter protein that contributes to biofilm formation and bladder colonization by uropathogenic Escherichia coli CFT073**. *Infection and immunity* 2010, **78**(4):1659-1669.

32. Fischbach MA, Lin H, Zhou L, Yu Y, Abergel RJ, Liu DR, Raymond KN, Wanner BL, Strong RK, Walsh CT *et al*: **The pathogen-associated iroA gene cluster mediates bacterial evasion of lipocalin 2**. *Proceedings of the National Academy of Sciences of the United States of America* 2006, **103**(44):16502-16507.

33. Raymond KN, Dertz EA, Kim SS: **Enterobactin: an archetype for microbial iron transport**. *Proceedings of the National Academy of Sciences of the United States of America* 2003, **100**(7):3584-3588.

34. Wiles TJ, Kulesus RR, Mulvey MA: **Origins and virulence mechanisms of uropathogenic Escherichia coli**. *Experimental and molecular pathology* 2008, **85**(1):11-19.

35. Davis JM, Rasmussen SB, O'Brien AD: **Cytotoxic necrotizing factor type 1 production by uropathogenic Escherichia coli modulates polymorphonuclear leukocyte function**. *Infection and immunity* 2005, **73**(9):5301-5310.

36. Yamamoto S: **Molecular epidemiology of uropathogenic Escherichia coli**. *Journal of infection and chemotherapy : official journal of the Japan Society of Chemotherapy* 2007, **13**(2):68-73.

37. Mills M, Meysick KC, O'Brien AD: **Cytotoxic necrotizing factor type 1 of uropathogenic Escherichia coli kills cultured human uroepithelial 5637 cells by an apoptotic mechanism**. *Infection and immunity* 2000, **68**.

38. Miraglia AG, Travaglione S, Meschini S, Falzano L, Matarrese P, Quaranta MG, Viora M, Fiorentini C, Fabbri A: **Cytotoxic necrotizing factor 1 prevents apoptosis via the Akt/IkappaB kinase pathway: role of nuclear factor-kappaB and Bcl-2**. *Molecular biology of the cell* 2007, **18**(7):2735-2744.

39. Justice SS, Hunstad DA, Cegelski L, Hultgren SJ: **Morphological plasticity as a bacterial survival strategy**. *Nature Reviews Microbiology* 2008, **6**(2).

40. Corno G, Jurgens K: **Direct and indirect effects of protist predation on population size structure of a bacterial strain with high phenotypic plasticity**. *Applied and environmental microbiology* 2006, **72**(1):78-86.

41. Chen K, Sun GW, Chua KL, Gan YH: **Modified virulence of antibiotic-induced Burkholderia pseudomallei filaments**. *Antimicrobial agents and chemotherapy* 2005, **49**(3):1002-1009.

42. Justice SS, Hung C, Theriot JA, Fletcher DA, Anderson GG, Footer MJ, Hultgren SJ: **Differentiation and developmental pathways of uropathogenic Escherichia coli in urinary tract pathogenesis**. *Proceedings of the National Academy of Sciences of the United States of America* 2004, **101**(5):1333-1338.

43. Andersen TE, Khandige S, Madelung M, Brewer J, Kolmos HJ, Moller-Jensen J: **Escherichia coli uropathogenesis in vitro: invasion, cellular escape, and secondary infection analyzed in a human bladder cell infection model**. *Infection and immunity* 2012, **80**(5):1858-1867.

44. Mulvey MA, Schilling JD, Hultgren SJ: **Establishment of a persistent Escherichia coli reservoir during the acute phase of a bladder infection**. *Infection and immunity* 2001, **69**(7):4572-4579.

45. Anderson GG, Palermo JJ, Schilling JD, Roth R, Heuser J, Hultgren SJ: **Intracellular bacterial biofilm-like pods in urinary tract infections**. *Science* 2003, **301**(5629):105-107.

46. Zhou G, Mo WJ, Sebbel P, Min G, Neubert TA, Glockshuber R, Wu XR, Sun TT, Kong XP: **Uroplakin Ia is the urothelial receptor for uropathogenic Escherichia coli: evidence from in vitro FimH binding**. *Journal of Cell Science* 2001, **114**.

47. Mulvey MA: **Induction and Evasion of Host Defenses by Type 1-Piliated Uropathogenic Escherichia coli**. *Science* 1998, **282**(5393):1494-1497.

48. Hasman H, Chakraborty T, Klemm P: **Antigen-43-mediated autoaggregation of Escherichia coli is blocked by fimbriation**. *Journal of bacteriology* 1999, **181**.

49. Reigstad CS, Hultgren SJ, Gordon JI: **Functional genomic studies of uropathogenic Escherichia coli and host urothelial cells when intracellular bacterial communities are assembled**. *The Journal of biological chemistry* 2007, **282**(29):21259-21267.

50. Hannan TJ, Mysorekar IU, Chen SL, Walker JN, Jones JM, Pinkner JS, Hultgren SJ, Seed PC: **LeuX tRNA-dependent and -independent mechanisms of Escherichia coli pathogenesis in acute cystitis**. *Molecular microbiology* 2008, **67**(1):116-128.

51. Justice SS, Lauer SR, Hultgren SJ, Hunstad DA: **Maturation of intracellular Escherichia coli communities requires SurA**. *Infection and immunity* 2006, **74**(8):4793-4800.

52. Billips BK, Schaeffer AJ, Klumpp DJ: **Molecular basis of uropathogenic Escherichia coli evasion of the innate immune response in the bladder**. *Infection and immunity* 2008, **76**(9):3891-3900.

53. Song J, Duncan MJ, Li G, Chan C, Grady R, Stapleton A, Abraham SN: **A novel TLR4-mediated signaling pathway leading to IL-6 responses in human bladder epithelial cells**. *PLoS pathogens* 2007, **3**(4):e60.

54. Justice SS, Hunstad DA, Seed PC, Hultgren SJ: **Filamentation by Escherichia coli subverts innate defenses during urinary tract infection**. *Proceedings of the National Academy of Sciences of the United States of America* 2006, **103**(52):19884-19889.

55. Greene SE, Hibbing ME, Janetka J, Chen SL, Hultgren SJ: **Human Urine Decreases Function and Expression of Type 1 Pili in Uropathogenic Escherichia coli**. *mBio* 2015, **6**(4):e00820.

56. Weichhart T, Haidinger M, Horl WH, Saemann MD: **Current concepts of molecular defence mechanisms operative during urinary tract infection**. *European journal of clinical investigation* 2008, **38 Suppl 2**:29-38.

57. Bister B, Bischoff D, Nicholson GJ, Valdebenito M, Schneider K, Winkelmann G, Hantke K, Sussmuth RD: **The structure of salmochelins: C-glucosylated enterobactins of Salmonella enterica**. *BioMetals* 2004, **17**(4).

58. Smith KD: **Iron metabolism at the host pathogen interface: lipocalin 2 and the pathogen-associated iroA gene cluster**. *The international journal of biochemistry & cell biology* 2007, **39**(10):1776-1780.

59. Hunstad DA, Justice SS, Hung CS, Lauer SR, Hultgren SJ: **Suppression of bladder epithelial cytokine responses by uropathogenic Escherichia coli**. *Infection and immunity* 2005, **73**(7):3999-4006.

60. Wu LJ, Errington J: **Nucleoid occlusion and bacterial cell division**. *Nature reviews Microbiology* 2011, **10**(1):8-12.

61. Adams DW, Errington J: **Bacterial cell division: assembly, maintenance and disassembly of the Z ring**. *Nature reviews Microbiology* 2009, **7**(9):642-653.

62. Harry EJ: **Bacterial cell division: regulating Z-ring formation**. *Molecular Microbilogy* 2001, **40**.

63. Thanbichler M: **Synchronization of chromosome dynamics and cell division in bacteria**. *Cold Spring Harbor perspectives in biology* 2010, **2**(1):a000331.

64. Jensen RB: **Coordination between chromosome replication, segregation, and cell division in Caulobacter crescentus**. *Journal of bacteriology* 2006, **188**(6):2244-2253.

65. Mulder E, Woldringh CL: **Actively replicating nucleoids influence positioning of division sites in Escherichia coli filaments forming cells lacking DNA**. *Journal of bacteriology* 1989, **171**.

66. Nielsen HJ, Youngren B, Hansen FG, Austin S: **Dynamics of Escherichia coli chromosome segregation during multifork replication**. *Journal of bacteriology* 2007, **189**(23):8660-8666.

67. Jensen RB, Wang SC, Shapiro L: **A moving DNA replication factory in Caulobacter cresentus**. *The EMBO Journal* 2001, **20**.

68. Bernhardt TG, de Boer PA: **SlmA, a nucleoid-associated, FtsZ binding protein required for blocking septal ring assembly over Chromosomes in E. coli**. *Molecular cell* 2005, **18**(5):555-564.

69. Tonthat NK, Milam SL, Chinnam N, Whitfill T, Margolin W, Schumacher MA: **SlmA forms a higher-order structure on DNA that inhibits cytokinetic Z-ring formation over the nucleoid**. *Proceedings of the National Academy of Sciences of the United States of America* 2013, **110**.

70. Dajkovic A, Lan G, Sun SX, Wirtz D, Lutkenhaus J: **MinC spatially controls bacterial cytokinesis by antagonizing the scaffolding function of FtsZ**. *Current biology : CB* 2008, **18**(4):235-244.

71. Park KT, Wu W, Lovell S, Lutkenhaus J: **Mechanism of the asymmetric activation of the MinD ATPase by MinE**. *Molecular microbiology* 2012, **85**(2):271-281.

72. Shih YL, Zheng M: **Spatial control of the cell division site by the Min system in Escherichia coli**. *Environmental microbiology* 2013, **15**(12):3229-3239.

73. Lutkenhaus J: **Assembly dynamics of the bacterial MinCDE system and spatial regulation of the Z ring**. *Annual review of biochemistry* 2007, **76**:539-562.

74. Mukherjee A, Cao C, Lutkenhaus J: **Inhibition of FtsZ polymerization by SulA, an inhibitor of septation in Escherichia coli**. *Proceedings of the National Academy of Sciences of the United States of America* 1998, **95**.

75. Trusca D, Scott S, Thompson C, Bramhill D: **Bacterial SOS Checkpoint Protein SulA Inhibits Polymerization of Purified FtsZ Cell Division Protein**. *Journal of bacteriology* 1998, **180**(15).

76. Arends SJ, Williams K, Scott RJ, Rolong S, Popham DL, Weiss DS: **Discovery and characterization of three new Escherichia coli septal ring proteins that contain a SPOR domain: DamX, DedD, and RlpA**. *Journal of bacteriology* 2010, **192**(1):242-255.

77. Gerding MA, Liu B, Bendezu FO, Hale CA, Bernhardt TG, de Boer PA: **Self-enhanced accumulation of FtsN at Division Sites and Roles for Other Proteins with a SPOR domain (DamX, DedD, and RlpA) in Escherichia coli cell constriction**. *Journal of bacteriology* 2009, **191**(24):7383-7401.

78. Halbert CL, Demers GW, Galloway DA: **The E7 Gene of Human Papillomavirus Type 16 is Sufficient for Immortalization of Human Epithelial Cells**. *Journal of Virology* 1991, **65**(1).

79. Graham FL, Smiley J, Russell WC, Nairn R: **Characteristics of a Human Cell Line Transformed by DNA from Human Adenovirus Type 5**. *The Journal of General Virology* 1977, **36**(1).

80. Burke C, Liu M, Britton W, Triccas JA, Thomas T, Smith AL, Allen S, Salomon R, Harry E: **Harnessing single cell sorting to identify cell division genes and regulators in bacteria**. *PLoS One* 2013, **8**(4):e60964.

81. Carey AJ, Tan CK, Ipe DS, Sullivan MJ, Cripps AW, Schembri MA, Ulett GC: **Urinary tract infection of mice to model human disease: Practicalities, implications and limitations**. *Critical reviews in microbiology* 2016, **42**(5):780-799.

82. Wright KJ, Seed PC, Hultgren SJ: **Development of intracellular bacterial communities of uropathogenic Escherichia coli depends on type 1 pili**. *Cellular microbiology* 2007, **9**(9):2230-2241.

83. Elsinghorst EA: **Measurement of invasion by gentamicin resistance**. *Methods in Enzymology* 1994, **236**.

84. Weiser JN, Chong ST, Greenberg D, Fong W: **Identification and characterization of a cell envelope protein of Haemophilus influenzae contributing to phase variation in colony opacity and nasopharyngeal colonization**. *Molecular microbiology* 1995, **17**(3):555-564.

85. Dower WJ, Miller JF, Ragsdale CW: **High efficiency transformation of E. coli by high voltage electroporation**. *Nucleic acids research* 1988, **16**(13):6127-6145.

86. Ghosal D, Trambaiolo D, Amos LA, Lowe J: **MinCD cell division proteins form alternating copolymeric cytomotive filaments**. *Nature communications* 2014, **5**:5341.

87. Romih R, Korosec P, de Mello W, Jr., Jezernik K: **Differentiation of epithelial cells in the urinary tract**. *Cell and tissue research* 2005, **320**(2):259-268.

88. Urban JH, Vogel J: **Translational control and target recognition by Escherichia coli small RNAs in vivo**. *Nucleic acids research* 2007, **35**(3):1018-1037.

89. Robinson JM, Karnovsky MJ: **Evaluation of the Polyene Antibiotic Filipin as a Cytochemical Probe for Membrane Cholesterol**. *The Journal of Histochemistry and Cytochemistry* 1980, **28**(2).

90. Awasthi-Kalia M, Schnetkamp PP, Deans JP: **Differential Effects of Filipin and Methyl-beta-cyclodextrin on B Cell Receptor Signalling**. *Biochemical and Biophysical Research Communications* 2001, **287**(1).

91. Shaner NC, Steinbach PA, Tsien RY: **A guide to choosing fluorescent proteins**. *Nature methods* 2005, **2**(12):905-909.

92. Ellermeier CD, Janakiraman A, Slauch JM: **Construction of targeted single copy lac fusions using lambda Red and FLP-mediated site-specific recombination in bacteria**. *Gene* 2002, **290**(1-2):153-161.

93. Murphy KC, Campellone KG: **Lambda Red-mediated recombinogenic engineering of enterohemorrhagic and enteropathogenic E. coli**. *BMC Molecular Biology* 2003.

94. Datsenko KA, Wanner BL: **One-step inactivation of chromosomal genes in Escherichia coli K-12 using PCR products**. *Proceedings of the National Academy of Sciences of the United States of America* 2000, **97**(12):6640-6645.

95. Murphy KC: **Use of bacteriophage lambda recombination functions to promote gene replacement in Escherichia coli**. *Journal of bacteriology* 1998, **180**(8).

96. Klein K, Palarasah Y, Kolmos HJ, Moller-Jensen J, Andersen TE: **Quantification of filamentation by uropathogenic Escherichia coli during experimental bladder cell infection by using semi-automated image analysis**. *Journal of microbiological methods* 2015, **109**:110-116.

97. Staerk K, Khandige S, Kolmos HJ, Moller-Jensen J, Andersen TE: **Uropathogenic Escherichia coli Express Type 1 Fimbriae Only in Surface Adherent Populations Under Physiological Growth Conditions**. *J Infect Dis* 2016, **213**(3):386-394.

98. Whitesides GM: **The origins and the future of microfluidics**. *Nature* 2006, **442**(7101):368-373.

99. Wlodkowic D, Darzynkiewicz Z: **Rise of the micromachines: microfluidics and the future of cytometry**. *Methods in cell biology* 2011, **102**:105-125.

100. Lee PJ, Gaige TA, Hung PJ: **Dynamic cell culture: a microfluidic function generator for live cell microscopy**. *Lab on a chip* 2009, **9**(1).

101. **CellASIC ONIX Microfluidic Platform**. In. Edited by Millipore M. USA: EMD Millipore Corporation; 2014.

102. **CellASIC ONIX M04S-03 Microfluidic Plates**. In. Edited by Millipore M. USA: EMD Millipore Corporation; 2012.

103. Lee PJ, Gaige TA, Ghorashian N, Hung PJ: **Microfluidic tissue model for live cell screening**. *Biotechnology progress* 2007, **23**(4):946-951.

104. Lee PJ, Ghorashian N, Gaige TA, Hung PJ: **Microfluidic System for Automated Cell-based Assays**. *JALA Charlottesville Va* 2007, **12**(6).

105. Khandige S, Asferg CA, Rasmussen KJ, Larsen MJ, Overgaard M, Andersen TE, Moller-Jensen J: **DamX Controls Reversible Cell Morphology Switching in Uropathogenic Escherichia coli**. *mBio* 2016, **7**(4).

106. Ipe DS, Horton E, Ulett GC: **The Basics of Bacteriuria: Strategies of Microbes for Persistence in Urine**. *Frontiers in cellular and infection microbiology* 2016, **6**:14.

107. D'ari R, Huisman O: **Novel Mechanism of Cell Division Inhibition Associated with the SOS Response in Escherichia coli**. *Journal of bacteriology* 1983, **156**(1).

108. Maguin E, Brody H, Hill CW, D'ari R: **SOS-Associated Division Inhibition Gene sfiC is Part of Excisable Element e14 in Escherichia coli**. *Journal of bacteriology* 1986, **168**(1).

109. Shields-Cutler RR, Crowley JR, Hung CS, Stapleton AE, Aldrich CC, Marschall J, Henderson JP: **Human Urinary Composition Controls Antibacterial Activity of Siderocalin**. *The Journal of biological chemistry* 2015, **290**(26):15949-15960.

110. Bouatra S, Aziat F, Mandal R, Guo AC, Wilson MR, Knox C, Bjorndahl TC, Krishnamurthy R, Saleem F, Liu P *et al*: **The Human Urine Metabolome**. *Plos ONE* 2013, **8**(9).

111. Yasuda T, Morimatsu T, H., Nagata T, Ohmori H: **Inhibition of Escherichia coli RecA coprotease activities by DinI**. *The EMBO Journal* 1998, **17**(11).

112. Voloshin ON, Ramirez BE, Bax A, Camerini-Otero RD: **A model for the abrogation of the SOS response by an SOS protein: a negatively charged helix in DinI mimics DNA in its interaction with RecA**. *Genes and Development* 2001.

113. Brooks T, Keevil CW: **A simple artificial urine for the growth of urinary pathogens**. *Letters in Applied Microbiology* 1997, **24**(3).

114. Schuerch DW, Wilson-Kubalek EM, Tweten RK: **Molecular basis of listeriolysin O pH dependence**. *Proceedings of the National Academy of Sciences of the United States of America* 2005, **102**(35):12537-12542.

115. Pinzon-Arango PA, Liu Y, Camesano TA: **Role of cranberry on bacterial adhesion forces and implications for Escherichia coli-uroepithelial cell attachment**. *Journal of medicinal food* 2009, **12**(2):259-270.

116. Liu Y, Gallardo-Moreno AM, Pinzon-Arango PA, Reynolds Y, Rodriguez G, Camesano TA: **Cranberry changes the physicochemical surface properties of E. coli and adhesion with uroepithelial cells**. *Colloids and surfaces B, Biointerfaces* 2008, **65**(1):35-42.

117. Micali S, Isgro G, Bianchi G, Miceli N, Calapai G, Navarra M: **Cranberry and recurrent cystitis: more than marketing?** *Critical reviews in food science and nutrition* 2014, **54**(8):1063-1075.

118. Spaulding CN, Klein RD, Ruer S, Kau AL, Schreiber HL, Cusumano ZT, Dodson KW, Pinkner JS, Fremont DH, Janetka JW *et al*: **Selective depletion of uropathogenic E. coli from the gut by a FimH antagonist**. *Nature* 2017, **546**(7659):528-532.